Temperature Coefficients and Thermal Uniformity Mapping of PV Modules and Plants

by

Ashwini Pavgi

A Thesis Presented in Partial Fulfillment
of the Requirements for the Degree
Master of Science

Approved July 2016 by the
Graduate Supervisory Committee:

Govindasamy Tamizhmani, Co-Chair
Patrick Phelan, Co-Chair
Liping Wang

ARIZONA STATE UNIVERSITY

August 2016

ABSTRACT

The operating temperature of photovoltaic (PV) modules is affected by external factors such as irradiance, wind speed and ambient temperature as well as internal factors like material properties and design properties. These factors can make a difference in the operating temperatures between cells within a module and between modules within a plant. This is a three-part thesis.

Part 1 investigates the behavior of temperature distribution of PV cells within a module through outdoor temperature monitoring under various operating conditions (Pmax, Voc and Isc) and examines deviation in the temperature coefficient values pertaining to this temperature variation. ANOVA, a statistical tool, was used to study the influence of various factors on temperature variation. This study also investigated the thermal non-uniformity affecting I-V parameters and performance of four different PV technologies (crystalline silicon, CdTe, CIGS, a-Si). Two new approaches (black-colored frame and aluminum tape on back-sheet) were implemented in addition to the two previously-used approaches (thermally insulating the frame, and frame and back sheet) to study temperature uniformity improvements within c-Si PV modules on a fixed latitude-tilt array. This thesis concludes that frame thermal insulation and black frame help reducing thermal gradients and next best viable option to improve temperature uniformity measurements is by using average of four thermocouples as per IEC 61853-2 standard.

Part 2 analyzes the temperature data for two power plants (fixed-tilt and one-axis) to study the temperature variation across the cells in a module and across the modules in a power plant. The module placed in the center of one-axis power plant had higher temperature, whereas in fixed-tilt power plant, the module in north-west direction had

higher temperatures. Higher average operating temperatures were observed in one-axis tracking as compared to the fixed-tilt PV power plant, thereby expected to lowering their lifetime.

Part 3 focuses on the determination of a thermal model coefficients, using parameters similar to U_c and U_v thermal loss factors in PVsyst, for the modules of four different PV technologies experiencing hot-desert climate conditions by statistically correlating a year-long monitored data. Thermal models help to effectively quantity factors influencing module temperatures to estimate performance and energy models.

To,

My parents, Arun Mahadeo Pavgi and Alpana Arun Pavgi, for their constant support, encouragement and unconditional love throughout my master's program.

My mentors and friends, whose guidance and affection motivated me in the thesis work.

ACKNOWLEDGMENTS

I would like to extend my gratitude to Dr. Govindasamy Tamizhmani for providing me an opportunity to work in the research group ASU-PRL (Photovoltaic Reliability Laboratory) and also for his constant guidance and support throughout the thesis work. It was a great experience to work with such a hardworking and knowledgeable person, whose expertise and supervision helped me to excel in my work.

I would also like to thank my committee members, Dr. Patrick Phelan and Dr. Liping Wang for their support during the thesis work. I am really grateful to Dr. Joseph Kuitche for extending his constant guidance and expertise during the thesis work.

In addition, I would like to thank Sai Tatapudi, laboratory technical manager for his motivation and technical support during the course of my project. I would like to acknowledge Salt River Project (SRP) for the funding a part of this thesis work.

I would also like to appreciate the opportunity to work with a group of members, who are helpful, hard-working and fun-filled. I am thankful to each and every laboratory member, whose presence and support made this Master's program journey a great experience.

TABLE OF CONTENTS

Page

CHAPTER Page

LIST OF TABLES

Table Page

Table Page

LIST OF FIGURES

Figure Page

Figure Page

Figure Page

Figure Page

Figure Page

PART 1: THERMAL UNIFORMITY IMPROVEMENT OF PV MODULES

1.1 INTRODUCTION

1.1.1 Background

The operating temperature of a PV module is influenced by the irradiance, wind speed, material and electrical configuration. Though the effect of irradiance and wind seems to be dominant on PV module temperature, material properties also impact the transfer of heat through the module and thereby affecting module temperature. There exists a thermal equilibrium between the heat absorbed, heat essentially generated by the module and heat lost to the surroundings by conduction, convection and radiation. These heat loss modes are dependent on the thermal and optical properties of the module materials as well as the ambient conditions. The conduction heat transfer takes place between various materials of module packaging, convection heat transfer occurs between the module surfaces and the air around and the radiation heat transfer happens between module surfaces and the atmosphere.

It is known that the performance parameters of a PV module are irradiance and temperature, wherein current is affected by the irradiance on a module while operating temperature of the PV module affects the voltage. Generally, for crystalline silicon modules, voltage decreases by 1% for every 2.5^{o}C rise in temperature and power decreases by 1% for every 2.2°C rise in temperature. In addition, higher temperatures increase stresses associated with thermal expansion, thereby resulting into several failures and

degradation modes of a PV module. Therefore, temperature is a significant factor affecting the performance of a PV module.

1.1.2 Problem Statement

As per ASTM 1036 – 15 module performance is usually reported at standard test conditions (STC) for selection and tests of the module by system designers and energy analysts but the outdoor operating conditions deviate from STC. Moreover temperature coefficients are also based on indoor solar simulator results with the controlled conditions, while a module in field operates in varying ambient conditions. Factors such as wind, clouds, dust, physical irregularities due to module components, etc. can affect the temperature uniformity. This paper attempts to study the effect of these factors on variation of temperature in modules with different cell technologies and thermal insulation configurations in order to reduce the differences by suggesting some methods for temperature uniformity in crystalline silicon technology modules.

1.1.3 Scope of the Work

i. Selection of different PV technologies (crystalline silicon, amorphous, cadmium telluride and CIGS) to analyze module level spatial temperature variation.
ii. Implementing various strategies on crystalline silicon technology modules to viable better uniform temperature variation by using different back sheets, frame and insulation.

iii. Baseline test to obtain temperature coefficients of all the modules to compare the deviation in temperature coefficients due to non-uniform temperature distribution within a module.

iv. Installing the modules on fixed tilt rack along with some balance of system components.

v. Setting up multi-curve tracer for continuously monitoring all the modules at MPPT conditions and simultaneously recording temperature values in the data loggers for four locations in each module respectively.

vi. Statistically analyzing the data using ANOVA designs to identify the significant factors affecting the temperature variation within a module.

vii. Performing few experiments on a sample to identify the point of maximum temperature within a module.

viii. Monitoring the temperature at four different locations in all the modules (with different technologies and module packaging) mounted on the fixed tilt rack at various electrical configurations for a short period (~ 30 minutes around solar noon) to analyze the effect of different combinations on temperature variability.

ix. Also monitoring the temperature for a long-term period (3 days) at four different locations in all the modules mounted on fixed tilt rack at Pmax and Voc to analyze the repeatability in the measurements.

x. Quantifying the impact of thermal non-uniformity within a module based on I-V parameters collected continuously at Pmax conditions.

xi. Statistically analyzing the temperature data by using a three-factorial design (with different levels and blocks) in Minitab and JMP to identify technology and configuration with the most uniformity.

1.2 LITERATURE REVIEW

1.2.1 Influence of Temperature on PV Module Performance

Several studies have been performed in the past to represent the impact of module operating temperature on PV performance and reliability. Various correlations presented by E. Skoplaki et. al. [1] show linear dependence of both electrical efficiency and module power output on operating temperature. Increase in temperature decreases band gap of a solar cell and allows longer wavelength photons to get absorbed. This leads to a rapid decrease in Voc and a slight increase in Isc causing an overall drop in fill factor and efficiency [2].Thus solar cell similar to any other semiconductor device is sensitive to temperature changes [3]. Different cell technologies distinctly influence the module temperature and its efficiency [2].

1.2.2 Effect of Various Parameters on Module Temperature Variability

The IV parameters and temperature coefficients are reported at standard test conditions based on indoor solar simulator results with controlled conditions. David King et. al. studied that about 15 to 25 minutes were required for modules with different front and back surfaces to reach their quasi-steady operating temperatures during the outdoor test [4] . Thus transient outdoor tests introduce temperature variations due to influence of wind, intermittent sunshine, module design and mount.

K. Emery et. al. discusses the temperature dependence of cells, modules and systems for various technologies [5]. C. Schwingshackl et. al. suggests varying indications of model performances with wind estimations for different technologies [6]. H. Goverde et. al. observed significant temperature variations across a module due to presence of variations

in wind speed and suggested solar cell performance models to integrate location-dependent heat transfer models [7]. A number of studies have also investigated the effect of various electrical configurations on module operating temperatures and performance [8], [9], [10].

Various studies in the past have discussed and analyzed the prevalent temperature distributions in modules and systems. D. Faiman studied an approximate 2K cell-to-cell temperature differences with center cells typically warmer than the corner cells [11]. The prevailing non-uniform temperature variations of 2-4 ^{O}C depending on ambient conditions present within cells of a module was determined by Neelesh in his MS Thesis [9]. Two precautions could be taken to minimize these variations which can be typically less than 5^{o}C. The module temperature sensors should be carefully placed on the back surface in order to minimize the errors introduced between measured and junction temperature [5]. D.L. King et. al. suggests that judicious placement of multiple temperature sensors on back surface of the modules and averaging these measurements can compensate for spatial temperature variations present in the system [12].

1.2.3 Effect of Various Parameters on Module Temperature Uniformity

Multiple authors have attempted to propose methods to minimize the temperature differences in modules. D. L. King suggested addition of thermal insulation for more uniform cell temperature distribution, lower thermal influence of junction box and metal frame and to achieve back surface module temperatures are more compatible to actual cell temperatures [4]. ASU-PRL further studied various insulation configurations to eliminate back sheet insulated only module after initial short term monitoring test and concluded

least temperature variations using frame insulation [9]. A study was performed at ASU-PTL (Photovoltaic Testing Laboratory) to improve module temperature uniformity with the help of phase change material on back surface [13].

The approach of this thesis is to further study the temperature differences present in various cell locations in each module of various PV technologies under different electrical configurations and sky conditions. It also investigates crystalline silicon technology PV modules with variations in frame, back sheet and frame and back sheet to viable uniform temperature measurements.

1.3 METHODOLOGY

This study consists of data collection through outdoor temperature monitoring and its analysis. This section discusses the various parameters and tests used to study the temperature variation

1.3.1 Test Modules

The test modules of various PV technologies were installed on latitude (33.4^{O}) fixed tilt rack system in the landscape mode with almost uniform spacing between the modules as shown in the Figure 1. This avoids the generation of low and high temperature currents, thereby minimizing thermal and electrical mismatch leading to temperature variation. This also helps to reduce the variability due to wind and soiling effect. Dummy modules were placed at both the ends to minimize effect of weather parameters and maintain least possible variation. The test modules under study were crystalline-Silicon, amorphous-Silicon, Cadmium Telluride (CdTe) and Copper Indium Gallium Selenide (CIGS) PV cell technologies. The label numbers mentioned in the Figure 1 corresponds to the module specifications as provided in Table 1.

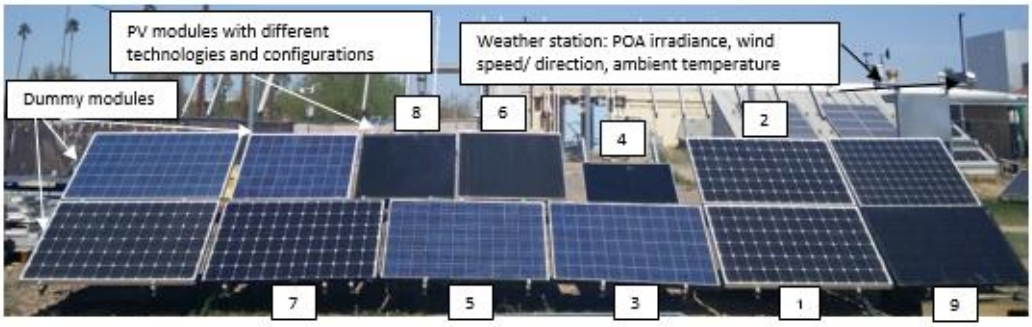

Figure 1: PV Modules with Different Technologies and Thermal Insulation Configurations Mounted on an Open Rack System at Latitude Tilt.

Table 1: Specifications of Various PV Modules Installed on the Open-Rack System

Sr No	Module configuration	PV Technology	Pmax (W)	Vmp (V)	Imp (A)	Voc (V)	Isc (A)
1	Non-insulated cSi module	monocrystalline-Si	285	35.8	7.96	44.7	8.52
2	Aluminum tape covered back sheet module	monocrystalline-Si	285	36.72	7.77	44.64	8.36
3	Frame insulated module	polycrystalline-Si	285	36.72	7.77	44.64	8.36
4	Thin-film module	CdTe	60	62	0.96	62	1.12
5	Frame and back sheet insulated module	polycrystalline-Si	285	36.36	7.84	44.5	8.35
6	Thin-film module	amorphous-Silicon	128	186	0.688	238	0.846
7	Thin-film module	CIGS	150	79	1.9	110	2.1
8	Black-frame module	monocrystalline-Si	310	36.871	8.408	46.377	8.829
9	Black frame and back sheet module	monocrystalline-Si	240	30	8	37.4	8.5

1.3.2 Determination of Temperature Coefficients Using Baseline IV Parameters

The temperature coefficients are applicable to three performance parameters namely current, voltage and power of a PV module. It can be defined for a particular PV performance parameter as the ratio of rate of change of that parameter to temperature. The modules were first placed in the cold chamber, in order to bring operating temperatures for modules around 10^{o}C. The IV parameters were recorded for temperature coefficient measurements on each module at four locations on a single-axis tracker on a clear sunny day around solar noon time (eliminating the angle of incidence effect) for a specific range of module operating temperatures (20-30^{o}C). These parameters were plotted against temperature to obtain the temperature coefficients respectively and then compared to their

rated values. These coefficients calculated for four different locations were plotted to study the temperature variability amongst coefficients for a particular module.

The table of temperature coefficients for the new modules added on the setup at four different locations is provided in Appendix A.

1.3.3 Thermocouple Locations

The temperature sensors were located at four locations on back surface of the test modules as mentioned in IEC standard 61853-2 draft in order to account more module area and study overall module temperature. The various thermocouple locations in a module as per the standard are shown in the following Figure 2:

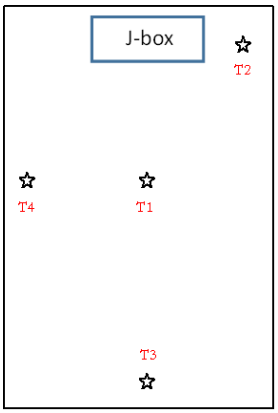

Figure 2: Various Thermocouple Locations in a Module Per IEC Standard Draft 61853-2

The K-type thermocouples were located at four locations in each module simultaneously for all the modules for each and every test. HOBO 4-channel data loggers as shown in Figure 3 were used to record the data at one minute interval using these temperature sensors. The data was monitored using these data loggers and retrieved periodically. These HOBO data loggers proved to be very convenient providing ease of simultaneous data collection and retrieval for long-term period.

Figure 3: HOBO 4-Channel Data Logger

1.3.4 Weather Parameters

A weather station including irradiance sensor, wind sensor and rain gauge was installed near the rack system to monitor various weather parameters like solar irradiance, ambient temperature, wind speed and wind velocity. The data from these sensors was recorded and stored every minute using Campbell Scientific CR1000 data logger and retrieved periodically.

The irradiance sensor used was a Kipp and Zonen pyranometer mounted at latitude tilt about 12 feet from the test modules as shown in Figure 1 (Reference cell). An ultrasonic wind sensor and rain gauge were mounted horizontally to measure the wind speed and precipitation. Temperature sensor was also installed on this setup to record ambient temperature values. These weather parameters were used to determine the sky conditions at two levels: clear sunny sky and overcast/cloudy sky. An average irradiance of above 900 W/m^2 during the solar window time without the presence of clouds surrounding the sun was considered as clear sunny sky conditions.

1.3.5 Electrical Conditions

The temperatures were monitored at four locations in the test modules under different electrical conditions.

A. Short-Circuit Condition

A test module under short-circuit condition is operating at zero voltage and when the module leads are connected without any load. Practically, short-circuit current is the largest current drawn from the cell. The test modules were monitored under short-circuit condition for short term period to avoid damaging the module by operating it under short-circuit for longer time.

B. Open-Circuit Condition

A test module under open-circuit condition is operating at its maximum voltage available and occurs when the net current through it is zero. The temperature measurements were under this condition when PV module leads were not connected. The test modules were monitored under open-circuit condition for two term periods: short term ($\sim$ 30 minutes around solar noon) and long term period.

C. Maximum Power Point Tracking Condition

The Daystar, Inc. MT5 multi-curve tracer comprising of load and control unit was used to run all the modules under maximum power for short-term and long term (2 days) period. It was also used to take IV curves at every minute interval simultaneously. It tracks the peak- power point by using an algorithm which continually changes the operating voltage in the same direction until the power drops relative to the last measurement. MT5 Control

unit consists of input ports for temperature sensors which accepts standard T-type thermocouples. The Load unit consists of module channel ports which can withstand maximum of 300 W, 100 V and 10A, except 2 ports for maximum configurations of 100 W, 100 V and 10 A. Due to these limits, amorphous silicon technology (with configurations of 128 W, 238 V and 0.846 A) module was not tested at P_{max} conditions.

1.3.6 IV Curve Measurements for Performance Monitoring

The multi- curve tracer was set to monitor the performance of all the modules simultaneously every hour for 2 consecutive clear sunny days (during solar window from 10am to 2pm). These recorded I-V curves would then be translated to STC condition (rated module values) based on the measured temperature at four locations on the module. This approach helps to analyze the effect of module temperature variability on performance prediction.

1.3.7 Thermography under Steady State Conditions

Thermography or also known as infrared (IR) imaging allows analysis of thermal and electrical failures in PV modules in the field under working conditions. Thermography measurements can be performed in individual or large scale system PV modules under steady state conditions. These measurements help to study the temperature variations induced by supplying external current (comparable to short circuit current) or by applying light to the modules.

The IR imaging was performed using uncooled-IR camera as shown in Figure 4 on a clear, sunny day with about ideal ambient temperature and low wind speed. These measurements

were performed from back side and glass side at a view angle close to 90^{o}. Thermography help to detect the module defects and temperature gradients within PV module or array occurring due to convective heat transfer.

Figure 4: IR Imaging Camera Used to Study Temperature Gradients

1.3.8 Various Strategies on c-Si Modules to Implement Temperature Uniformity

This approach involved crystalline silicon technology PV modules with variations in frame, back sheet and frame and back sheet mounted simultaneously on the rack system to minimize the temperature variation. Figure 5 represents two materials used on crystalline silicon modules (frame and/or back sheet). In a previous study done at ASU, the effects of insulation on edge cells and temperature variations was studied [9]. Under

that study, the module back sheet was insulated using foam insulation of R-value 9.6. The inner surface of the frame was insulated using rigid foam board while the inner surface using self-sealing R-1 foam tape. Back sheet insulated only module was eliminated after an initial short term temperature monitoring since insulation did not improve temperature uniformity.

Figure 5: Various Materials Used for Module Insulation

This study utilized two modules: Module with frame insulation, Module with frame and back sheet insulation from the previous study simultaneously with other test modules. It also extended the approach of experimenting PV module boundaries by introducing three modules: Module with black frame, module with black frame and back sheet and module

back sheet covered with aluminum tape. Thermally conductive aluminum tape was covered on back sheet of monocrystalline silicon and the module was mounted on top of crystalline silicon module. The specifications of these test modules are as follows in Table 2. In order to analyze the effect of aluminum tape for viability of temperature uniformity, IR images from glass and back surface were captured. A DC Voltage Transducer as shown in Figure 6 having specifications of input range 0-100 VDC and output range 0-5 VDC was used for the voltage measurements. Figure 7 shows voltage transducer with power source were connected to the module leads of the crystalline silicon and the other crystalline silicon module with aluminum tape back sheet to measure the open-circuit voltage of those modules. The voltage and temperature measurements were recorded using the data loggers and compared for further analysis.

Figure 6: DC Voltage Transducer Used to Record Voc using Voltage Data Loggers

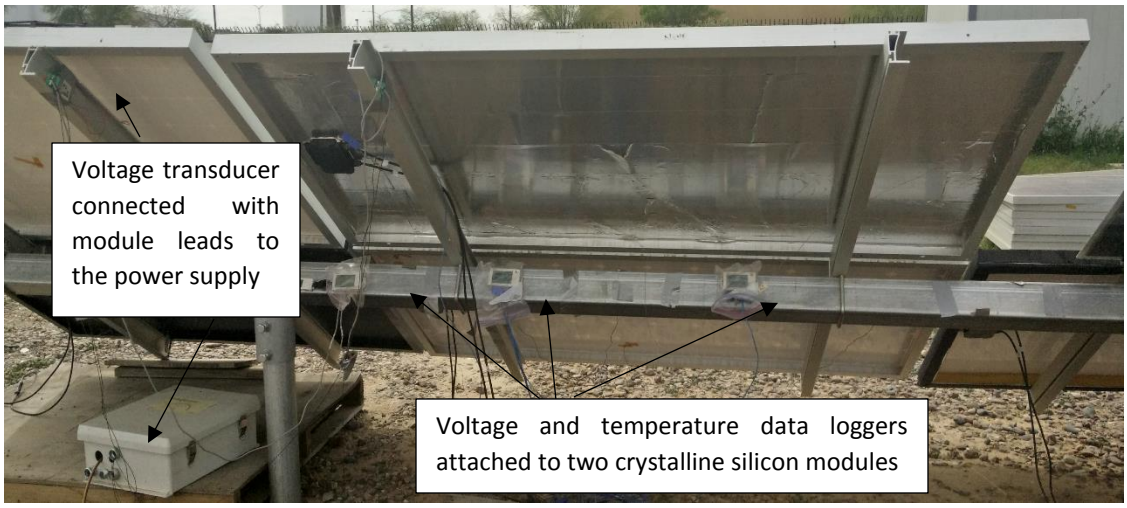

Figure 7: Voltage Transducer Connected with Module Leads and Voltage Data Loggers

1.3.9 Response Surface Methodology for Determination of Point of Maximum Temperature within a PV Module

The objective of a response surface methodology (RSM) used on a PV module whose temperature values are influenced by several variables is to determine the point of maximum temperature using a 2^2 factorial design.

The cell (amongst the four cells) which recorded the maximum temperature was considered as the center-point and RSM was applied with respect to this point using a 2^2 factorial design. Since irradiance has a significant effect on module temperatures, it was considered as one of the factors. Since an optimized point was to be determined on the surface of PV module, the number of cells with respect to the center-point cell was considered as the second factor. Each factor had two levels: high and low in the design. The RSM flowchart as shown in Figure 8 was used for the determination of point of maximum temperature within a PV module.

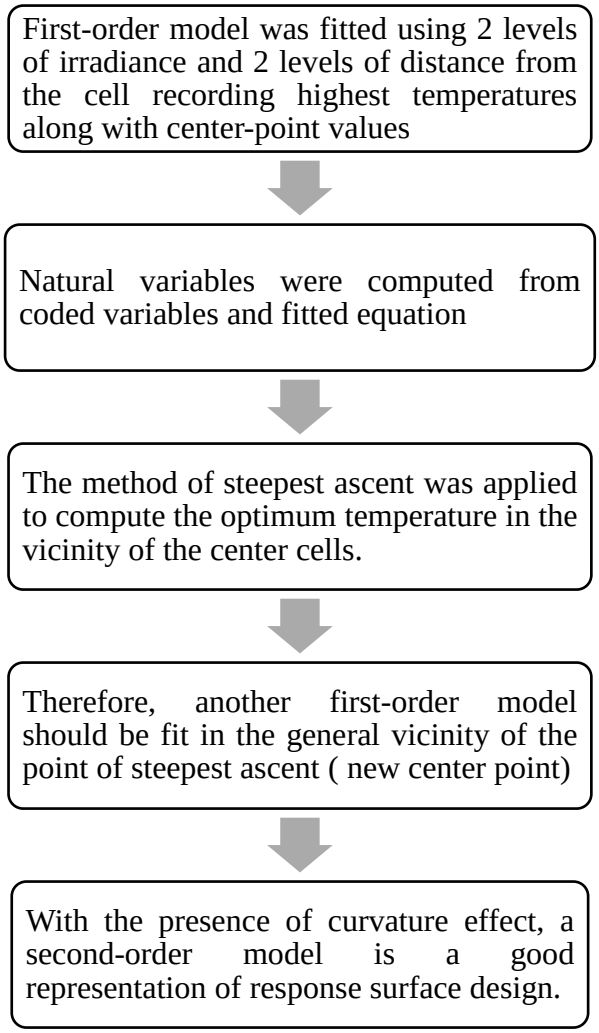

Figure 8: Flowchart for Response Surface Methodology

The following sets of experiments were performed on the sample PV module on two clear sunny days for determination and optimization of response.

i. Initial experiment for 2 levels of irradiance and 2 levels of distance from the cell recording highest temperatures with respect to the center-point.

ii. Next experiment using two new levels of irradiance and new levels of distance from the cells recording highest temperatures in the general vicinity of the point of steepest ascent. (new center point)

1.4 RESULTS AND DISCUSSIONS

This part of the chapter discusses the effect of various PV technologies and thermal insulation configurations on temperature variability. As mentioned in Section 1.3.5, a-Si PV technology module is not considered for further plots, except for plots representing variation in temperature coefficients for Isc, Voc and Pmax at different thermocouple locations.

1.4.1 Thermal Variation Based on PV Technologies

I. Variation in Temperature Coefficient Values for Isc, Voc and Pmax at Different Thermocouple Locations

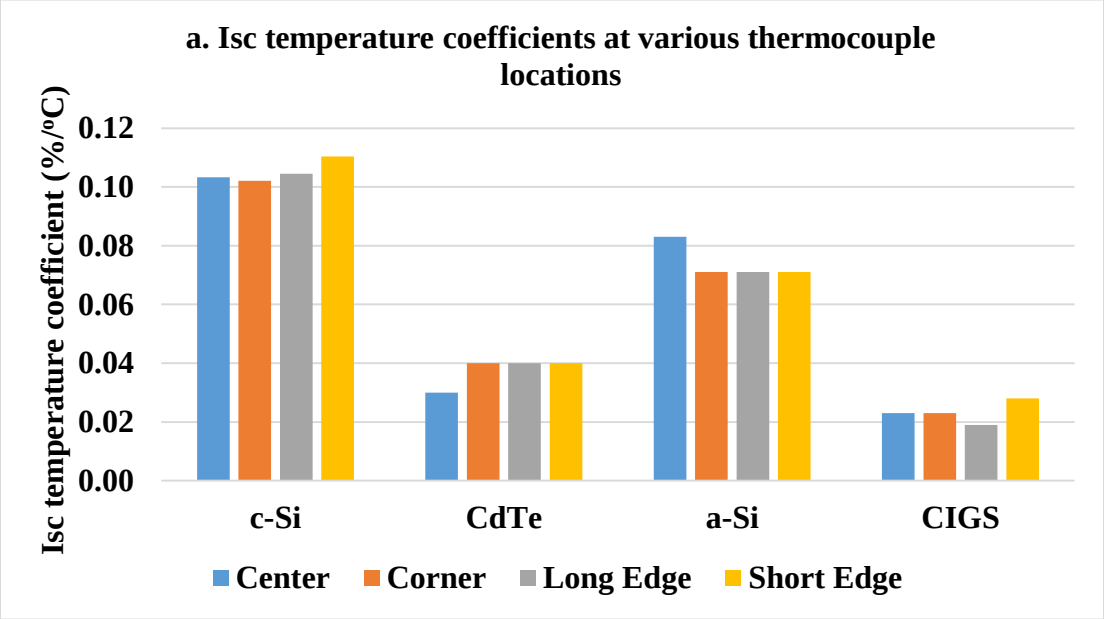

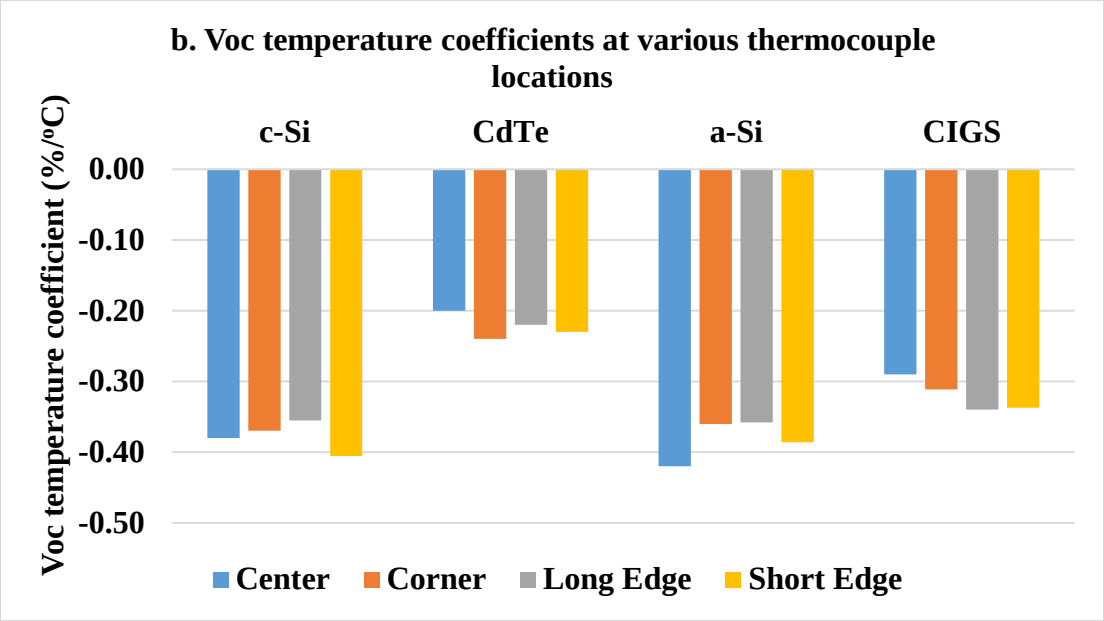

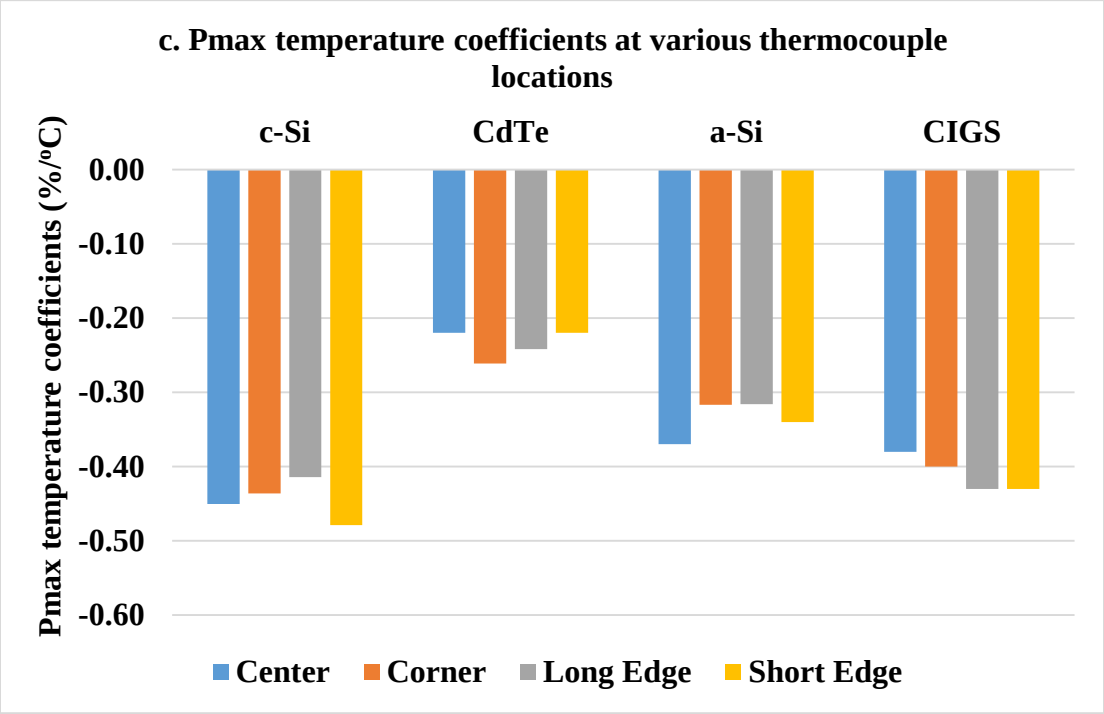

Figure 9: Isc, Voc and Pmax Temperature Coefficients for Various PV Technologies (c-Si, CdTe, CIGS and a-Si) at Different Thermocouple Locations

The short edge has the highest temperature coefficient values for c-Si and CIGS PV technologies. This could be influenced by thermal mass of frames/edges. The center cell

has the highest temperature coefficient values for a-Si (amorphous silicon) PV technology. The double-junction a-Si PV technology has higher Voc (%/^{o}C) temperature coefficient values compared to other PV technologies because of higher bandgap leading to higher Voc. The variation in the Isc, Voc and Pmax temperature coefficient values at four different thermocouple locations is not consistent due to G/G/FR construction type of CdTe PV technology leading to higher influence of wind on the values.

II. ANOVA Design for PV Technologies, Electrical Conditions and Thermocouple Locations

The ANOVA (Analysis of Variance) of fixed effect model was executed to study the significance of various factors and their interactions on the module temperature. The three factors (PV technology, electrical condition and thermocouple locations) with different levels were studied through ANOVA design as represented in Table 2.

Table 2: Model Summary for PV Technologies (PV Tech), Electrical Conditions (EC) and Thermocouple Locations (TL)

Factor	Type	Levels	Values
PV Tech	**Fixed**	**3**	**1 2 3**
EC	**Fixed**	**3**	**1 2 3**
TL	**Fixed**	**4**	**1 2 3 4**

The experiments for this design were conducted on a clear sunny day with irradiance >950W/m^2. For the time frame from 10am-2pm, the average irradiance was 1015W/m^2 and average wind speed was 1.3m/s. The ANOVA for this experiment is as shown in Table 3:

Table 3: ANOVA Design for PV Technologies (PV Tech), Electrical Conditions (EC) and Thermocouple Locations (TL)

Source	DF	SS	MS	F	P
PV Tech	2	56.901	28.45	71.2	0
EC	2	75.625	37.812	94.63	0
TL	3	28.271	9.424	23.58	0
PV Tech*EC	4	5.632	1.408	3.52	0.04
EC*TL	6	2.048	0.341	0.85	0.554
PV Tech*TL	6	131.11	21.852	54.j69	0
Error	12	4.795	0.4		
Total	35	304.39			

It can be seen that p-value for all factors is less than 0.05. Therefore all the three factors (PV technology, electrical conditions and thermocouple locations) have significant effect on the temperature variation. The p-value for interaction between PV technology and thermocouple location and PV technology and electrical conditions is also less than 0.05. Therefore these interactions have significant effect.

A. Interaction and Main Effects Plot on a Clear Sunny Day

Since the factors and interactions had significant effect, further the factorial plots were considered to study the temperature variation on a clear sunny day. The various levels of the three factors are represented in the Table 4.

Table 4: Various Levels of Factors for PV Technology (PV Tech), Electrical Condition (EC) and Thermocouple Location (TL) (a. Clear Sunny Day)

Levels of PV Tech (PV technologies)	Levels of EC (electrical conditions)	Levels of TL (thermocouple locations)
c-Si	Short circuit	Center
CdTe	Open circuit	Corner
CIGS	Maximum power point	Long edge
		Short edge

The interactions plot and the effects plot for temperature variation on a clear sunny day are shown in Figure 10.

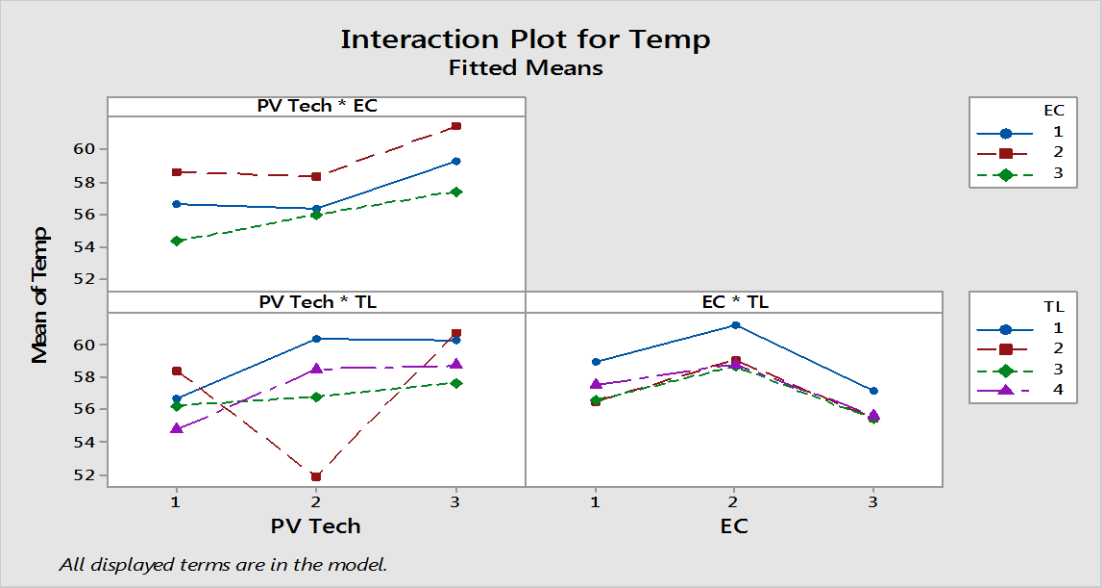

Figure 10: Interactions Plot for Temperature Variation Based on 3 PV Technologies (c-Si, CdTe, CIGS), 3 EC (Electrical Conditions) and 4 Thermocouple Locations on a Clear Sunny Day

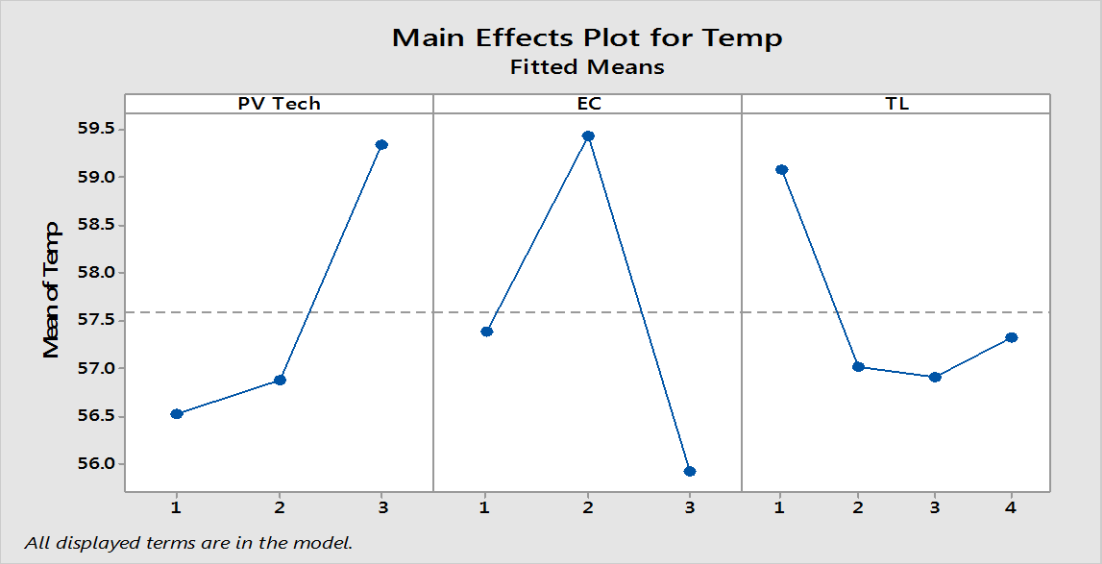

Figure 11: Main Effects Plot for Temperature Variation Based on Various PV Technologies (c-Si, CdTe, CIGS), 3 EC (Electrical Conditions) and 4 Thermocouple Locations on a Clear Sunny Day

It can be studied from the main effects plot for responses that, CIGS PV technologies operating at VOC have highest temperature value at the center of the module. The three PV technology modules irrespective of the thermocouple location in a module have higher operating temperatures at VOC conditions and lowest at Pmax conditions. The center thermocouple has higher operating temperature irrespective of the electrical conditions. On the other hand, the influence of other thermocouple locations is not that distinct. Mostly the center thermocouple locations have higher temperature values than the other locations for all PV technologies.

B. Interactions and main effects plot for temperature variation around solar noon

The interactions and main effects plot to study the temperature variation around solar noon for the readings taken on three consecutive days for three different electrical conditions are as shown in Figure 12, 13. The various levels of each factor is as shown in the table 4.b.

Table 4: Various Levels of Factors for PV Technology (PV Tech), Electrical Condition (EC) and Thermocouple Location (TL) (b. around Solar Noon)

Levels of PV Tech (PV technologies)	Levels of EC (electrical conditions)	Levels of TL (thermocouple locations)
cSi	Maximum power point	Center
CdTe	Open circuit	Corner
CIGS	Short circuit	Long edge
		Short edge

The average irradiance was in the range of 1007-1015 W/m^2, the average wind speed was in the range of 0.7-0.8 m/s and the ambient temperature was in the range of 22-24 ^{o}C.

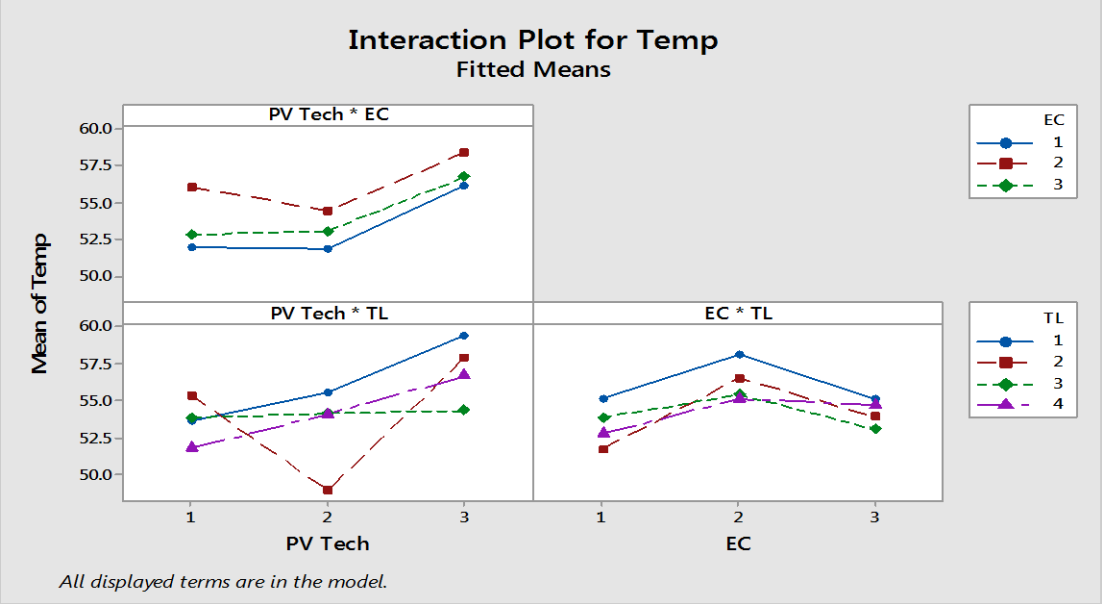

Figure 12: Interactions Plot for Temperature Variation Based on Various PV Technologies (c-Si, CdTe, CIGS), 3 EC (Electrical Conditions) and 4 Thermocouple Locations around Solar Noon

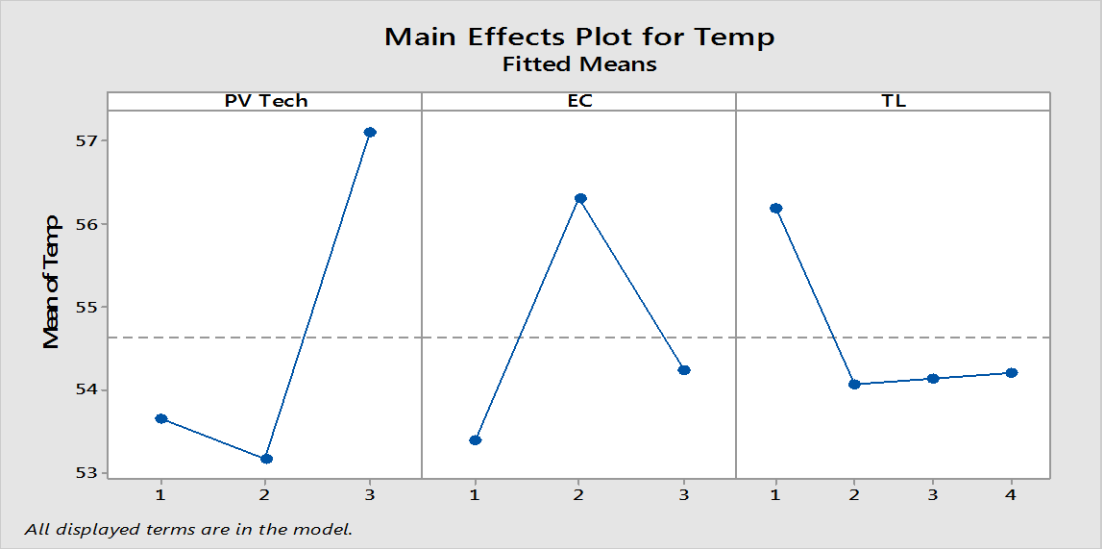

Figure 13: Main Effects Plot for Temperature Variation Based on Various PV Technologies (c-Si, CdTe, CIGS), 3 EC (Electrical Conditions) and 4 Thermocouple Locations around Solar Noon

It can be studied from the main effects plot for responses that, CIGS PV technologies operating at VOC have highest temperature value at the center of the module. The three PV technology modules irrespective of the thermocouple location in a module have lower operating temperatures at Pmax conditions. The center thermocouple has higher operating temperature irrespective of the electrical conditions. On the other hand, the influence of other thermocouple locations is not too distinct.

C. Interaction Plot to Study the Variation of the Edge and Corner Cell Temperatures with Respect to the Center

Since the center cell of the module show highest temperature among all the four cells, a further experimentation was performed to study the variation of the edge and corner cell temperatures with respect to the center cell. The following three factors A, B, C were used in the study the temperature variation using interaction plot. The various levels of each

factor is included in the Table 5. The interactions plot of a 3^3 factorial design as shown in Figure 14 was analyzed to study the temperature variation.

Factor A: Various PV technologies,

Factor B: Various electrical conditions

Factor C: Difference between center and various thermocouple locations

Table 5: Various Levels of Factors for PV Technologies, Electrical Conditions and Distance between Center and Other Thermocouple Locations

Levels of A	Levels of B	Levels of C
cSi	Short circuit	Center- Corner
CdTe	Open circuit	Center- long edge
CIGS	Maximum power point	Center- Short edge

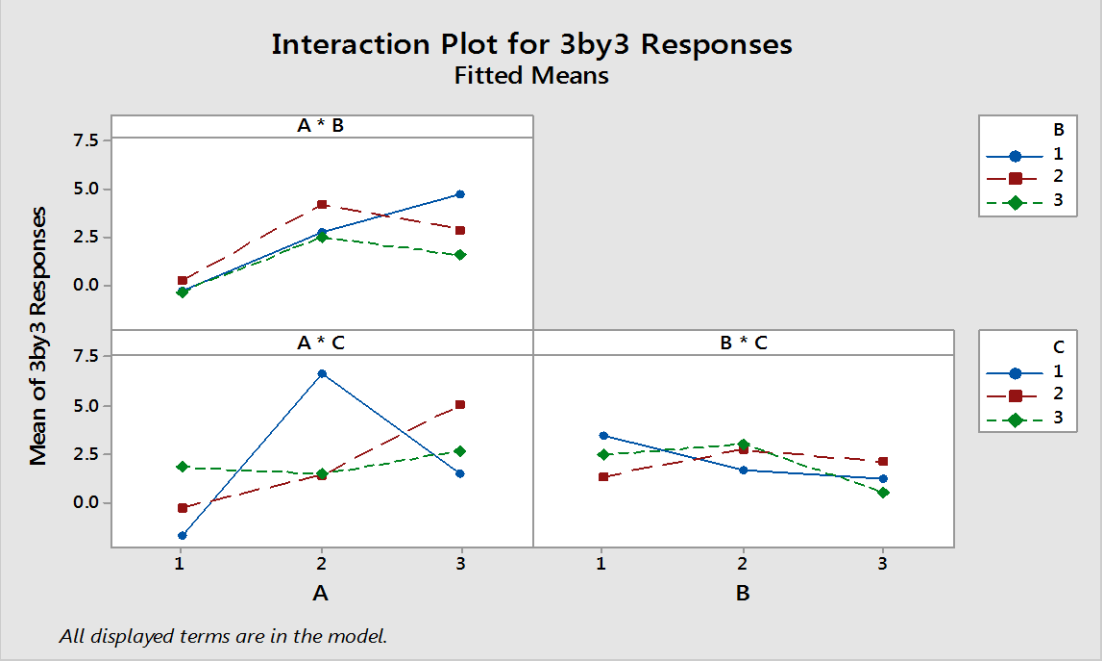

Figure 14: Main Effects Plot for Various PV Technologies, Electrical Conditions and Distance between Center and Other Thermocouple Locations

Since center cell recorded maximum temperature values, a further analysis was performed to study interaction of the other three cells with respect to the center cell. As variation in values for factor C is high, a further center-point design was constructed to design a maximum point on module.

III. Response Surface Methodology to Determine the Maximum Temperature Point and Optimize the Response

The center-point design and the response surface plot were evaluated using the methodology as mentioned in the flowchart in Section 1.3.9. The two levels of irradiance considered as initial design parameters are as follows: low level value as 300 and high level value as 1000. The two levels of distance from the center is cell number 3 as low and cell number 6 as high level value. Table 6 shows the initial design parameters used to fit a linear model obtained after analyzing the factorial design. The design used to collect the data is a 2^2 factorial design augmented with center points. The replicates of center point help to estimate the experimental error and to check the first-order model adequacy.

Table 6: Original Design Parameters of 2^2 Factorial Design

Factors and levels	**Irradiance (x1)**	**Number of cells/ Distance from the center cell (x2)**
High	**1000**	**6**
Low	**300**	**3**
Origin	**800**	**0**

The first-order model obtained in the coded variables x1 and x2 are as shown in the Equation 1.

$y = -0.415 + 0.580\ x1 - 0.125\ x2$ Equation 1

The method of steepest ascent was used to move sequentially in the direction of the maximum increase in the response. In order to move along the path of steepest ascent, we need to move by 77.8 units in the opposite x1 direction for every one unit in the x2 direction. Thus the path passes through the point (x1=0, x2=0) with a slope of 4.5/350. The basic step size was decided based on the feasible values of irradiance. Table 7 shows the step size, followed by Table 8 denoting the steepest ascent experiment for the natural variables.

Table 7: Determination of Natural Variables and Step Size

x	**(e - 650)/350**	**(e - 4.5)/1.5**
e	**350x + 650**	**1.5x + 4.5**
Δx	**1**	**-0.215517241**
Δe	**350 Δx**	**4.5 Δx**

Table 8: Steepest Ascent Experiment using Natural Variables

Steps	**e1**	**e2**	**y**
Origin	**800**	**0**	
Δ	**0.2**	**-0.22**	
Base + Δ	**350**	**0**	
Base + 2Δ	**720**	**4.18**	**47.15**
Base + 3Δ	**790**	**3.85**	**49.41**
Base + 4Δ	**860**	**3.53**	**52.06**
Base + 5Δ	**930**	**3.21**	**51.81**

The steps are computed along this path until a decrease in response was observed. Increases in response are observed through the fourth step; however, steps beyond this point result in a decrease in temperature. In this way the optimum temperature in the vicinity of the center cells/ center region of the PV module was obtained by performing the steepest ascent experiment. Again a first-order model was fitted around the new center-point: x1= 860, x2= 3 (i.e. 3rd cell from the center, between center and short edge) and a 2^2 factorial design wit center points was used. The low and high levels of this design are as shown in Table 9.

Table 9: Design Parameters for Second First-Order Model

	Irradiance (x1 or A)	**Distance (x2 or B)**
High	**930**	**4**
Low	**790**	**2**
origin	**860**	**3**

Table 10: First-Order Model Summary

S		**R-sq**	**R-sq(adj)**		**R-sq(pred)**	
0.610795		**95.89%**	**91.79%**		*	
Term	**Effect**	**Coef**	**SE Coef**	**T-Value**	**P-Value**	**VIF**
Constant		**47.26**	**0.305**	**154.75**	**0**	
A	**0.59**	**0.295**	**0.305**	**0.97**	**0.389**	**1**
B	**5.86**	**2.93**	**0.305**	**9.59**	**0.001**	**1**
A*B	**0.01**	**0.005**	**0.305**	**0.02**	**0.988**	**1**
Ct Pt		**0.268**	**0.41**	**0.65**	**0.549**	**1**

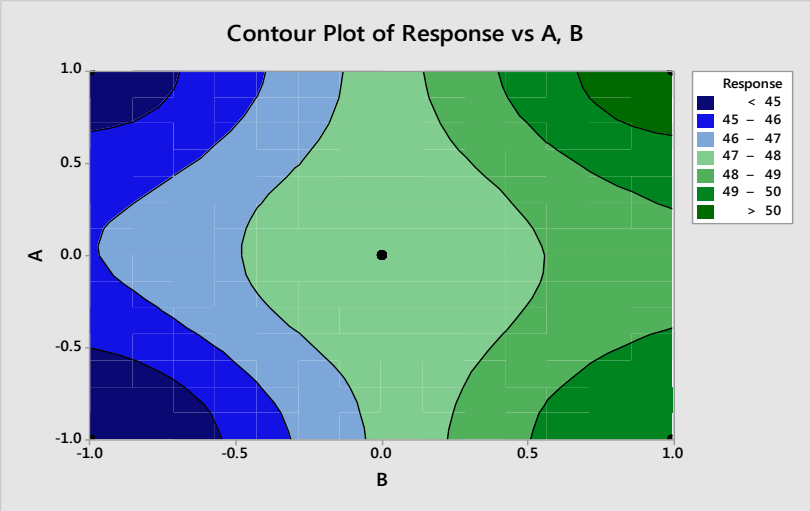

Figure 15: Contour Plot of Responses for First-Order Model Design

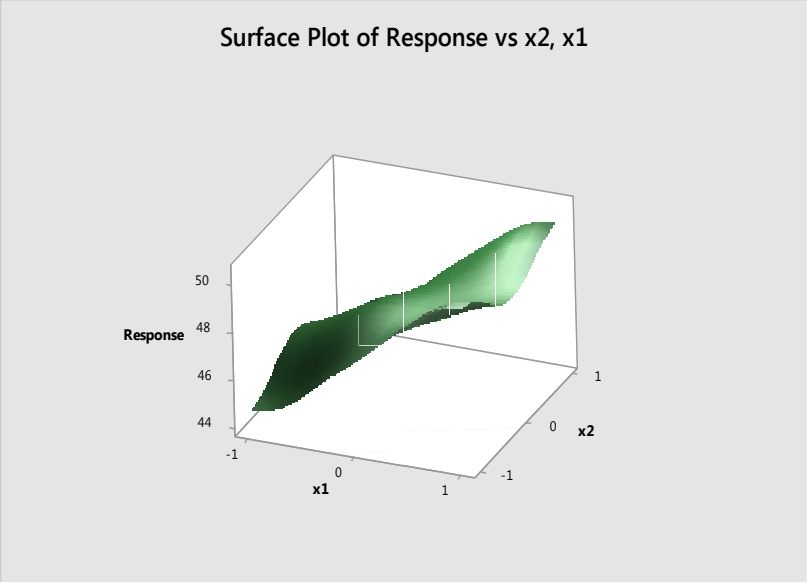

Figure 16: Surface Plot of Responses for First-Order Model Design

The curvature effect is calculated by $\mu_c - \mu_f = 0.268$.

The first-order model summary shown in Table 10 imply the presence of curvature effect and that the first-order model is not an adequate approximation. This curvature may imply that observations in the vicinity of the optimum. Therefore, further analysis must be performed to locate the optimum more precisely.

Due to the presence of curvature effect, second-order model using central composite design was analyzed to represent the response surface. This design considers the axial points as the extra center points in order to implement the second-order model near maximum. The fitted second-order model used is as shown in Equation 2.

$$y = 47.26 + 0.295\,A + 2.93\,B + 0.005\,A*B + 0.268\,Ct.\,pt. \qquad \text{Equation 2}$$

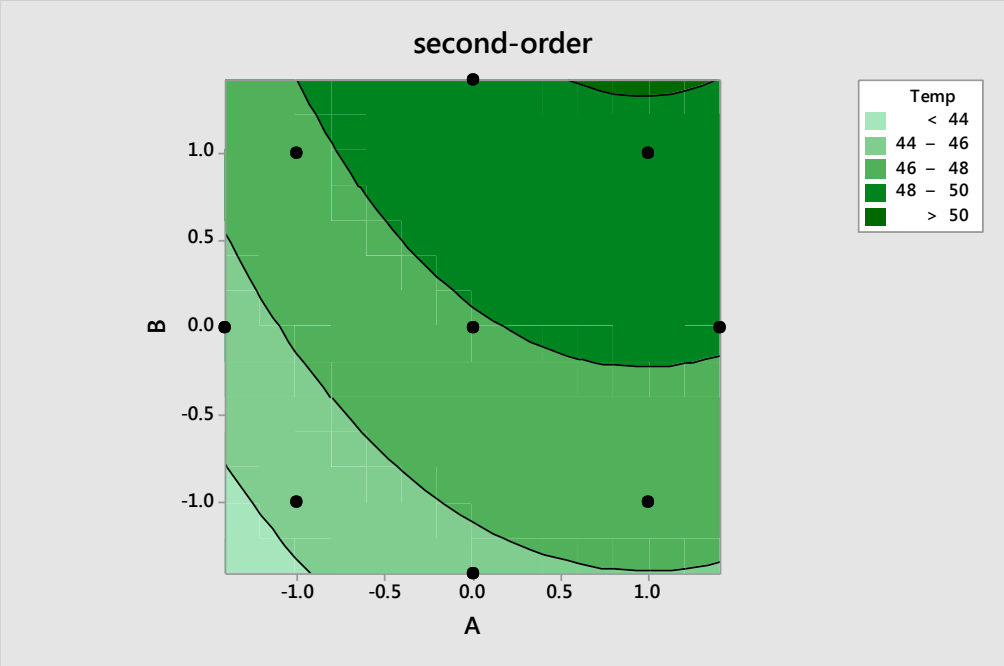

Figure 17: Contour Plot of Responses for Second-Order Model Design

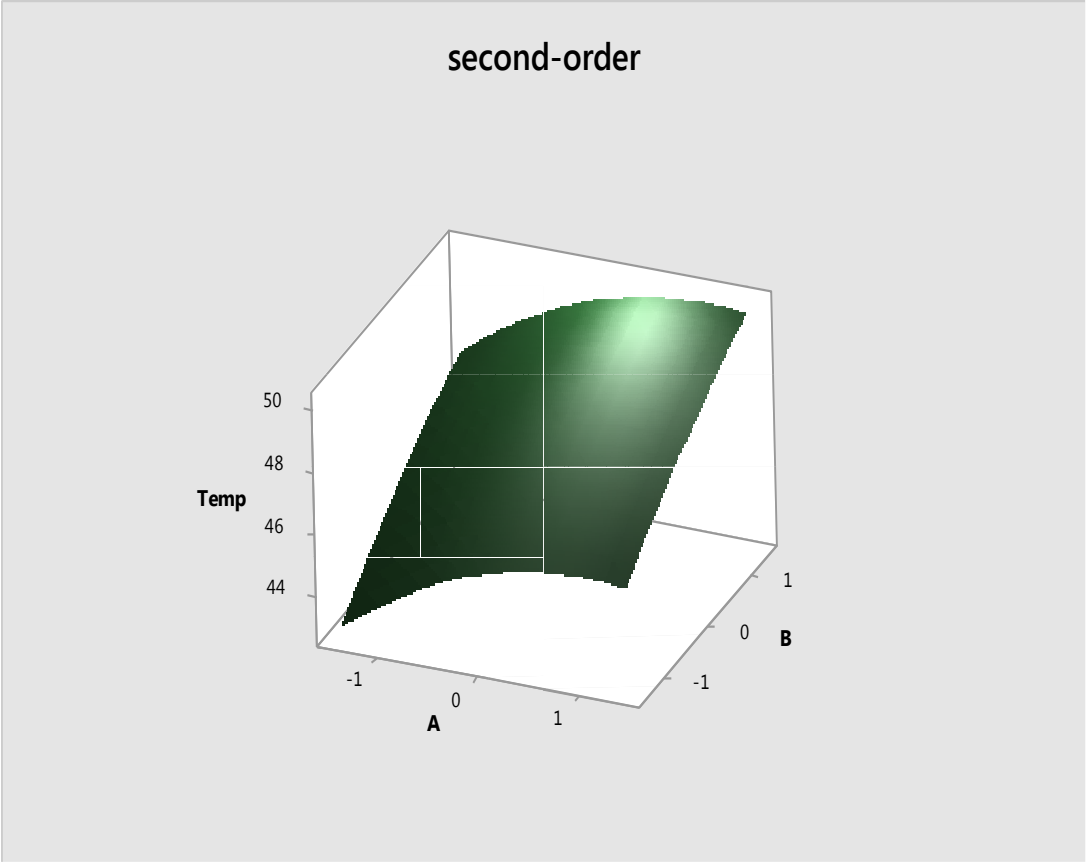

Figure 18: Surface Plot of Responses for Second-Order Model Design

The temperature at right-most corner (+1, +1) is higher than all the values. The stationary point represent the point of maximum response. Therefore response surface and contour plot illustrate a surface with a maximum. Therefore, the maximum point is the 3rd cell from the center-most cell, between the center-most cell and center cell along the short edge.

IV. Short-term temperature variation

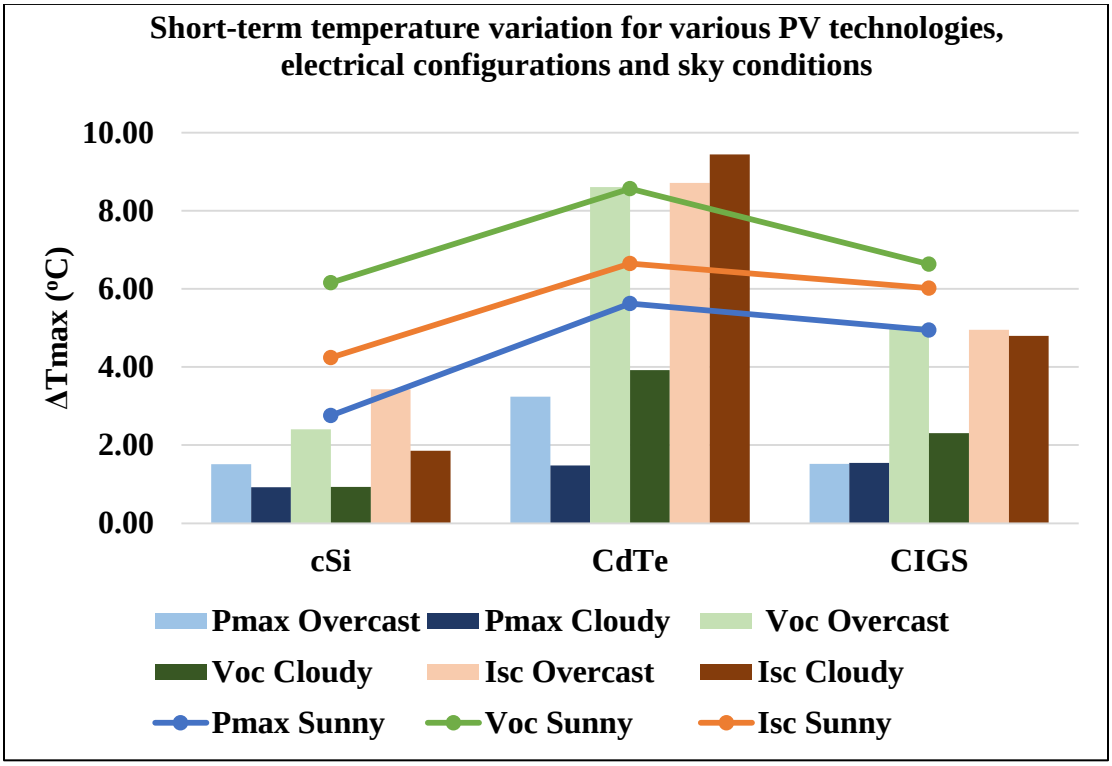

Figure 19: Short-Term Temperature Variation Analysis between Four Cell Locations within a PV Module (ΔT_{max}) at Various PV Technologies, Electrical and Sky Conditions

The temperature variation was least in crystalline silicon modules. The temperature variation is highest at Voc for any sky condition difference being as high as 4-5°C. Therefore, further temperature variation was studied at Voc under any sky conditions. Modules at Pmax operate at lower temperatures and have temperature variation lower by around 3-4°C on clear sunny days. Higher insolation leads to higher operating temperatures as well as higher temperature gradients. Therefore higher temperature variation is observed on clear sunny days. The temperature variation at Isc seems to be affected the most at various sky conditions because of significant variation in irradiance.

V. Impact of Thermal Non-Uniformity affecting IV Parameters

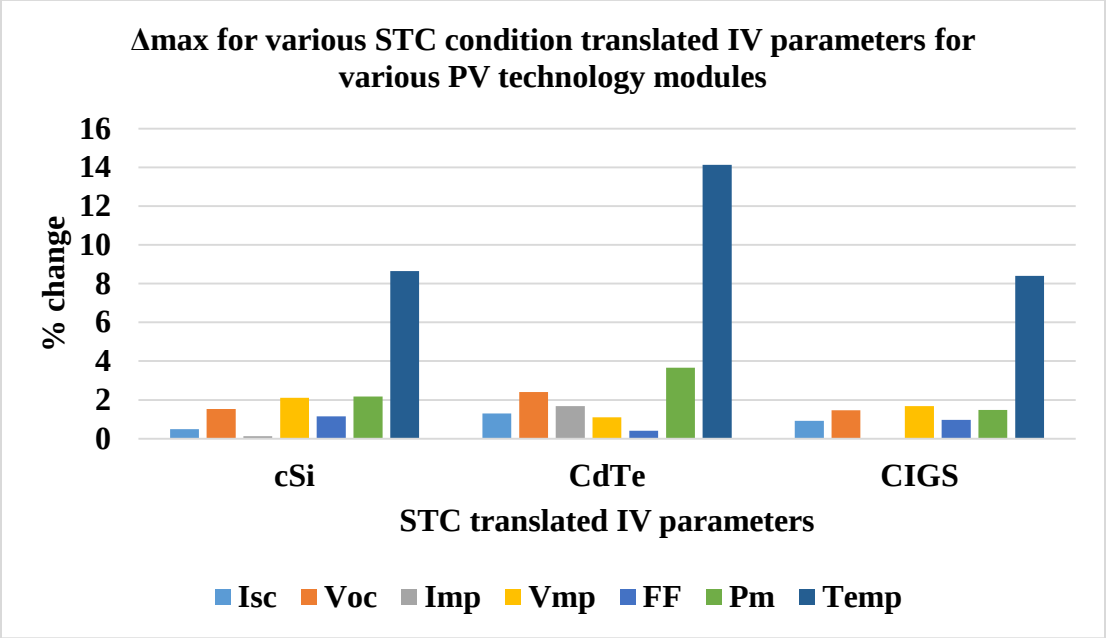

Figure 20: Thermal Non-Uniformity between Four Cell Locations within a PV Module (ΔTmax) in Various PV Technologies (c-Si, Cdte and CIGS) affecting IV Parameters

Pmax, Voc, Vmp and FF parameters are the main parameters affected by temperature variation. About 8% temperature variation within the cells in c-Si has caused only about 2% variation in Pmax. On the other hand about 14% variation in temperature seem to cause less than 4% variation in Pmax. Therefore, this high variation in temperature causing lower effect on performance could be because of G/G/FR construction type and higher effects of wind.

VI. Long Term Temperature Variation Analysis

The modules of various PV technologies operating at open-circuit and maximum power conditions were studied for a long-term period for the solar time frame window of 10am -

2pm. The crystalline silicon PV technology had the least variability at both Voc and Pmax conditions.

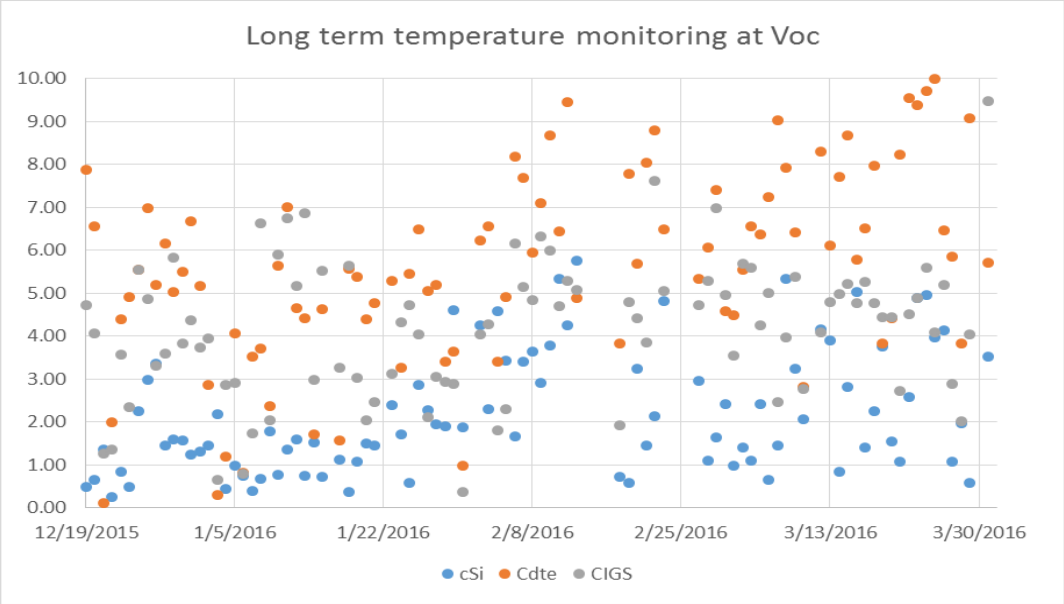

Figure 21: Thermal Variation for Various PV Technologies during Long Term Temperature Monitoring at Voc

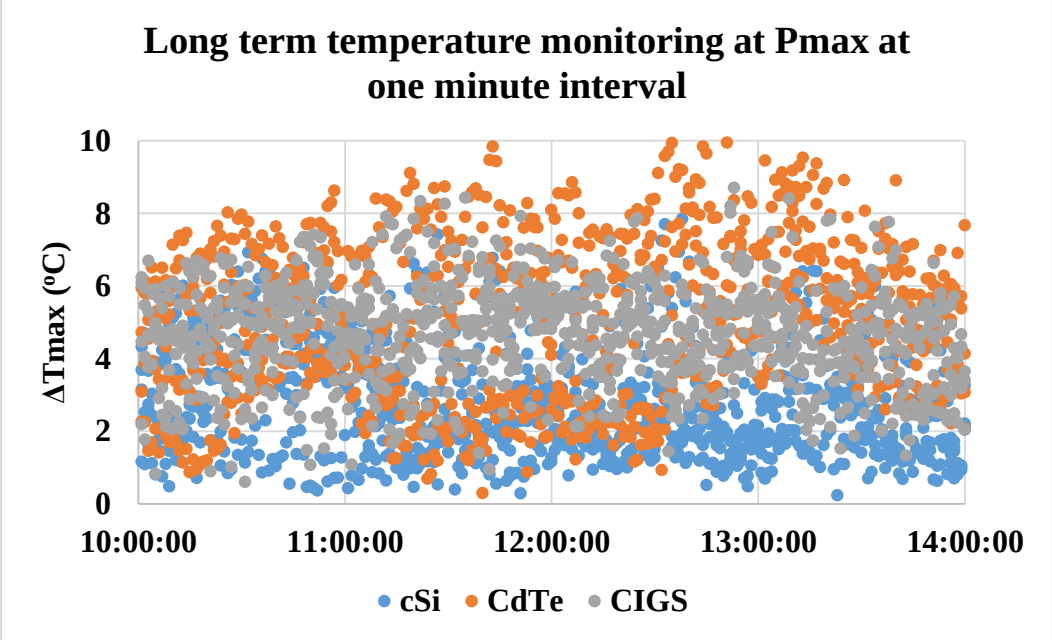

Figure 22: Thermal Variation for Various PV Technologies during Long Term Temperature Monitoring at Pmax

1.4.2 Thermal Variation Based on Various Thermal Insulation Configurations

I. Addition to Previous Study: Percentage Change in Temperature Coefficients with Respect to Different Temperature Sensors

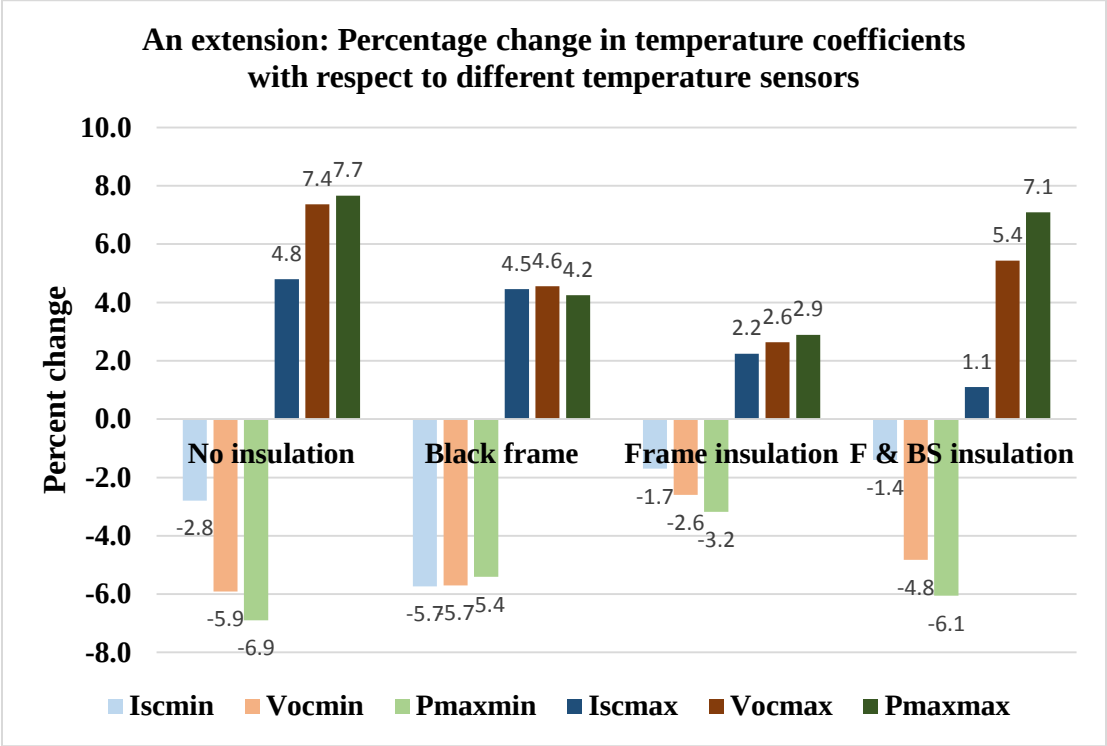

Figure 23: Addition: Percentage Change in Temperature Coefficients with Respect to Different Temperature Sensors

The individual graphs for variation in Isc, Voc and Pmax temperature coefficients at various thermocouple locations are included in Appendix A. Figure 23 is an addition to the previous study and therefore also includes previously used values. The least variation is observed in frame and back sheet insulated modules at Isc conditions. But overall, the variation in temperature coefficients is ±7 percent for frame and insulated modules. The least deviation of about ±3 percent is observed in frame insulated modules and the maximum deviation of about ±8 percent is observed in non-insulated modules.

II. ANOVA Design for Various Thermal Insulation Configurations, Electrical Conditions and Thermocouple Locations

The ANOVA (Analysis of Variance) of fixed effect model was executed to study the significance of various factors and their interactions on the module temperature. The three factors (thermal insulation configurations, electrical condition and thermocouple locations) with different levels were studied through ANOVA design as represented in Table 11.

Table 11: Model Summary for Thermal Insulation Configurations, Electrical Conditions and Thermocouple Locations

Factor	Type	Levels	Values
A (MC)	fixed	5	1 2 3 4 5
B (EC)	fixed	3	1 2 3
C (TL)	fixed	4	1 2 3 4

The experiments for this ANOVA design were conducted on a clear sunny day with irradiance >950W/m^2. For the time frame from 10am-2pm, the average irradiance was 1015W/m^2 and average wind speed was 1.3m/s. The ANOVA for this experiment is as shown in Table 12:

Table 12: ANOVA Design for Thermal Insulation Configurations, Electrical Conditions and Thermocouple Locations

Source	DF	SS	MS	F	P
MC	4	4661.8	1165.45	2308.56	0
EC	2	323.29	161.65	320.19	0
TL	3	161.41	53.8	106.57	0
MC*EC	8	29.55	3.69	7.32	0
EC*TL	6	15.2	2.53	5.02	0.002
MC*TL	12	92.51	7.71	15.27	0
Error	24	12.12	0.5		
Total	59	5295.9			

It can be seen that the p-value for all factors and interactions is less than 0.05. Therefore all the three factors (Module configurations, Electrical conditions and thermocouple locations) have significant effect on temperature variation. Interaction and main effects plot on a clear sunny day. Since the factors and interactions have significant effect, further the factorial plots were considered to study the temperature variation on a clear sunny day. The various levels of the three factors are represented in the Table 13.

Table 13: Various Levels of Factors for Thermal Insulation Configuration, Electrical Condition and Thermocouple Location

Levels of A	Levels of B	Levels of C
No insulation	Short circuit	Center
Black frame	Open circuit	Corner
Frame insulation	Maximum power point	Long edge
Frame and back sheet insulation		Short edge
Aluminum tape back sheet		

The interactions plot and the effects plot for temperature variation on a clear sunny day are shown in Figure 24 and 25.

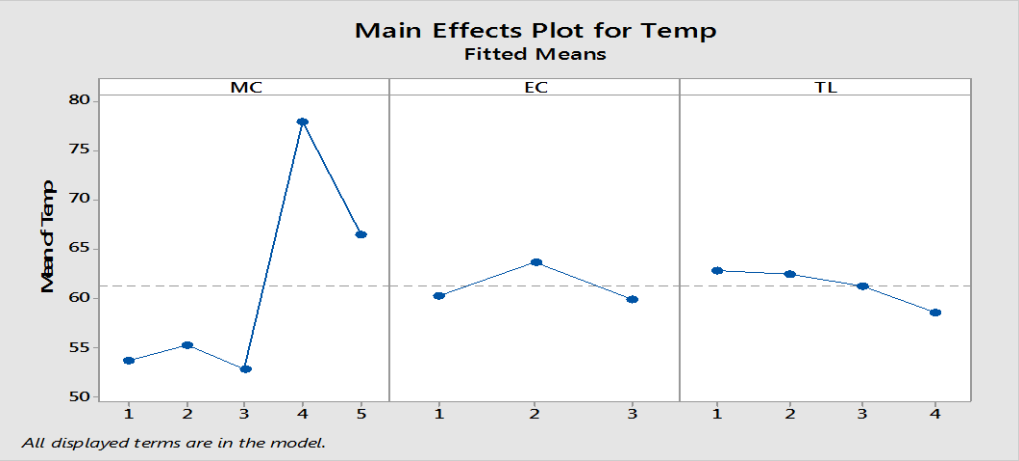

Figure 24: Main Effects Plot for Temperature Variation Based on Various Thermal Insulation Configurations on a Clear Sunny Day

The modules operating at open circuit conditions (VOC) have highest temperature value. The center of the module operate at higher temperature than the edges and corners of the module. This is because the center of the module is surrounded by other cells which also experience the similar high temperature and therefore the center cell has no proper heat transfer mechanism. On the other hand, frame of the PV module acts as a passive heat sink to the nearby cells, which results in comparatively lower operating temperatures near the edges and corners. The module with frame and back sheet insulation has the highest operating temperature. This is because the back sheet of the module is covered with an insulated foam, which blocks the radiative heat loss through the back sheet, therefore an increase in temperature is observed. Similar trend can be seen for the module back sheet covered with aluminum tape having higher temperature. On the other hand, module with frame insulation has lowest operating temperatures.

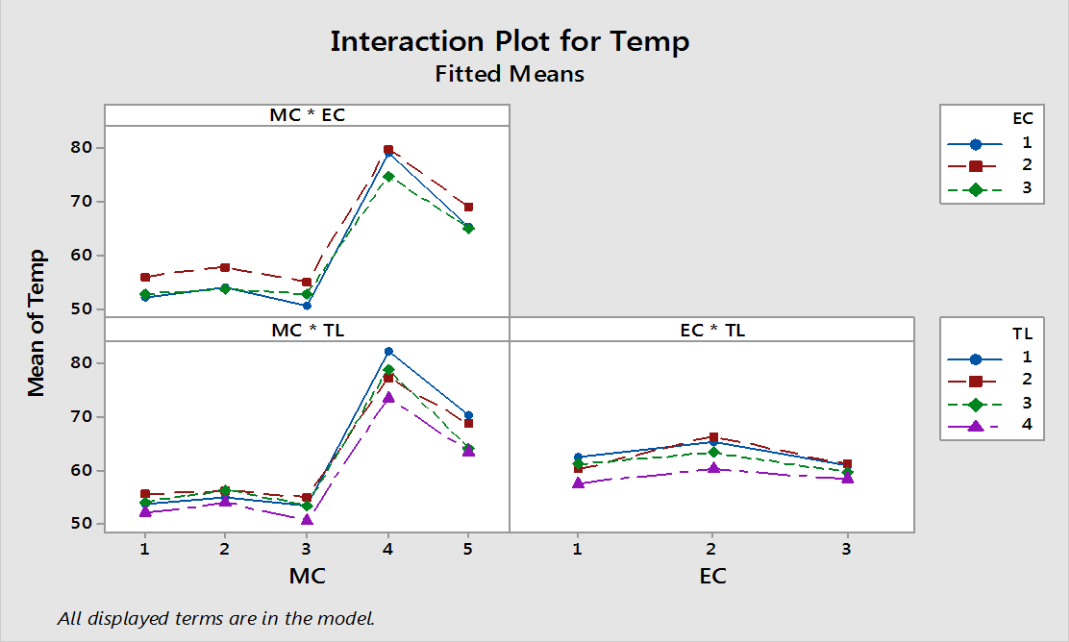

Figure 25: Interactions Plot for Temperature Variation Based on Various Thermal Insulation Configurations on a Clear Sunny Day

The modules with various thermal insulation configurations irrespective of the thermocouple location in a module have higher operating temperatures at open circuit (VOC) conditions. The center thermocouple has higher operating temperature irrespective of the electrical conditions while the thermocouple placed along the center of short edge has lowest operating temperature. On the other hand, the influence of other thermocouple locations is not too distinct.

III. Temperature Variability for Various Thermal Insulation Configurations around Solar Noon

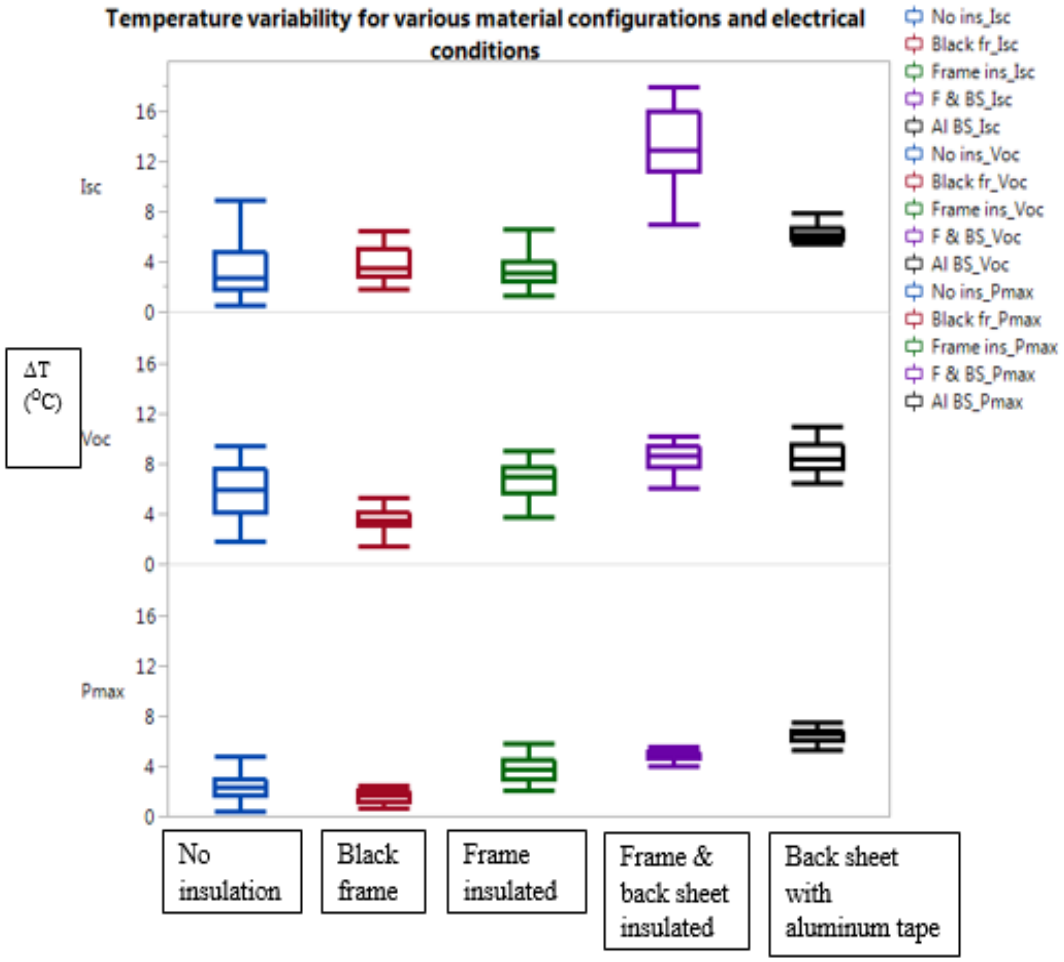

Figure 26: Temperature Variability for c-Si PV Modules with Various Thermal Insulation Configurations at Isc, Voc and Pmax around Solar Noon (35 Data Points Each)

The average irradiance was in the range of 1007-1015 W/m^2, the average wind speed was in the range of 0.7-0.8 m/s and the ambient temperature was in the range of 22-24 ^oC.

It can be studied from the boxplots that there is least variability in the temperatures in Black frame module, followed by frame insulated module considering any of the three electrical configurations. Moreover the least variability in maximum temperatures values within a module is observed at maximum power condition. At Pmax, general operating conditions of PV modules, the maximum variability was observed in the non-insulated PV modules. The maximum variability was observed for the module with frame and back sheet insulation at Isc conditions. Even though range of ΔT values for the module with aluminum tape on back sheet is higher, the standard deviation is lower. Therefore aluminum tape could be a good solution to improve thermal uniformity provided appropriate measures are taken to lower the operating temperatures.

IV. Short-Term Temperature Variation Analysis

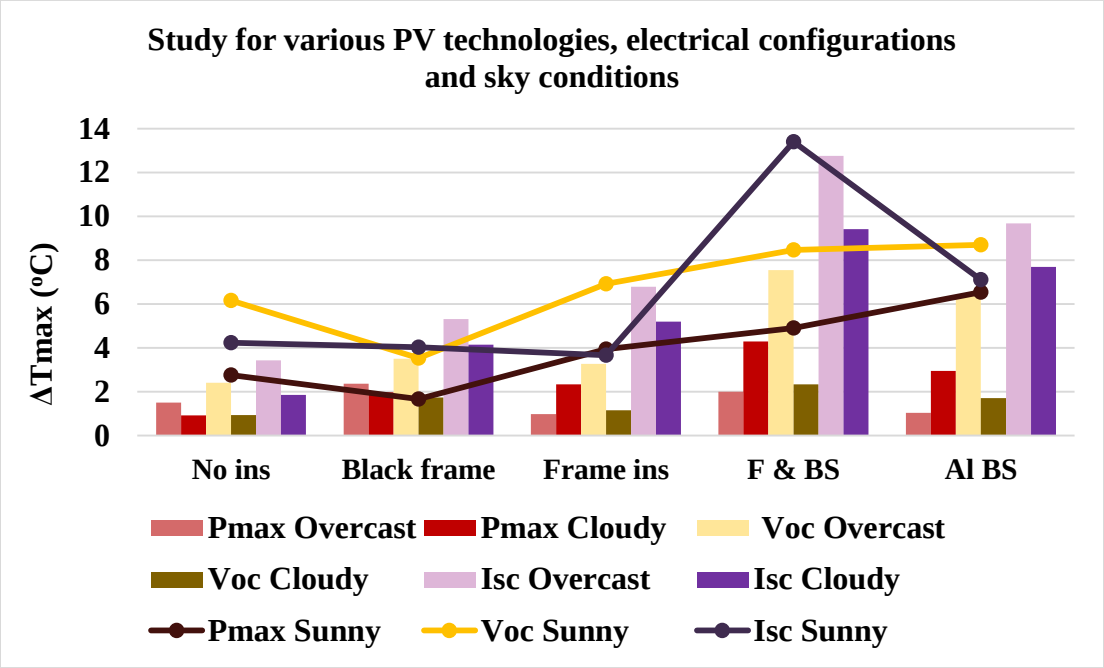

Figure 27: Short-Term Temperature Variation Analysis between Four Cell Locations within a PV Module for Various Thermal Insulation Configurations

Considering the modules operating at all the three electrical conditions, the least variation in the temperature values is observed in the module with black frame, followed by the module with frame insulation on clear sunny day. The modules are expected to have higher temperature variations on a clear sunny day because of higher insolation and higher temperatures. On the other hand, the least variation on cloudy/overcast days were observed in non-insulated PV modules. This might be due to effect of dominant wind conditions. The least variation in temperature values was observed at Pmax conditions. Therefore further study of the temperature variation on IV parameters rated at STC conditions was performed at Pmax conditions.

V. Long-Term Temperature Analysis

In order to further study the temperature variation on clear sunny days around solar noon (12-1pm), long-term temperature analysis was performed. The data for five days was considered having irradiance value > 900W/m^2.

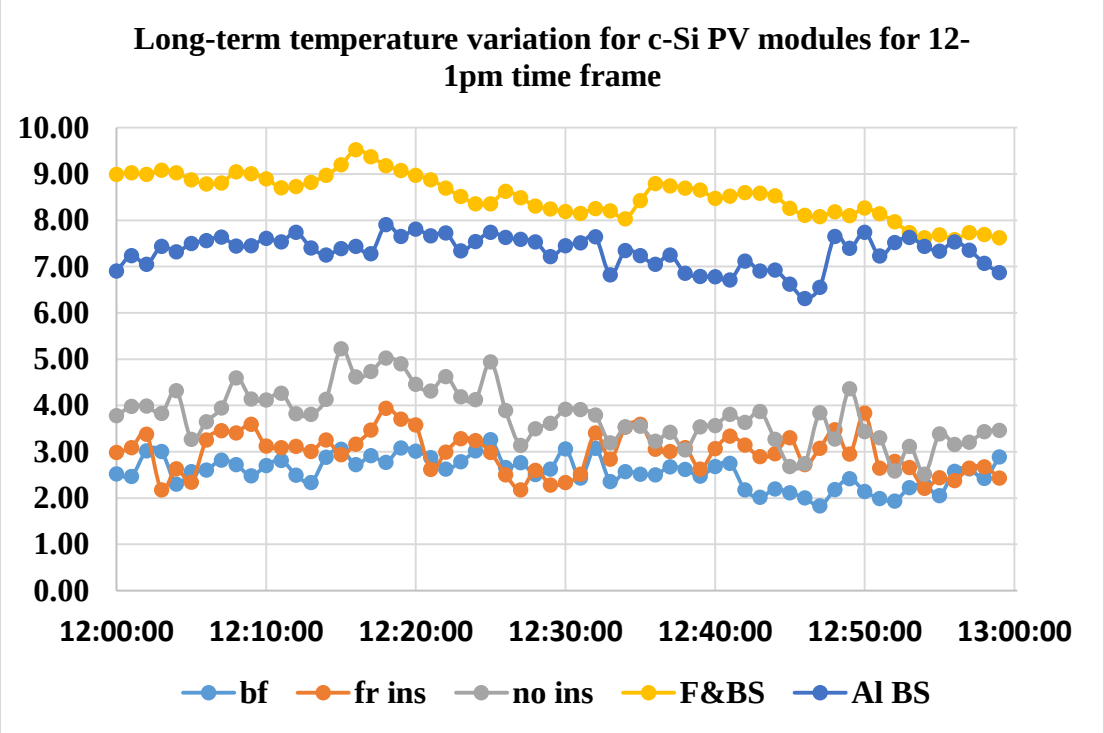

Figure 28: Long-Term Temperature Variation for c-Si PV Modules with Various Thermal Insulation Configurations on Clear Sunny Days for 12-1pm Time Frame

This variation in temperature is consistent with the observations obtained for short-term temperature analysis at three electrical conditions as shown in Figure 27.

The principle that the frame of the PV module acts as passive heat sink, which results in the cells near the frame to operate at comparatively lower temperatures than the center cells is well-known. Now when the frame is insulated, the heat transfer in this direction is blocked resulting into more uniformity in the temperature. But on the other hand, the

thermal insulation is not effective for the module with frame and back sheet insulation. This is because with the back sheet insulated with foam blocks the heat transfer to the surroundings. Similar trend is observed in the module with aluminum tape on the back sheet.

1.4.3Aluminum Tape Back Sheet versus Conventional Polymer White Back Sheet Study for Temperature Variation

I. Voltage versus temperature

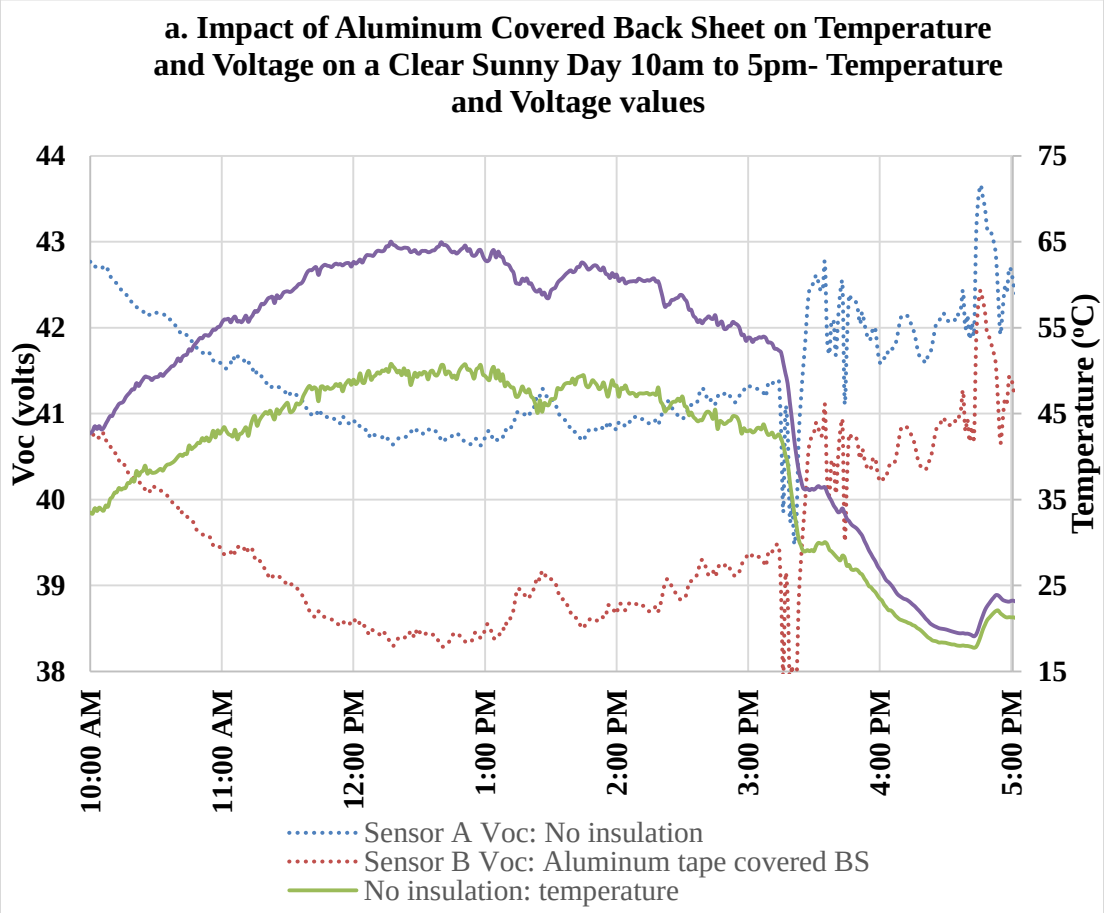

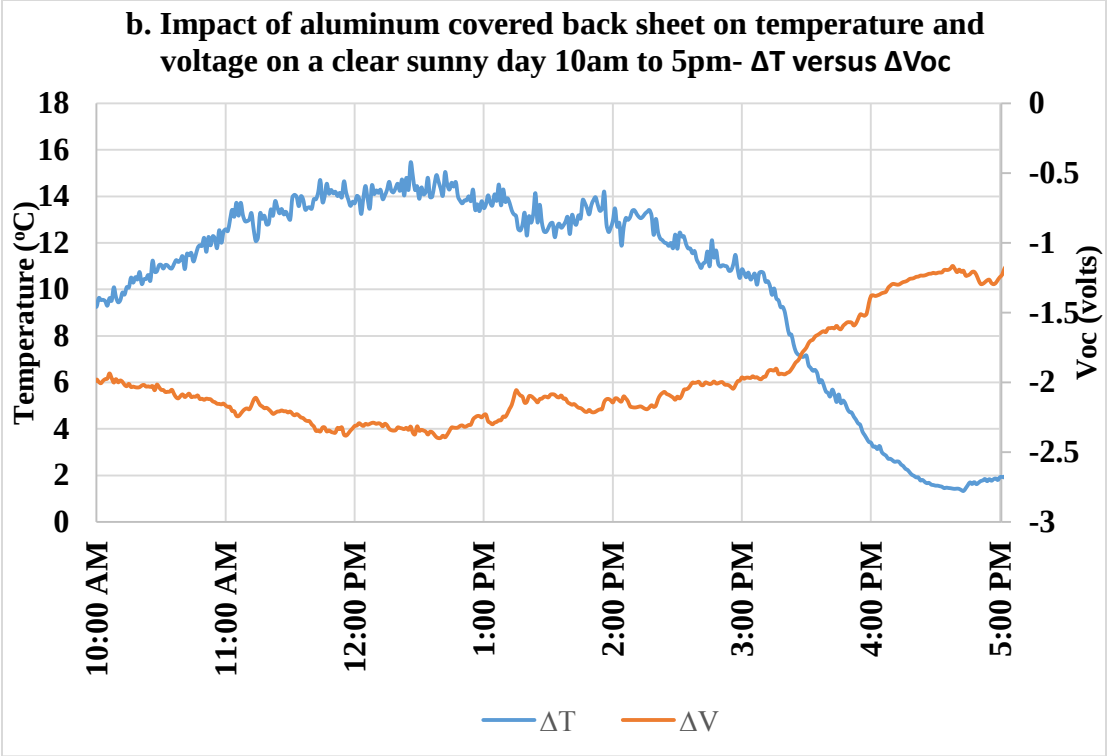

Figure 29: Impact of Aluminum Covered Back Sheet on Temperature and Voltage on a Clear Sunny Day 10am to 5pm

The module operating temperatures monitored on white back sheet covered with aluminum tape are higher than those monitored on white back sheet module without aluminum tape especially from 10:00 am to 3:00 pm. Temperature difference as high as 15ºC was observed around solar noon. The difference of the voltage and temperature values were plotted and it was observed that as the temperature increases, voltage decreases i.e. voltage and temperature values were inversely proportional. The value of the slope is equal to 0.39%/ºC. This value is generally the voltage temperature coefficient of crystalline silicon modules.

II. Infrared Imaging

Thermography measurements were performed on clear sunny day to study the temperature variations induced by supplying short circuit current) to the modules. The weather conditions were as follows: Irradiance= 1019 W/m2, wind speed= 1.213 m/s, ambient temperature= 24.9 ºC. The module in the bottom row is the conventional polymer white back sheet PV module and the PV module placed on the top row has aluminum tape on its back sheet.

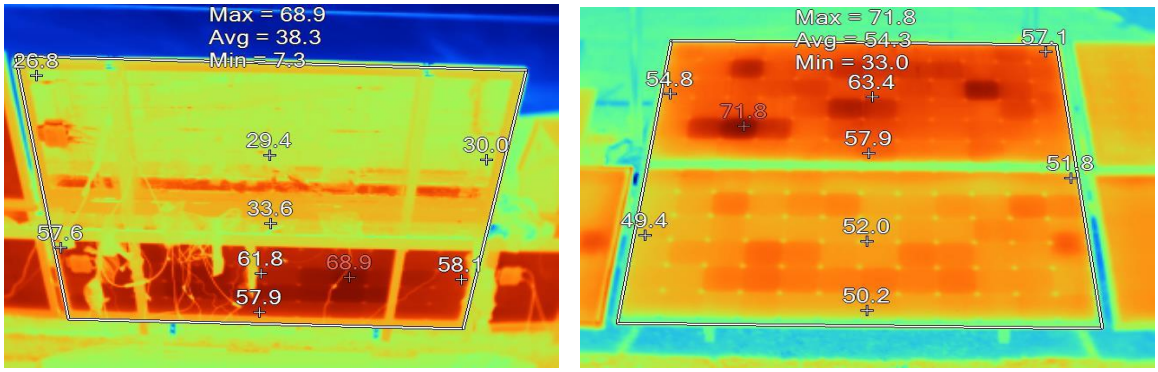

Figure 30: Front and Back Side of Aluminum Tape Back Sheet and Conventional Polymer White Back Sheet PV Module

Table 14: Temperatures Recorded on the Front and Back Side (a. Conventional Polymer White Back Sheet PV Module)

No insulation	**Center**	**Corner**	**Long Edge**	**Short Edge**
Module temperature	**54.79**	**58.77**	**56.52**	**54.97**
IR image: Back sheet	**61.9**	**57.6**	**57.9**	**58.1**
IR image: Front side	**52**	**51.8**	**50.2**	**49.4**
ΔT between front side and back sheet	**9.9**	**5.8**	**7.7**	**8.7**
ΔT between back sheet IR image and module temperature	**7.11**	**1.17**	**1.38**	**3.13**

Table 14: Temperatures Recorded on the Front and Back Side (b. Aluminum Tape Back Sheet PV Module)

Aluminum back sheet	**Center**	**Corner**	**Long Edge**	**Short Edge**
Module temperature	**74.08**	**71.7**	**70.1**	**68.45**
IR image: Back sheet	**29.4**	**26.8**	**33.6**	**30**
IR image: Front side	**63.4**	**57.1**	**54.8**	**57.9**
ΔT between front side and back sheet	**34**	**30.3**	**21.2**	**27.9**
ΔT between back sheet IR image and module temperature	**44.68**	**44.9**	**36.5**	**38.45**

Aluminum tape on the back sheet of the module can also act as a passive heat sink. Therefore comparing the results for module with frame insulation, it was projected that the module with aluminum back sheet will have lower operating temperatures and less temperature variability. But on the other, the aluminum tape on the back sheet blocked radiative loss and resulted in comparative increase in operating temperatures as well as temperature variations. It is can be said from the above values, that the temperature corresponding to the blockage of radiative loss is = 61.9 - 29.4 = 32.5^{o}C. This indicates that if we have good conductive encapsulant and back sheet, there is a potential to cool the module by as high as 32 ^{o}C. It is equivalent to the module will be operating at close to ambient temperature.

III. New Approach: Effect of Aluminum Tape on Black Back Sheet PV Module

To further study the effect of heat transfer using aluminum tape on back sheet, a PV module with black frame and back sheet was introduced in the setup. The preliminary experiment

only involved one thermocouple sensor on black back sheet only and one under aluminum tape.

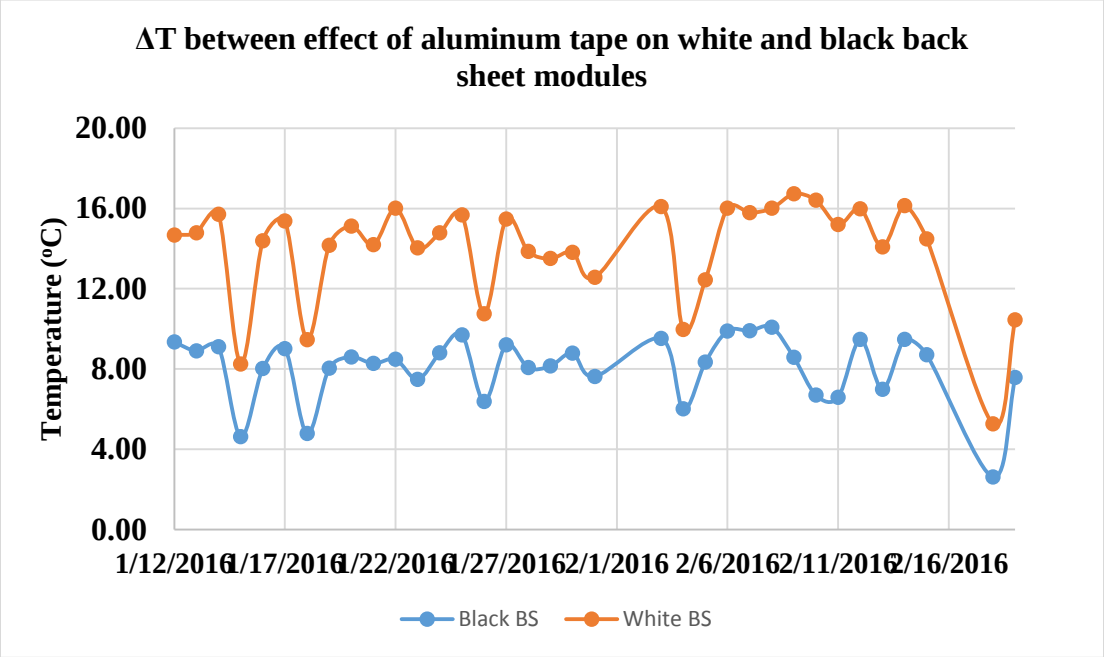

Figure 31: New Approach- Effect of Aluminum Tape on Black Back Sheet PV Module

The average temperature difference between the aluminum tape with black and white back sheet is about 6°C. The temperature difference on a clear sunny day is as high as 9.7°C. The aluminum tape on the white back sheet leads to blocking of radiative loss causing comparatively higher temperature variations. On the other hand, aluminum tape on black back sheet seems to cause lower radiative loss blockage due to presence of black back sheet (good emissivity properties).

Therefore, similar to the modules with white back sheet, the study of effect of aluminum tape on black back sheet using four thermocouples is recommended by including one more similar module with black back sheet on the setup.

1.5 CONCLUSIONS

This part investigated the effect of temperature variation between cells across a PV module on performance measurements through extended outdoor field monitoring. Based on this temperature monitoring of PV modules of four different technologies (c-Si, CdTe, CIGS and a-Si) and thermal insulation configurations and under different sets of conditions (electrical terminations and sky conditions), following conclusions can be outlined.

- The least deviation in the temperature coefficient values of about ±3 percent is observed in frame insulated modules c-Si PV module, followed by that in black-frame PV module of about ±6 percent.

- The least temperature variation of about 8% was observed in a c-Si PV technology module and the highest of about 14% was observed in CdTe PV module. However, the effect of this 8% and 14% variation of temperature between the cells in the module caused a variation of only about 2% and 4% in power, respectively.

- ANOVA, a statistical tool, identified the significant factors among all factors that are affecting temperature variations and they are: PV technology, thermal insulation configurations, electrical conditions and thermocouple. Typically, it was observed that the center cells of the module operate at higher temperature than the cells in the edges and corners of a module. The modules operate at higher temperatures at Voc than at Pmax, causing about 3-4^{o}C temperature variation on a clear sunny day. The least variation in temperatures was observed at Pmax conditions.

- On an average, the aluminum-covered white back sheet module experienced about 8^{o}C higher temperature than the conventional white back sheet module. Surprisingly, this

difference increased to as high as 15^{o}C at solar noon, caused mainly due to blocking of radiative thermal losses from the cells.

- Frame insulated and black frame PV modules are good and viable options to reduce thermal gradients between cells within a module on clear sunny day. Using the average of four temperature sensors for uninsulated crystalline silicon PV module would be the second best viable option to reduce thermal gradients between cells within a module for any irradiance level and sky condition.

PART 2: THERMAL UNIFORMITY MAPPING OF PV POWER PLANTS

2.1 INTRODUCTION

2.1.1 Background

The non-uniform temperature between the cells within a module, between the modules within a string, between the strings in an array and between arrays within a system could cause both the performance issues due to thermal-mismatch induced electrical-electrical mismatch, and the durability (lifetime) or reliability (failure) issues due to differential thermal stresses. The non-uniform temperature between the cells within a module and modules in a PV power plant could be caused due to frame-cooling effect in a module and due to local parameters like wind speed and direction or the site layout (e.g. closely packed arrays, wind breakers such as walls and trees) [14]. The performance issue is caused by the change in the voltage of individual cells due to variation of temperature at cell and module level and the corresponding effect on the negative temperature coefficients of voltage. The durability issues are caused by the higher degradation rates for power plant due to non-uniform temperature variation at plant level as well as the higher operating temperatures. Thermal mapping at module and plant level will help to understand the performance and reliability issues due to non-uniform temperature distribution present in the power plants.

2.1.2 Problem Statement

This study involves examining two photovoltaic (PV) power plants based on the operating temperature measurements obtained from various modules in these power plants as well as various cells in few of the modules in the power plants. The data obtained from this study proves that the assumption that modules and power plants operate at same cell/module is not correct. In addition, the data obtained in this study would be useful to understand the

temperature variation and study the various affecting factors for this variation. The purpose of this study is to evaluate temperature variation at module as well as plant level with respect to the weather parameters and power plant performance parameters and map these temperature variations over the power plant systems.

The scope of the work included analyzing the plant level non-uniform temperature distribution, mapping the instantaneous values for various solar windows (time periods) and statistically determining the factors affecting variation in the plant.

2.2 LITERATURE REVIEW

2.2.1 Spatial Temperature Variations in PV Arrays

The prevalent spatial temperature variations present in the modules of PV array was discussed in part 1A of this study. M.G Farr et. al. through their study concluded array temperature variations for two different climate sites to be as high as 10 C during time between 10am and 3pm [15]. D.L. King et. al. in their discussed the difficulties in calculating temperature coefficients for an array due to presence of temperature anomalies and also suggested some methods [4]. The temperature coefficients for an array can also be estimated using regression analysis method [16].

2.2.2 System Description

A study was conducted to analyze failure and degradation modes of PV modules for two power plants, Site 4a and Site 4c in hot dry climate [17], [18].The modules of Site 4a power plant were initially installed on a single axis tracking system in Gilbert, Arizona for the first seven years and have been operating at their current location in Mesa, Arizona for the last nine years at fixed horizontal tilt and the modules of Site 4c power plant have been located in Mesa, Arizona since past seven years. Both the sites (Gilbert, Mesa) experience hot-dry desert climate. The Site 4a power plant has 1512 modules (named as AZ3) provides 113.4 kW DC output and Site 4c power plant has 1,280 modules (named as AZ5) which provide 243 kW DC output. It also reported a module degradation rate of 1.25% and 0.96% respectively under maximum power operating conditions. A soiling loss of 11% (two times higher loss) for Site4a as compared to the Site4c based modules (5.5% soiling loss) for the

same site (urban surrounding) was reported. Table 15 provides an overview of the two systems.

Table 15: System Description

System	Tilt/ orientation	DC rating (kW)	AC rating (kW)	Years fielded	Year Commissioned	Model Type	Number of modules
Site 4a	Horizontal fixed	113.4	100	19	1997	AZ3	1512
Site 4c	One-axis tracking	243.2	204.3	7	2009	AZ5	1280

This part further investigates two power plants using temperature measurements recorded from 20 different locations at each system. This study is approached to attempt mapping the temperature distributions observed in these two systems.

2.3 METHODOLOGY

2.3.1 System Layout

Each site have HOBO temperature data loggers installed in the five directions (one each in NW direction, NE direction, SW direction, SE direction and Centre most module). The strings of the modules in these power plants are not closely packed. The layout of these plants along with the location of HOBOs is shown in Figure 34. AZ3 plant has no wind barriers around it. But on the other hand, AZ5 plant is to the south of AZ3 and is about 4 feet lower, so some wind obstruction exists. There is also a 15 foot high wall on the south side of AZ5 plant and this wall is about 30 feet away from the array leading to some wind obstructions.

Four thermocouples (HOBOs) are attached within each of these five modules. The location of these four thermocouples is shown in Figure 2. These HOBOs as shown in Figure 35 are setup to monitor the temperatures every five minutes.

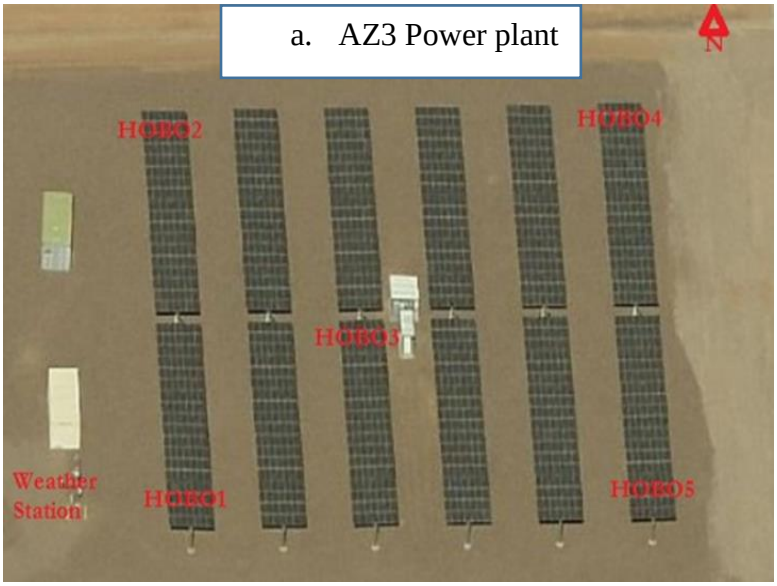

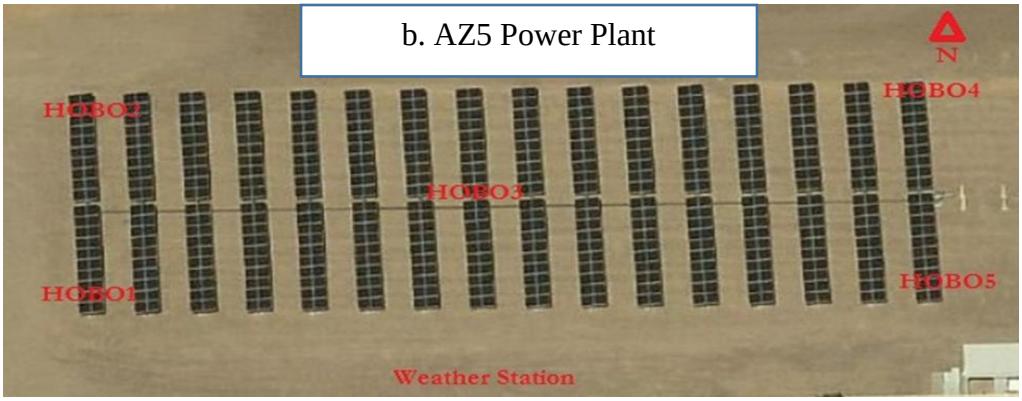

Figure 32: Thermal Mapping at Five Locations for AZ3 and AZ5 power plant

Figure 33: Location of Each HOBO under an Array

2.3.2 MATLAB Program Flowchart

The data recorded by HOBO data loggers was retrieved by using HOBOware software and converted into Excel file type. MATLAB was used to code a program to interpolate and map the temperature values on a grid representative of PV module or a power plant. Figure 34 represents a flowchart discussing various steps involved in MATLAB program code.

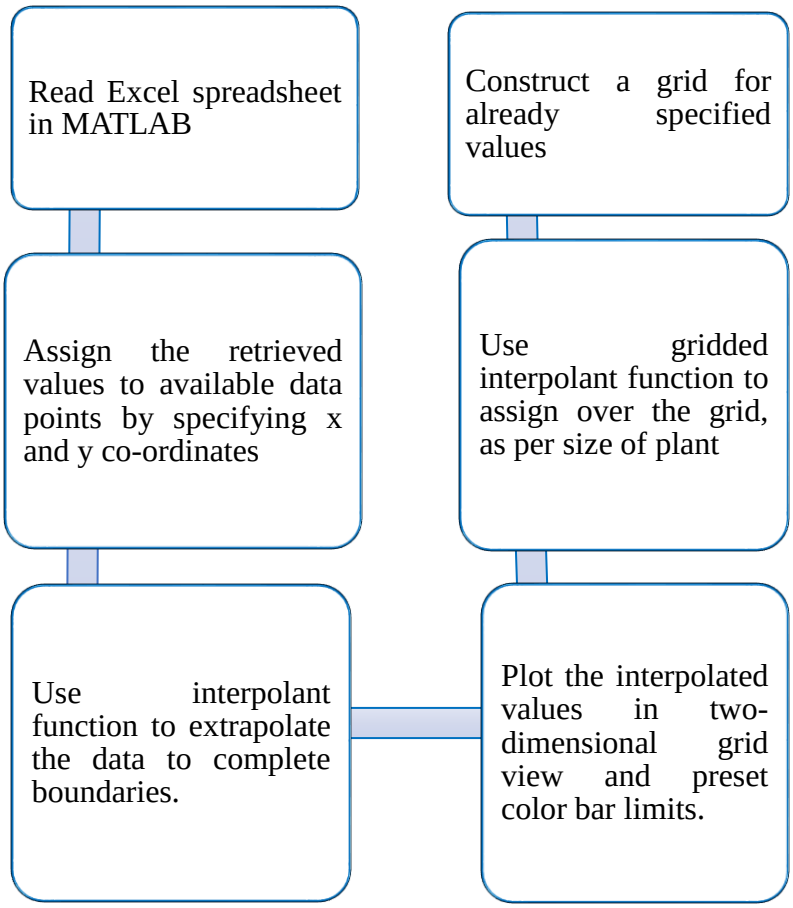

Figure 34: Program Flowchart Diagram

The following steps describe in detail various processes used in MATLAB program to map the temperature values on a two dimensional grid.

1. Input required for the program code is temperature data retrieved from Excel spreadsheet.
2. The next step would be to modify data as required. For example calculating mean of the values from 9am to 5pm solar window time period.
3. Define the x and y co-ordinates for which the temperature data is available.
4. Using these co-ordinates and data values interpolate and extrapolate the data with the help of interpolant function.

5. Use the nine point data values using the above generated data to assign them to a closed grid structure.
6. Use a grid function to create rectangular grid in ND space with specified dimensions. (This depends on size of the module/ power plant)
7. Use gridded interpolant function to interpolate the temperature values over the constructed grid.
8. Again use a grid function to further recreate the same grid with small intervals. (This depends on the size of cells in a module/modules in a power plant)
9. A pseudo color plot function was used to assign the interpolated values (created on the grid) to a rectangular array of cells determined by colors.
10. A function was used to preset the limits based on common minimum and maximum values.
11. The same above steps can be repeated for other dataset. The only variables are temperature dataset, temperature locations and dimensions of the grid.

2.4 RESULTS AND DISCUSSIONS

This part analyzes the temperature variation data recorded from 04/17/2015 to 09/30/2015 across the modules of a fixed-tilt and a one-axis tracking PV power plants.

I. Plant Level Temperature Distribution

The data for AZ3 and AZ5 PV power plants, which was recorded at five minute interval, was averaged and analyzed for a day, from 9am to 5pm and around solar noon (12 to 1 pm). The solar noon time period was selected from 12pm to 1 pm, since the solar noon time values for the days when the data was collected, fall in the range between 12 and 1 pm. Data collected from 9am-5pm excludes high AOI and large air mass effects in early morning and late afternoon.

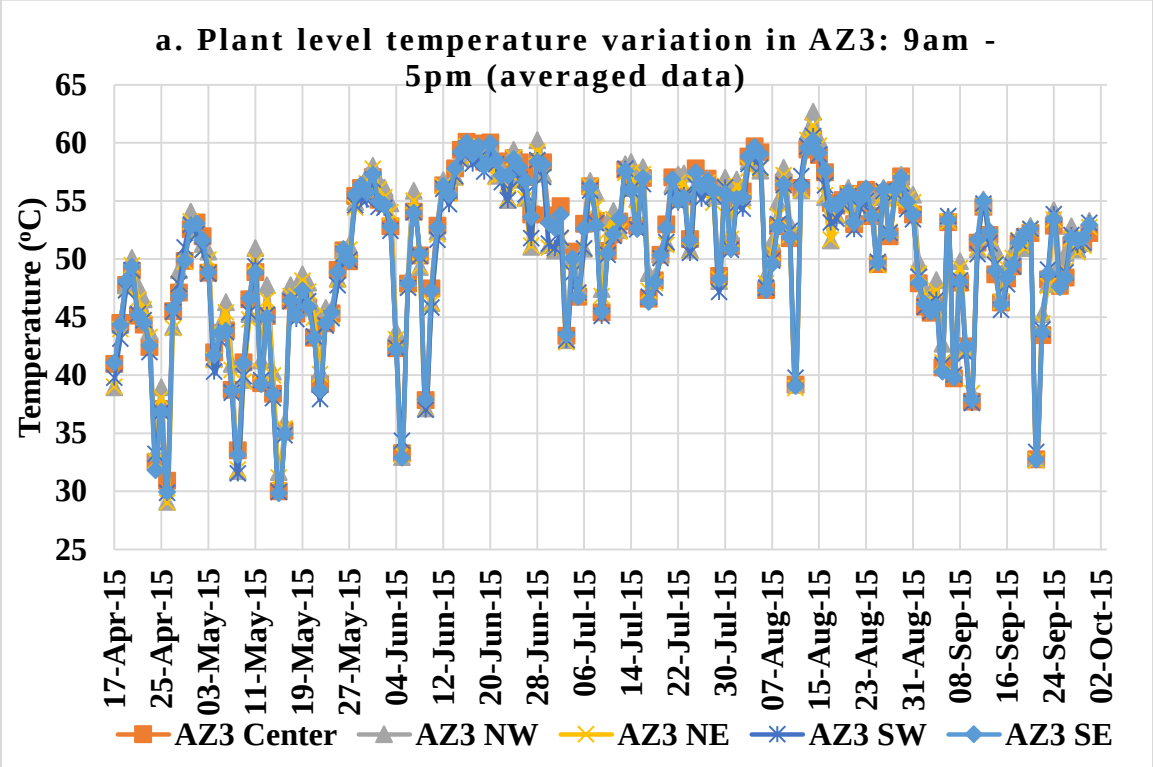

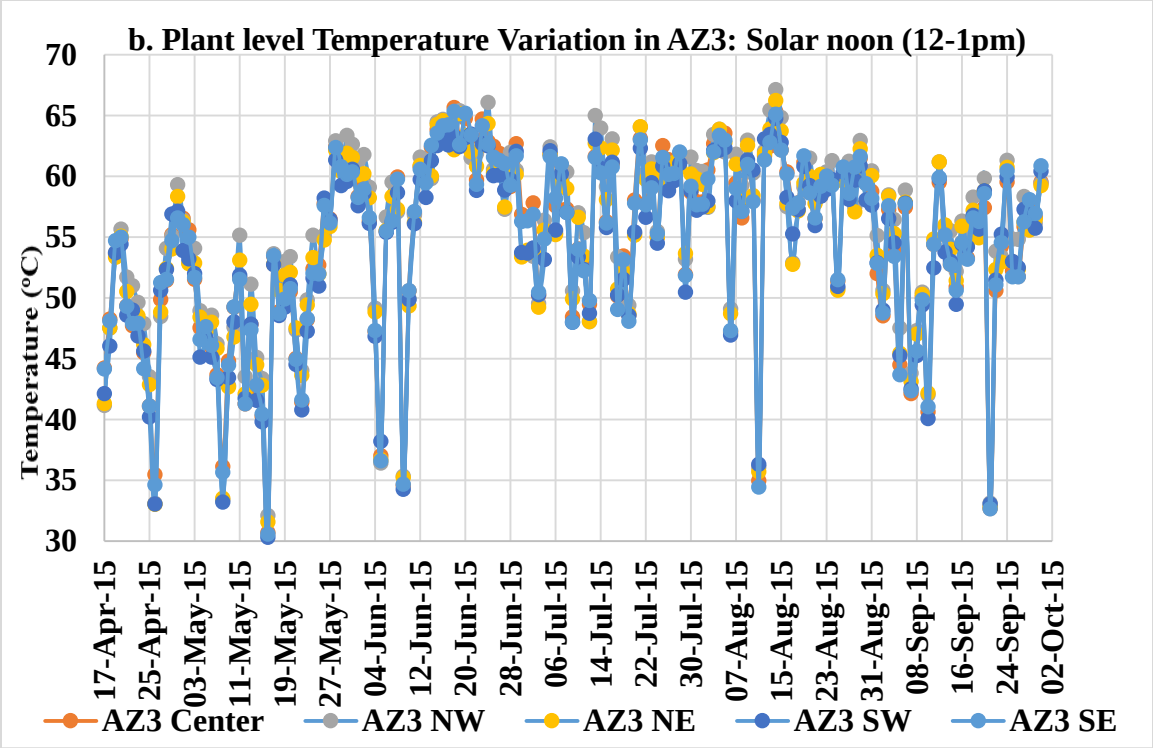

Figure 35: Plant Level Temperature Variation in AZ3

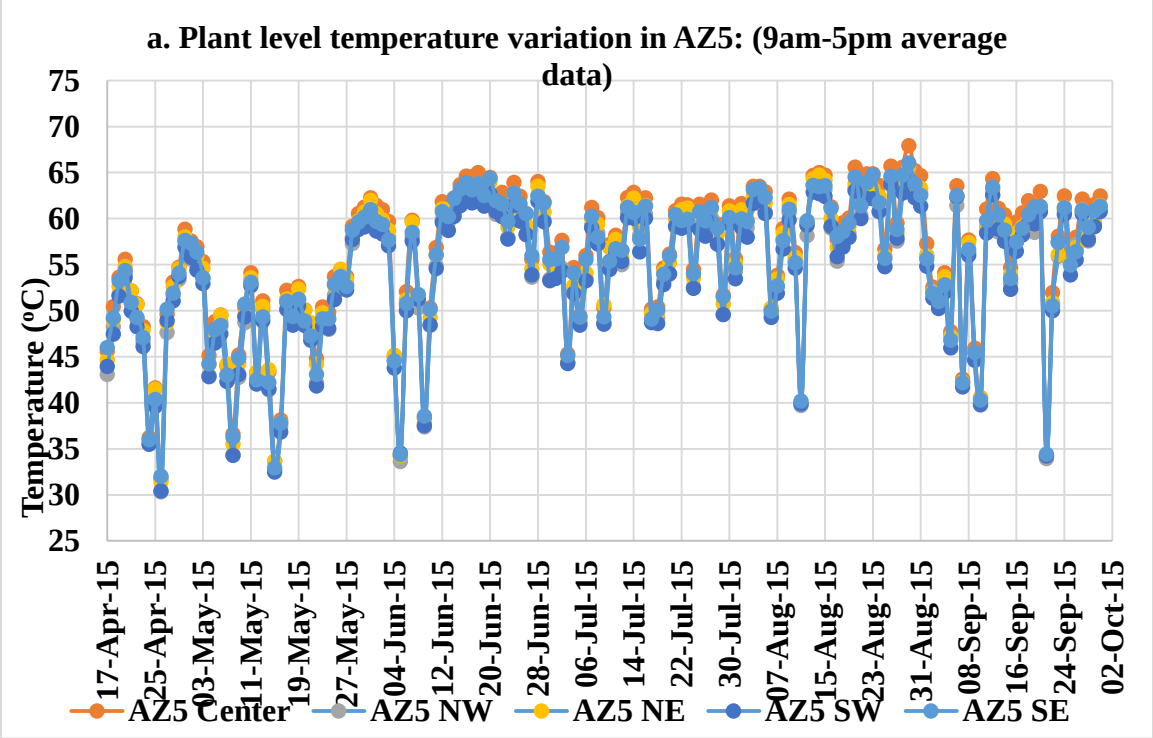

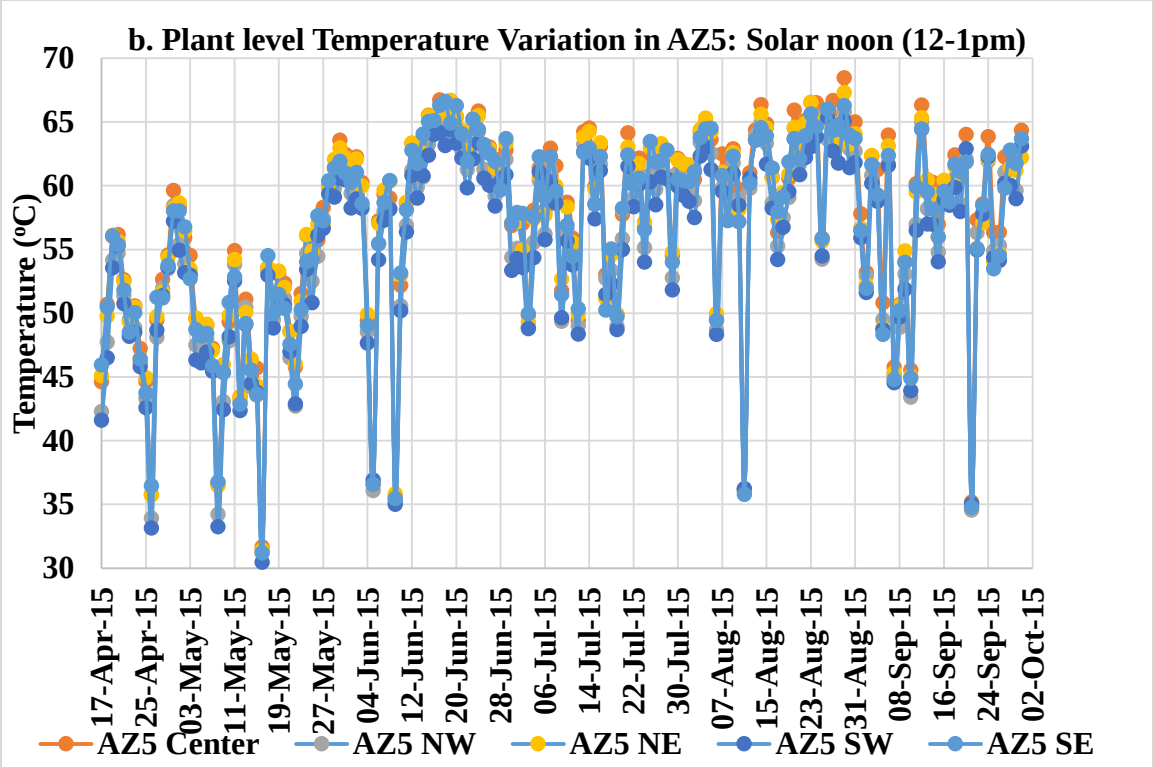

Figure 36: Plant Level Temperature Variation in AZ5

Figures 35 and 36 show the plant level temperature variation trend at different time periods (i.e. 9am-5pm, 12-1pm) within the five modules placed in AZ3 and AZ5 power plants respectively. The plant level temperature variations averaged throughout the day are included in Appendix B. It is observed that for AZ3, a fixed-tilt PV system, typically the module in north-west direction is the hottest while the module in south-west direction is the coolest amongst the five modules. On the other hand, for AZ5, a one-axis tracking system, typically the module in the center of the plant is the hottest, while the module in S direction is the coolest. This trend is mainly dominated by the influence of wind direction. In order to study this trend further, thermal mapping was performed on the PV modules of AZ3 and AZ5 as well as the complete power plants on a clear sunny day around solar noon time period from 12 to 1 pm. The average irradiance during the PSH time frame from 10am to 2pm is 971W/m^2 and the average wind speed of 3m/s.

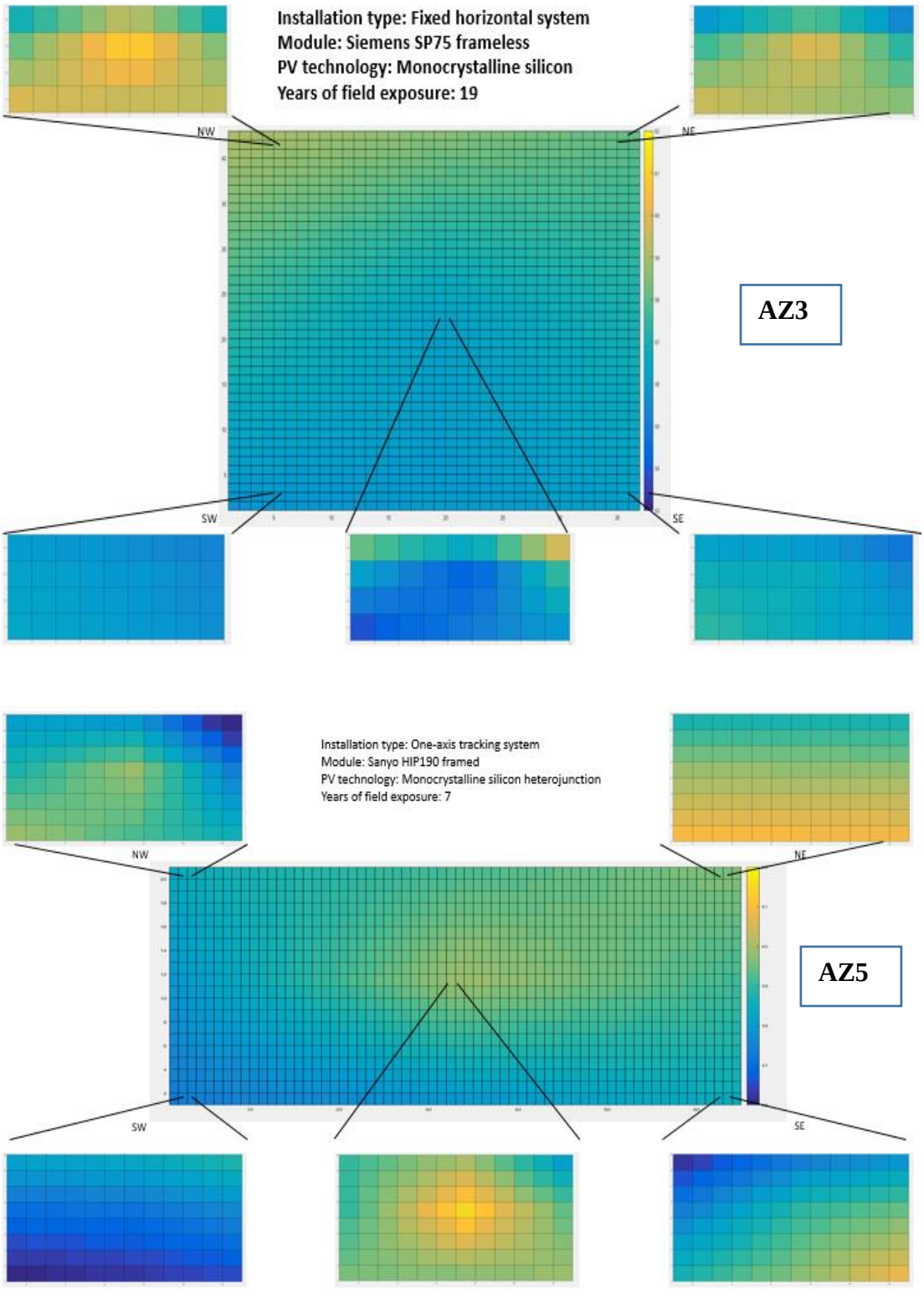

Figure 37: Thermal Mapping around Solar Noon in AZ3 and AZ5 power plant

The temperature variation at plant level was denoted in the form of distribution of heat/thermal energy. This distribution of the plant level temperatures was compared for AZ3 and AZ5. The higher temperatures were obtained for AZ5 PV power plant for every time frame (9am-5pm, solar noon 12-1pm and daily average). Hence the percent difference was calculated with respect to the base value being 100% for AZ3 power plant as shown in Table 16. The highest increase of 9% in the temperature distribution values of AZ5 was observed for 9am-5pm time frame.

Table 16: Plant Level Temperature Data for AZ3 and AZ5

	9am-5pm data	Daily average data	Solar noon data
AZ3	100%	100%	100%
AZ5	109%	107%	103%

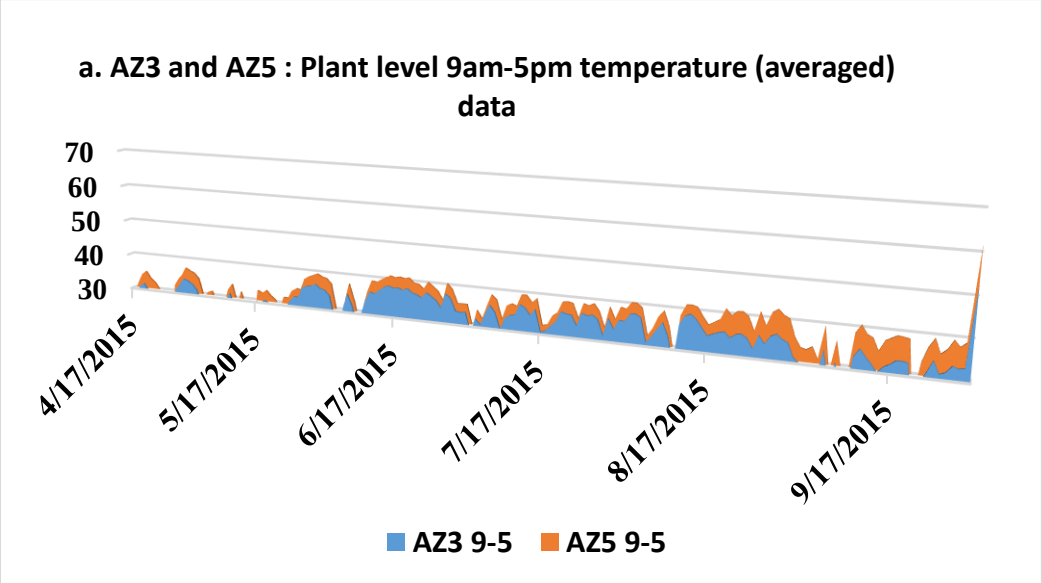

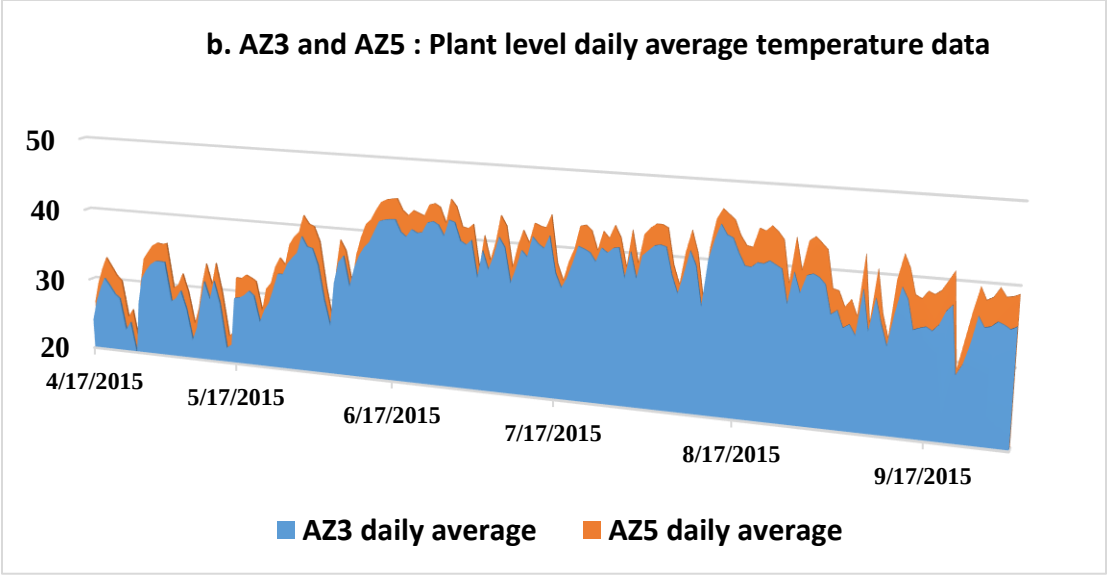

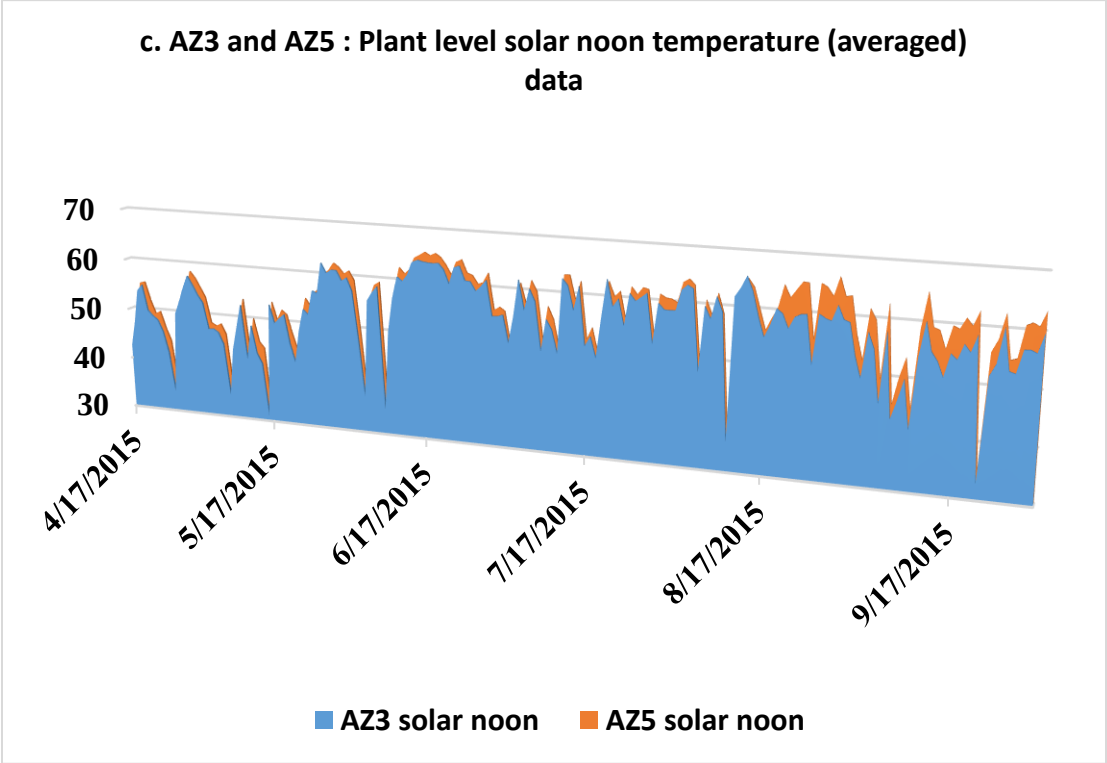

Figure 38: Plant Level Temperature Data for AZ3 and AZ5

II. Module Level Temperature Variation from 9am-5pm

Since the highest variation was observed during 9am-5pm time frame, the average temperatures for all the four cells within all the five modules from 9am to 5pm were compared for AZ3 and AZ5. The cell temperature difference within a module for AZ3/ fixed-tilt system was in the range of 0.8-3ºC with an average operating temperature of 50.4ºC. On the other hand, the cell temperature difference within a module for AZ5/one-axis system was in the range of 0.8-4ºC with an average operating temperature of 0.8-4ºC.

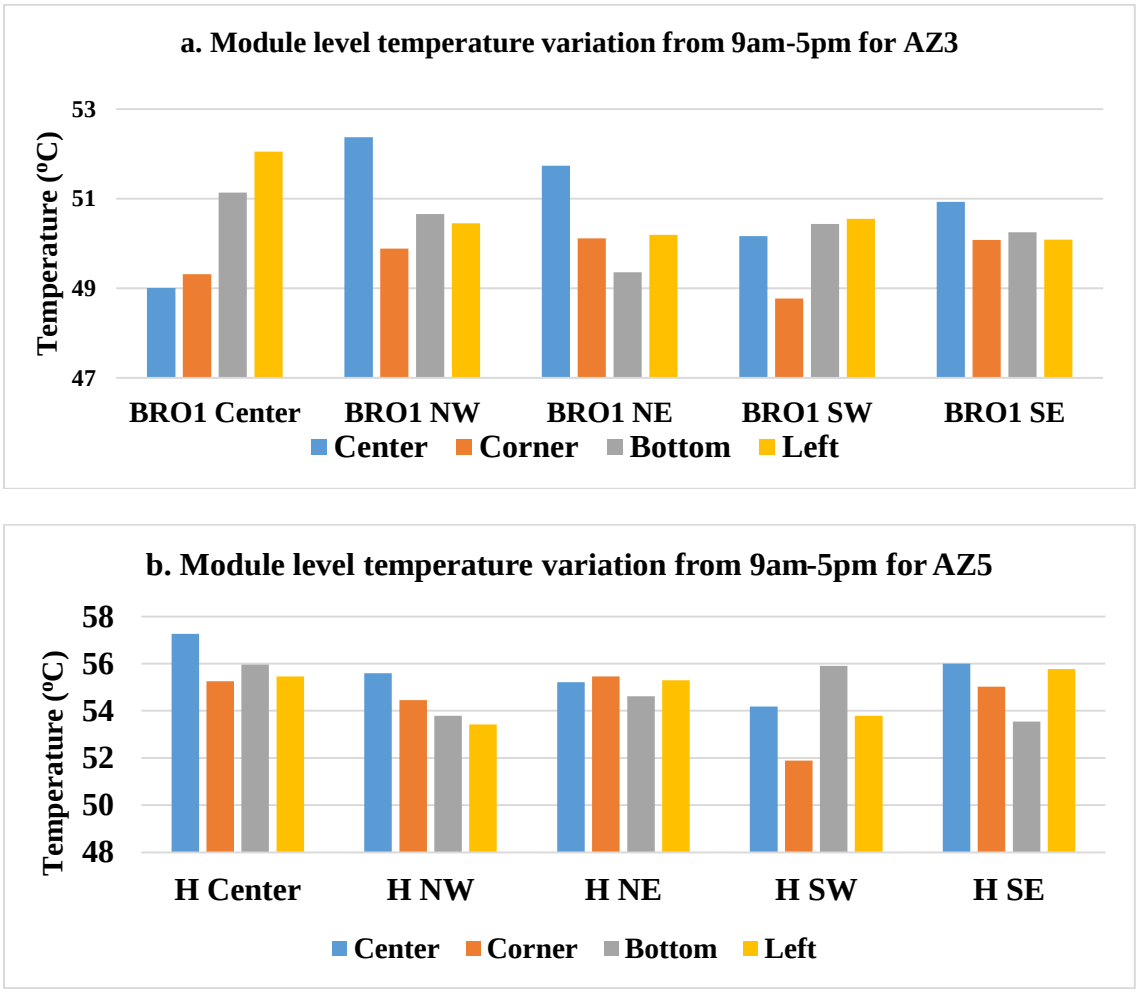

Figure 39: Module Level Temperature Variation from 9am-5pm for AZ3 and AZ5 power plant

The temperature variation within the modules of the plant was denoted in the form of distribution of heat/thermal energy and compared for AZ3 and AZ5. The least value of temperatures was observed in the modules in the south-west direction of both AZ3 and AZ5 power plants for the time frame from 9am to 5pm. Hence the percent difference was calculated with respect to the base value being 100% for the module in south-west direction of both the power plant as shown in Table 17. The highest increase of 9% in the temperature distribution values of AZ5 was observed for 9am-5pm time frame.

Table 17: Average Module Temperature for Five Modules Each in AZ3 and AZ5 Plant

Module location	AZ5	AZ3
Module at the center	104%	101%
Module in NW direction	101%	102%
Module in NE module	102%	101%
Module in SW direction	100%	100%
Module in SE direction	102%	101%

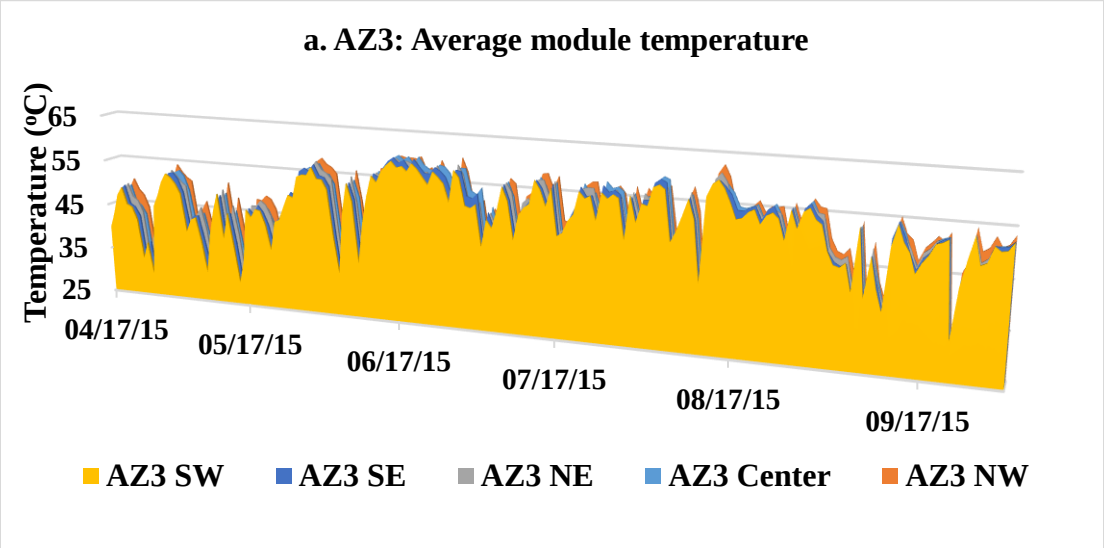

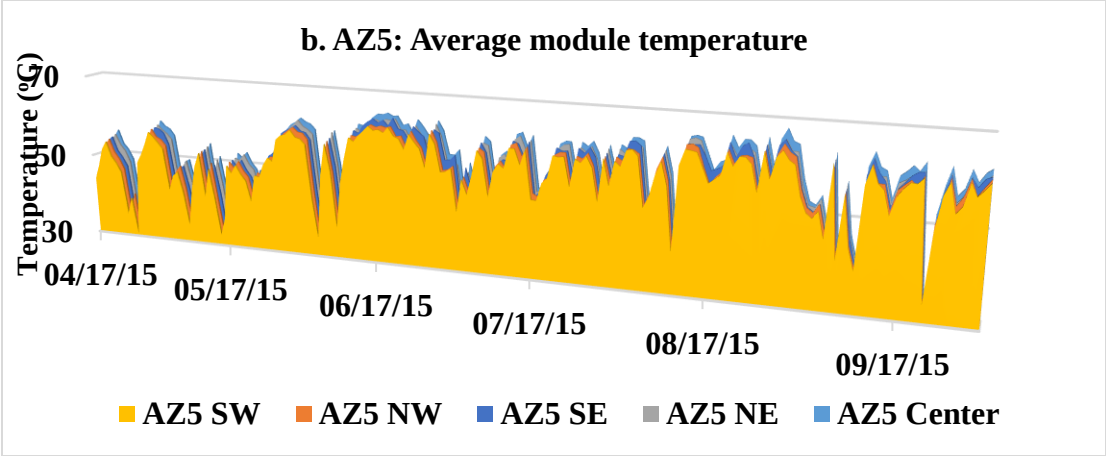

Figure 40: Average Module Temperature for Five Modules in Power Plant for AZ3 and AZ5 power plant

The difference between the highest and lowest cell temperature is highest at solar noon ($\Delta T_{avg} = 2.72$), followed by 9am-5pm averaged values ($\Delta T_{avg} = 2.1$), and least for the daily average data ($\Delta T_{avg} = 0.69$). This states that at highest temperatures the variation in the temperatures within the module is highest.

The difference between the highest and lowest cell temperature is highest for 9am-5pm averaged values ($\Delta T_{avg} = 2.276$), followed by solar noon ($\Delta T_{avg} = 2.15$) and least for the daily average data ($\Delta T_{avg} = 0.85$). This states that at highest temperatures the variation in the temperatures within the module is not the highest. This may be because the modules of AZ5 are constantly facing the sun at solar noon, when they obtain maximum insolation while facing the sun, the back of the modules experience convection flow. Therefore the maximum temperatures are not obtained during the solar noon. The graphs along with the values denoting the cell location with highest temperature are added in Appendix C.

III. Temperature Variation on a Clear Sunny and Cloudy Day

The temperature variation within the modules of the plant was denoted in the form of distribution of heat/thermal energy. This distribution of the cell level temperatures was compared for the center-most module of AZ3 and AZ5 power plants.

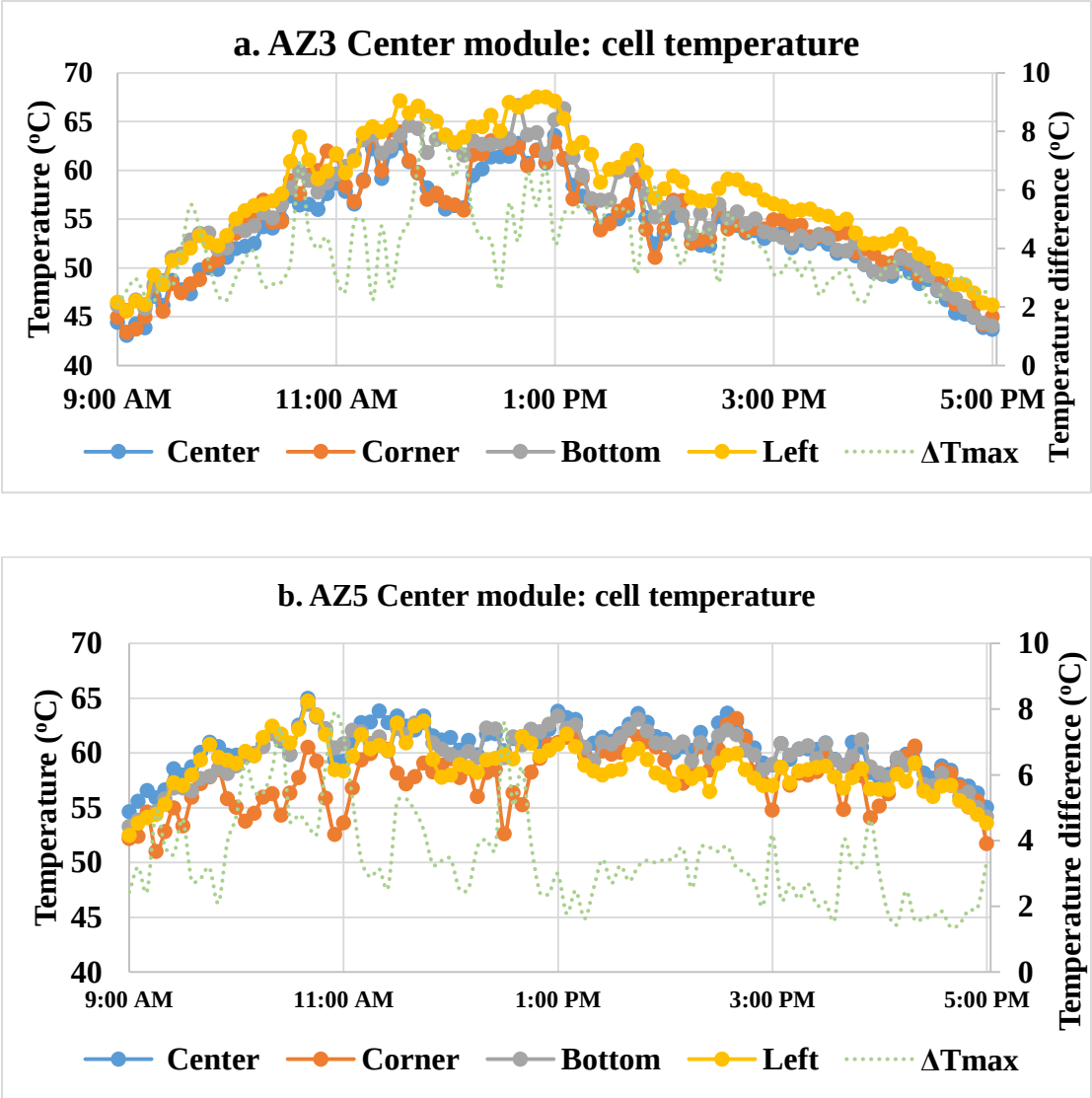

Figure 41: Cell Temperature Variation within the Center-Most Module on a Clear Sunny Day for AZ3 and AZ5 power plant

Table 18: Cell Temperature Variation within the Center-Most Module of AZ3 and AZ5 Power Plant (a. Clear Sunny Day)

	Center	Corner	Bottom	Left
AZ3	100%	101%	104%	107%
AZ5	105%	100%	104%	102%

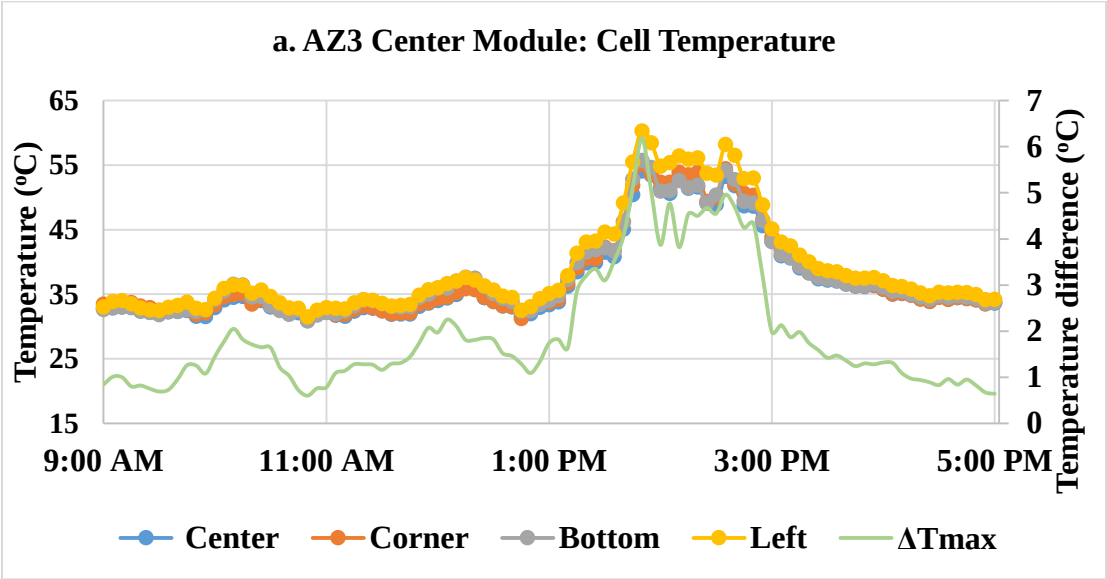

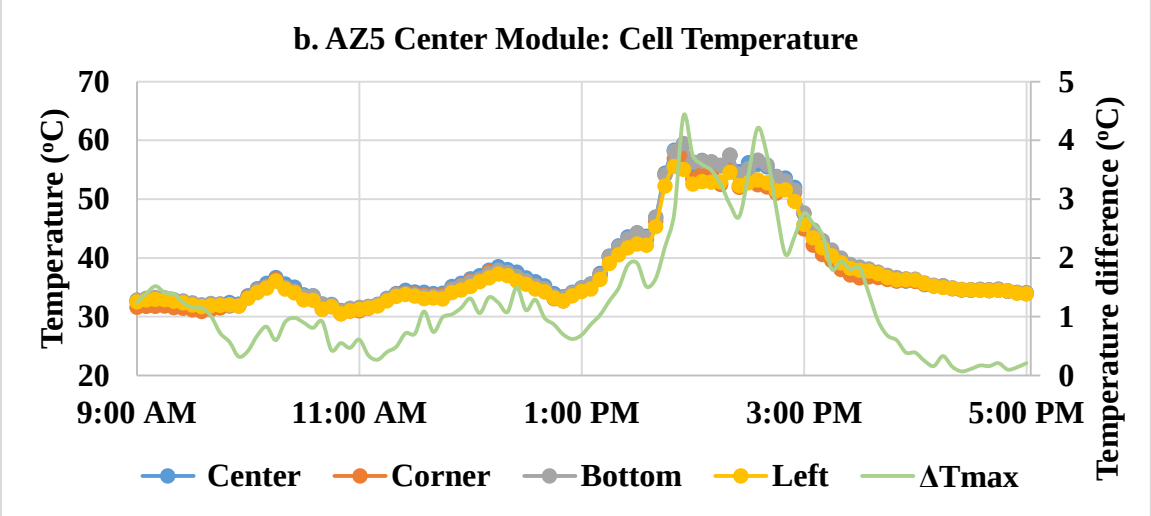

Figure 42: Cell Temperature Variation within the Center-Most Module on a Cloudy Day for AZ3 and AZ5 power plant

Table 18: Cell Temperature Variation within the Center-Most Module of AZ3 and AZ5 Power Plant (b. Cloudy Day)

	Center	Corner	Bottom	Left
AZ3	**100%**	**101%**	**102%**	**105%**
AZ5	**102%**	**100%**	**102%**	**100%**

The least value of temperatures was observed in the cells in the center of the module for AZ3 and in the corner-most cell of the module for AZ5 power plant. Hence the percent difference was calculated with respect to this base value being 100% for the cells in the center-most module of both the power plant as shown in Table 18.a and b. The highest increase of 7% in the left-most cell of the center-most module of AZ3 was observed on a clear sunny day from time frame of 9am-5pm. On the other hand, the highest increase of 5% in the left-most cell of the center-most module of AZ3 was observed on a cloudy day from the time frame of 9am-5pm.

IV. ANOVA Design

The ANOVA of effect model was performed to study significance of various factors and their interactions on the module temperature. The three factors (type of power plant, module locations and thermocouple locations) with different levels were studied on a clear sunny and cloudy day through ANOVA. Average irradiance recorded from 9am-5pm on a clear sunny day was 940 W/m^2 and on the cloudy day was 329 W/m^2. Average wind speed recorded on clear sunny day was 2m/s while that on a cloudy day was 4m/s.

ANOVA Design for AZ3 and AZ5 PV Plants on a Clear Sunny Day

Table 19: Analysis of Variance (ANOVA) Design Summary for AZ3 and AZ5 PV Plants on a Clear Sunny Day

Factor	Type	Levels	Values
Plant	fixed	2	1, 3
Module locations	random	5	1, 2, 3, 4, 5
Thermocouple	fixed	4	1, 2, 3, 4

Source	DF	SS	MS	F	P
Plant type	1	8.29	8.29	5.37	0.034
Module locations	4	18.216	4.554	2.95	0.05
Thermocouple	3	17.629	5.876	3.09	0.068
Plant*Thermocouple	3	1.686	0.562	0.36	0.78
Module locations*Thermocouple	12	22.827	1.902	1.23	0.342
Error	16	24.708	1.544		
Total	39	93.358			

Analysis of variance (ANOVA) design for AZ3 and AZ5 on cloudy day

Table 19.b: Analysis of Variance (ANOVA) Design Summary for AZ3 and AZ5 PV Plants on a Cloudy Day

Factor	Type	Levels	Values
Plant	fixed	2	1, 3
Module locations	random	5	1, 2, 3, 4, 5
Thermocouple	fixed	4	1, 2, 3, 4

Source	DF	SS	MS	F	P
Plant type	1	0.7317	0.7317	3.67	0.073
Module locations	4	2.7835	0.6959	3.49	0.031
Thermocouple	3	0.8957	0.2986	1.38	0.296
Plant*Thermocouple	3	0.6015	0.2005	1.01	0.416
Module locations*Thermocouple	12	2.5975	0.2165	1.09	0.43
Error	16	3.1907	0.1994		
Total	39	10.8007			

The response values are normally distributed and residual values fit had satisfactory pattern. The p value for plant type and module locations is less than 0.05 on a clear sunny day but on a cloudy day p-value only for module locations is less than 0.05.Therefore, plant type and module location has a significant effect on temperature variation on a sunny day. On the other hand, only module location has a significant effect on temperature variation on a cloudy day.

2.5 CONCLUSIONS

In this part, the data [04/17/2015 to 09/30/2015] for two power plants (fixed-tilt and one-axis) each with temperature monitoring of four modules in the corner and one in the center was analyzed to determine the temperature variation between cells within a module and between modules within a plant. This section provides a list of conclusions on the influence of temperature variation across the cells in a module and across the modules in a power plant.

- In AZ3 plant (fixed-horizontal), the module placed in NW corner has typically experienced higher temperatures; on the other hand, in AZ5 plant (1-axis), the module placed in the center of the plant has typically experienced higher temperatures.

- AZ3 (fixed-horizontal) power plant is operating at an average temperature of 50.4^{o}C. On the other hand, AZ5 (1-axis) is operating at a higher average temperature of 54.9^{o}C. Therefore, lower lifetime is expected for AZ5 power plant due to higher operating temperature. Within a module, the difference between cell temperatures is between 0.8 and 3.0^{o}C for fixed tilt and 0.8 and 4.0^{o}C for 1-axis modules.

- On a clear sunny day, the statistical analysis using ANOVA indicates that both module location and the plant type (fixed vs. 1-axis) play significant roles in temperature distribution. However, on a cloudy day, only module location within a plant plays a significant role in temperature distribution.

PART 3: THERMAL MODEL COEFFICIENTS OF PV MODULES

3.1 INTRODUCTION

3.1.1 Background

As discussed in part 1 of this thesis, module temperature depends on lots of factors including weather parameters like irradiance, wind speed, wind direction, ambient temperature as well as module parameters like module installation, module configuration, etc. Therefore testing and determining PV module temperature is complex by influence of these interactive factors. Thermal models help to effectively quantify these important factors and estimate the module operating temperature by considering their influence. These models help in reducing inherent uncertainty associated with module temperature estimation based on environmental or module parameters and in turn improve the accuracy of performance model [12]. These accurately determined models in turn play an important role to project annual energy production while designing a photovoltaic system [19].

3.1.2 Problem statement

Various thermal models are being put forward in the PV industry. This study discusses about the various thermal models used prominently by the PV industry. PVsyst is a widely used PC software package for simulation and data analysis of complete PV systems. It defines the thermal loss (for modules) by using thermal model parameters of U_c and U_v which is further used in predicting the energy output. PVsyst proposes U_c and U_v values for three different configurations: wind-dependent and wind-independent weather data for modules on free-standing arrays as well as for modules on fully insulated arrays. This study determines the thermal model coefficients (U_c and U_v) similar to the parameters determined

in PVsyst for modules mounted on free-standing arrays of various PV technologies experiencing hot-desert climate conditions by statistically correlating year-long data.

3.2 LITERATURE REVIEW

This part reviews various thermal models proposed on theoretical heat transfer approach or the empirical equations based on real time data. The various thermal models are as follows:

3.2.1 Simple Model

A simple thermal model relates the difference between the solar cell operating temperature and ambient temperature to be just about proportional to irradiance as shown in Equation 3 [20]. This model is specifically applicable for open rack system and low wind speed conditions and with no specific construction type differentiated.

$$T_{cell} = T_{amb} + (0.03 * Irr) \quad \text{Equation 3}$$

where T_{cell}= solar cell temperature (^oC)

T_{amb}= ambient temperature (^oC)

Irr= solar irradiance in (W/m^2)

3.2.2 NOCT (Nominal Operating Cell Temperature)

Nominal operating cell temperature per IEC 61215 standard is considered as one of the thermal performance parameters for PV design. The standard described a thermal model to calculate operating temperature as shown in Equation 4 [21].

$$T_{cell} = T_{amb} + (T_{NOCT} - 20) \times \frac{Irr}{800} \quad \text{Equation 4}$$

where T_{cell}= module temperature (^oC)

T_{amb}= ambient temperature (^oC)

T_{NOCT}= Nominal operating cell temperature (^oC)

Irr= solar irradiance (W/m^2)

Ty W. Neises et. al. developed a thermal model to analyze NOCT guidelines and suggested for multiple correction factor charts under different testing conditions [22]. A draft replacement for NOCT titled Nominal Module Operating Temperature is also under review and a study was performed by NREL in 2011 to evaluate difference in NMOT and NOCT procedures [23]. The primary difference between the two is, NOCT restricts the wind speed range and introduces a correction factor; on the other hand NMOT allows wide wind speed range but introduces a modelling approach with wind speed.

3.2.3 Sandia Module Temperature Model

Sandia National Laboratories developed a simple empirically based thermal model for expected module operating temperature and is been verified for an accuracy of about $\pm 5^{o}C$ [12].The empirically determined coefficients used in the model are influenced by module construction, mounting construction and location and height of wind speed measurements. Table 20 represents the empirical coefficients used in Sandia thermal model as shown in Equation 5.

$$T_m = E. \times \{e^{\,a+b\times WS}\} + T_a \qquad \text{Equation 5}$$

where T_m = back-surface PV module temperature (°C).

T_a = ambient air temperature (°C)

E = solar irradiance incident measured on surface of the module (W/m^2)

WS = wind speed measured at standard 10-m height (m/s)

a = Empirically-determined coefficient establishing the upper limit for module temperature at low wind speeds and high solar irradiance

b = Empirically-determined coefficient establishing the rate at which module temperature drops as wind speed increases

Table 20: Empirical coefficients used in Sandia thermal model

Module Type	Mount	a	b	ΔT (°C)
Glass/cell/glass	Open rack	-3.47	-.0594	3
Glass/cell/glass	Close roof mount	-2.98	-.0471	1
Glass/cell/polymer sheet	Open rack	-3.56	-.0750	3
Glass/cell/polymer sheet	Insulated back	-2.81	-.0455	0
Polymer/thin-film/steel	Open rack	-3.58	-.113	3
22X Linear Concentrator	Tracker	-3.23	-.130	13

Sandia also studied the back surface temperature to be different from cell temperature and deduced a relationship between both based on one dimensional thermal heat conduction as given by Equation 6.

$$T_c = T_m + \frac{EPOA}{Eo} \times \Delta T$$

Equation 6

where Tc= cell temperature

T_m= module temperature

E_{POA}= plane of array irradiance measured on module (W/m^2)

E= reference irradiance on module (1000 W/m

ΔT= Temperature difference measured between the cell and the module back surface at an irradiance level of 1000 W/m^2 (typically 2 to 3 °C for flat-plate modules on open-rack rack system)

3.2.4 Faiman Module Temperature Model

David Faiman measured POA irradiance, wind speed, ambient temperature and module temperature for seven different module types (with glass front surface and Tedlar back surface) to fit the data for heat loss coefficient values U_o and U_1 [11]. The module temperature model involving simple heat transfer phenomenon was represented as shown in Equation 7.

$$T_m = T_a + \frac{H}{UO + U1 \times v} \quad \text{Equation 7}$$

where T_m= module temperature (°C)

T_a= ambient air temperature (°C)

H= irradiance incident on the plane of the module or array (W/m^2)

Uo= constant heat transfer component (W/m^2 K)

U_1= convective heat transfer component (W/m^3.s.K)

v= wind speed (m/s)

3.2.5 PVsyst thermal model

PVsyst (a PV performance modelling software) implemented a cell temperature model based on Faiman module temperature model as shown in Equation 8 [24].

$$T_c = T_a + \frac{\alpha. \times EPOA \times (1 - \eta m)}{UO + U1 \times WS}$$

Equation 8

where T_c= cell temperature (°C)

T_a= ambient air temperature (°C)

α= adsorption coefficient of PV module (PVsyst default value = 0.9)

E_{POA}= irradiance incident on the plane of the module or array (W/m^2)

η_m = PV module efficiency (PVsyst default value = 0.1)

Uo= constant heat transfer component (W/m^2 K)

U_1= convective heat transfer component (W/m^3.s.K)

WS= wind speed (m/s)

PVsyst states that thermal behavior is characterized by a thermal loss factor and designed a U value split into two components: constant U_c component and wind proportional U_v component as shown in Equation 9 [25].

$$U = U_c + U_v \times v \qquad \text{Equation 9}$$

The following default U_c and U_v values were proposed for different installations.

As per an older version and accounting wind velocity influence on data, the default value proposed was:

U_c = 25 W/m²·K, U_v = 1.2 W/m²·K / m/s

With the wind velocity is not present in the data, PVsyst considers the wind-dependent contribution into U_c value by assuming an average speed of 1.5 m/s. Since version 4.0, for free-standing array, the default value is

U_c = 29 W/m²·K, U_v = 0 W/m²·K / m/s

The default value was halved in case of fully insulated arrays (with an assumption of average wind speed of 3.3 m/s) and was proposed to be:

U_c = 15 W/m²·K, U_v = 0 W/m²·K / m/s

3.2.6 ASU-PRL Thermal Model

Based on field monitored long-term real time data a mathematical model was developed to predict the module temperature using number of input parameter [26]. The model was

proposed to be fairly independent of site location and technology type. Equation 10 shows a simple linear regression between module temperature and the ambient conditions.

$$T_{module}\ (^{o}C) = 0.943 \times T_{ambient} + 0.028 \times Irradiance - 1.528 \times WindSpd + 4.3 \quad \text{Equation 10}$$

The coefficient for $T_{ambient}$ was evaluated to be less than 1, since the modules experience lower temperatures than the ambient during night-time due to radiation cooling effect. Moreover this model can be closely related to the PVsyst thermal model ($U = U_c + U_v$) considering coefficient for $T_{ambient}$ to be roughly as 1 and combining wind speed parameter and the constant together as a single term.

This study involves the determination of thermal loss factor constant (U_c and U_v) similar to the components used in PVsyst using a year-long data (2001) for modules of various PV technologies for hot desert specific climate conditions.

3.3 METHODOLOGY

3.3.1 System Description

A study was performed at the ASUE Williams Campus, Mesa, Arizona during the years 2000-2002, where PV modules from different manufacturers were installed for long-term field monitoring [26]. 14 PV modules under test as shown in Figure 13 included different PV technologies namely Monocrystalline Si, Polycrystalline Si, EFG-Polycrystalline Si, Amorphous Si, Copper Indium Diselenide and Cadmium Telluride. Table 21 provides information of various PV modules installed along with respective cell technology, front and back sheet material specifications and their manufacturers. The modules were installed on an open rack system at the site, which experiences hot desert climate conditions. The modules were operating near to their Pmax (maximum power) operating conditions with the help of power resistors. Weather station was installed near the rack systems to monitor wind speed and direction, ambient temperature and latitude-tilt global irradiance as shown in Figure 49. All the modules were installed on south facing, latitude-tilt racks with thermocouples attached on the substrate of each module as shown in Figure 48. The data was stored for every 5 minute interval in the data acquisition system and retrieved regularly. The quality of the collected data was verified periodically by normalized module temperature raise from ambient at 800 W/m^2 irradiance. Average wind speed measured throughout the year was 1.8 m/s and average ambient temperature was 23.6 ^oC. Average measured POA (annual) during the solar window time period was 837 W/m^2.

Figure 43: Modules Installed at PTL Site during 2000-2002 [26]

Table 21: Various PV modules Installed on the Rack (2001) [26]

Item	Cell Technology	Model Number	Serial Number	Manufacturer
1	Amorphous Si	US32	4464	USSC
2	Amorphous Si	US32	4463	USSC
3	Monocrystalline Si	SM55	2764	Siemens
4	Monocrystalline Si	SM55	2821	Siemens
5	Copper indium diselenide	ST40	2997	Siemens
6	Copper indium diselenide	ST40	975	Siemens
7	EFG-Polycrystalline Si	50ATF	4143	ASEA
8	EFG-Polycrystalline Si	50ATF	4149	ASEA
9	Polycrystalline Si	MSX60	2921	Solarex
10	Polycrystalline Si	MSX60	2907	Solarex
11	Cadmium telluride	N/A	1936	SCI
12	Cadmium telluride	N/A	1944	SCI
13	Amorphous Si	Millennium	3142	Solarex
14	Amorphous Si	Millennium	143	Solarex

3.3.2 Flowchart for Statistical Correlation

Excel and Minitab was used extensively to correlate the year-long data on a monthly and seasonal basis. The methodology as shown in Figure 44 was used to correlate the data and deduce U_c and U_v coefficients.

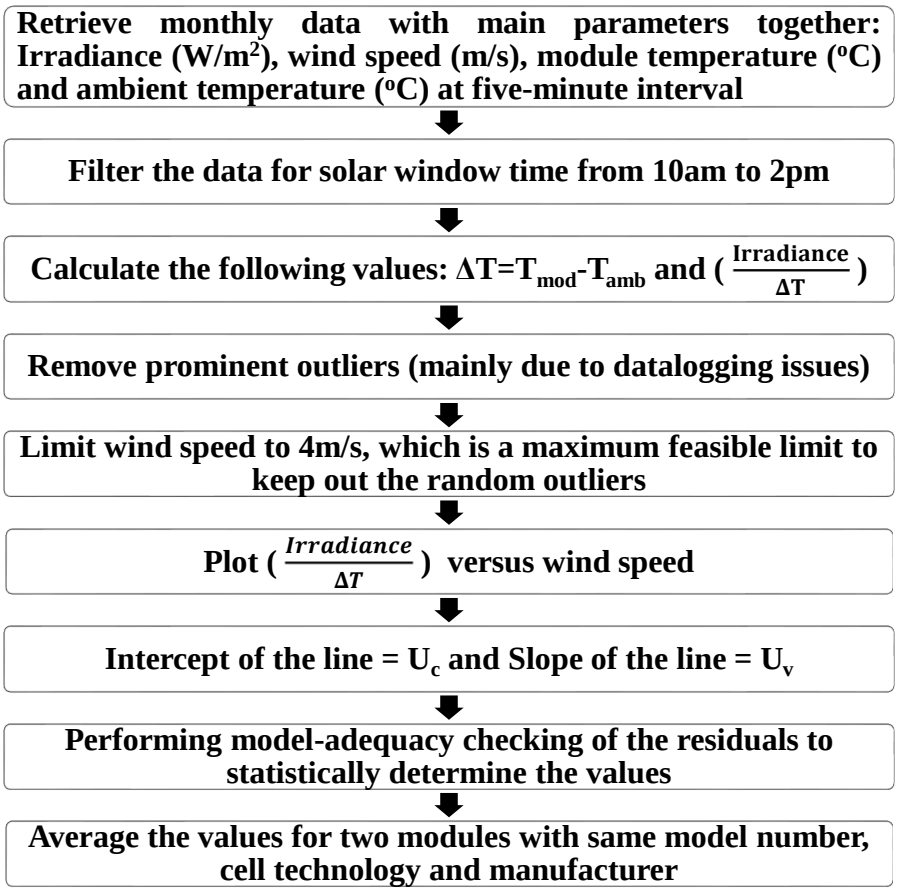

Figure 44: Flow Chart to determine Uc and Uv Coefficients

The various steps involved in determining the thermal coefficients are as follows:

1. First, monthly data having five minute interval was retrieved consisting of following main parameters: Solar irradiance (W/m^2), wind speed (m/s), module and ambient temperature (^oC).
2. The data was then filtered for solar window time period from 10 am to 2pm.
3. The following values were calculated using the retrieved parameters: $\Delta T = T_{mod} - T_{amb}$ and $\frac{\text{Irradiance}}{\Delta T}$

4. The data was checked to remove any prominent outliers present due to data logging issue.
5. Then $\frac{\text{Irradiance}}{\Delta T}$ was plotted against wind speed.
6. The trend line obtained in Excel represents the equation where intercept of the line is U_c and slope of the line is U_v.
7. Step 1: Plot the $\frac{\text{Irradiance}}{\Delta T}$ versus wind speed for all the technologies for the five-interval data.
8. Since it is difficult to perform model-adequacy checking of the residuals for these data points, other approach was used: U_c and U_v values for each month using five-minute interval data.
9. Another approach was used to determine an annual U_c and U_v value for each technology: one-hour data from 10am-2pm each day.
10. Step 2: Performed model-adequacy checking for the new data points and removed large unusual observations, obtained 95% confidence intervals and statistically determined the U_c and U_v values.
11. Verified non-dependence of the different technology and module on the values.
12. Averaged the values for two modules with same model, cell technology and manufacturer.

3.4 RESULTS AND DISCUSSIONS

This part presents the thermal loss parameters as thermal model coefficients for various PV technologies.

1. Determination of U_c and U_v Values using Five-Minute Interval Year-Long Data

As mentioned in section 3.3.2, Step 1 of the method mentioned in the flowchart was followed to fit the line and obtain U_c and U_v parameters for the available data of 1 year. In order to understand the outliers present in the data as shown in Figure 45, model adequacy checking was performed on these values. Even after limiting the y-axis co-ordinate to 120 W/m^2K, the R-square accuracy of the trend was 0.50. Moreover, due to presence of more than 10,000 data points, the residual plot as obtained in Figure 46 for a year-long data was difficult to analyze. Therefore, the data for each month for each technology was separately analyzed.

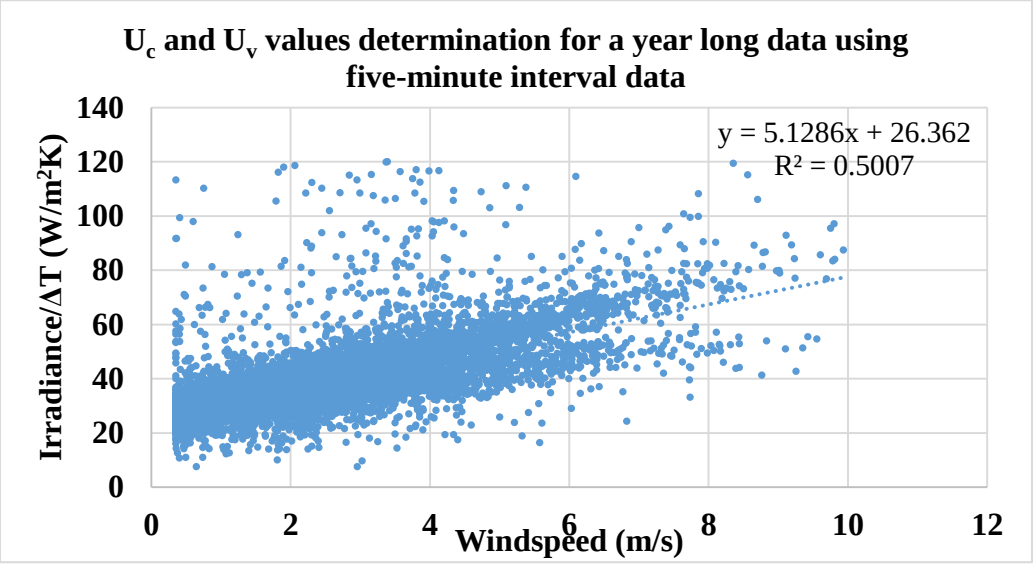

Figure 45: Determination of U_c and U_v Values for a Year-Long Data (2001) at Five-Minute Interval for Polycrystalline Silicon PV Technology

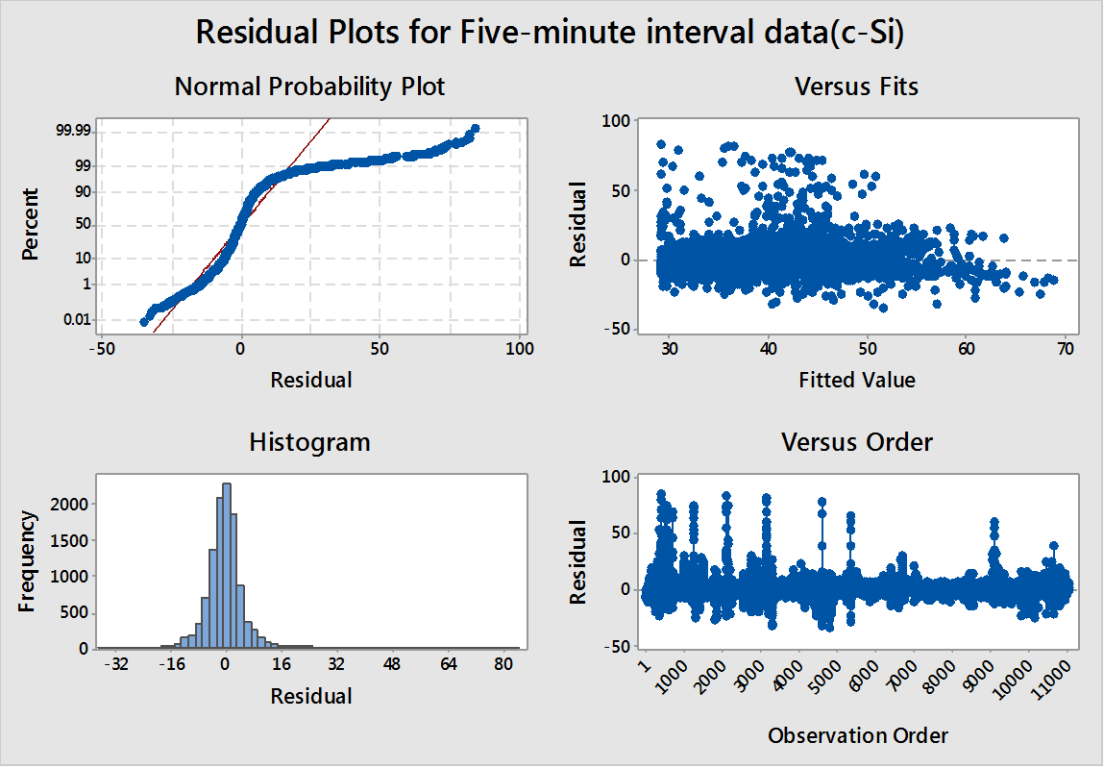

Figure 46: Residual plots for five-minute interval data for monocrystalline Silicon PV technology

2. Determination of U_c and U_v Values using Five Minute Interval Data for Each Month

The five-minute interval data available for about 1 year time period was analyzed for each month to obtain U_c and U_v values for each technology for each month and understand its trend. The summer and spring season tend to have higher U_c values as compared to winter and fall seasons. On the other hand, during the summer-spring season, U_v values are lower. Figure 47 represents U_c and U_v values for each month for polycrystalline PV technology. The graphs for all the technologies are included in Appendix D. Figure 48 represents U_c and U_v values for all PV technologies for one year data.

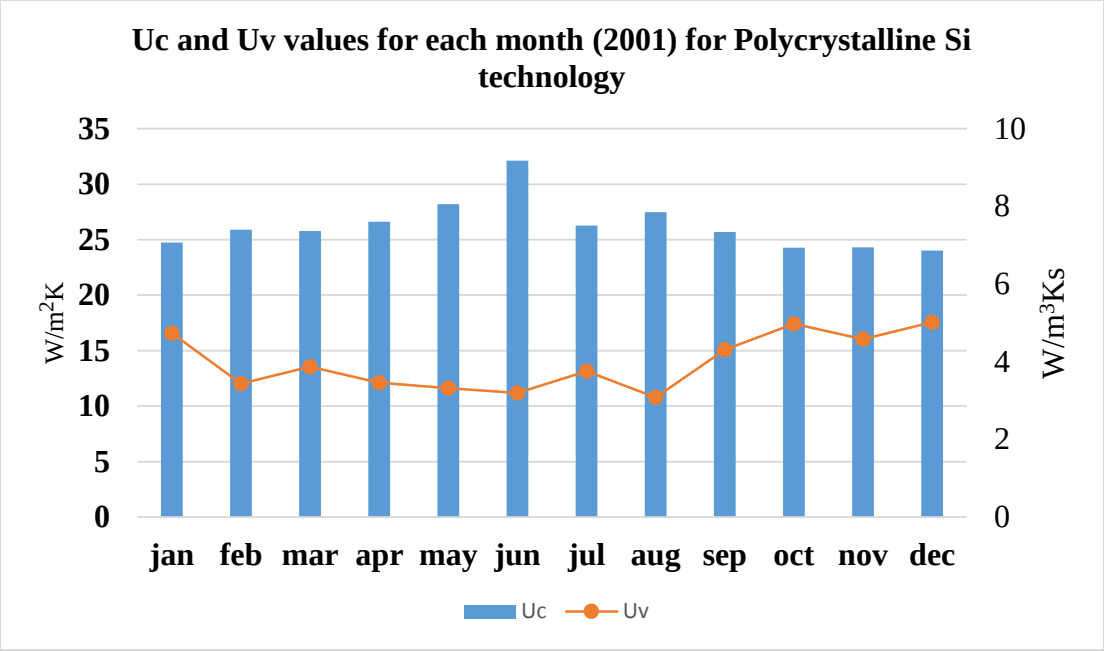

Figure 47: U_c and U_v Values for Each Month (2001) for Polycrystalline PV Technology

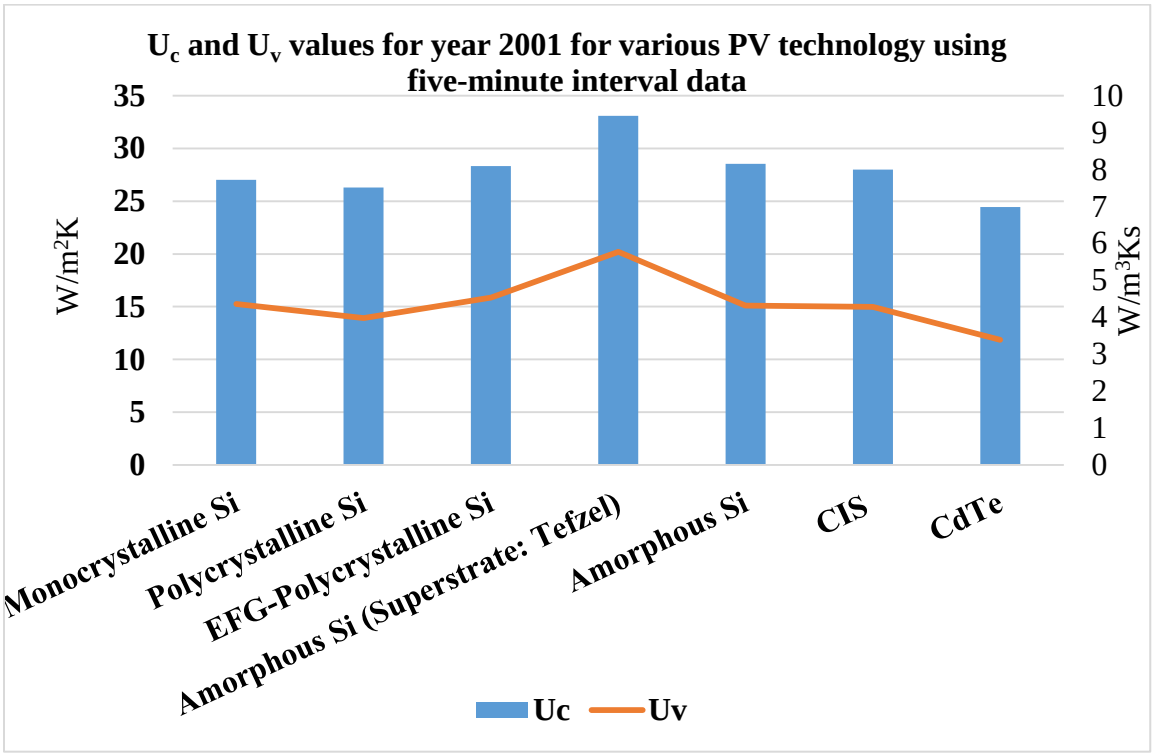

Figure 48: U_c and U_v values of Each Month Averaged for Year-2001 for Various PV Technology

In order to statistically correlate the U_c and U_v values and determine the residuals, model adequacy check was performed. For most of the plots, the residuals seem to follow satisfactory pattern and the data had normal distribution. But the normal probability plot was lightly tailed, or in other words, did not have normal distribution about the mean. Therefore another approach was followed.

3. Determination of Uc and Uv Values using Five-Minute Interval Data

In order to statistically determine the residuals for model-adequacy checking and to remove the outliers causing tailed distribution, the five-minute interval data was converted to hourly-data for full one year. The regression fit was obtained for a year-long data at one hour interval for polycrystalline Silicon PV technology with an R-square value of 0.6866 as shown in Figure 49.

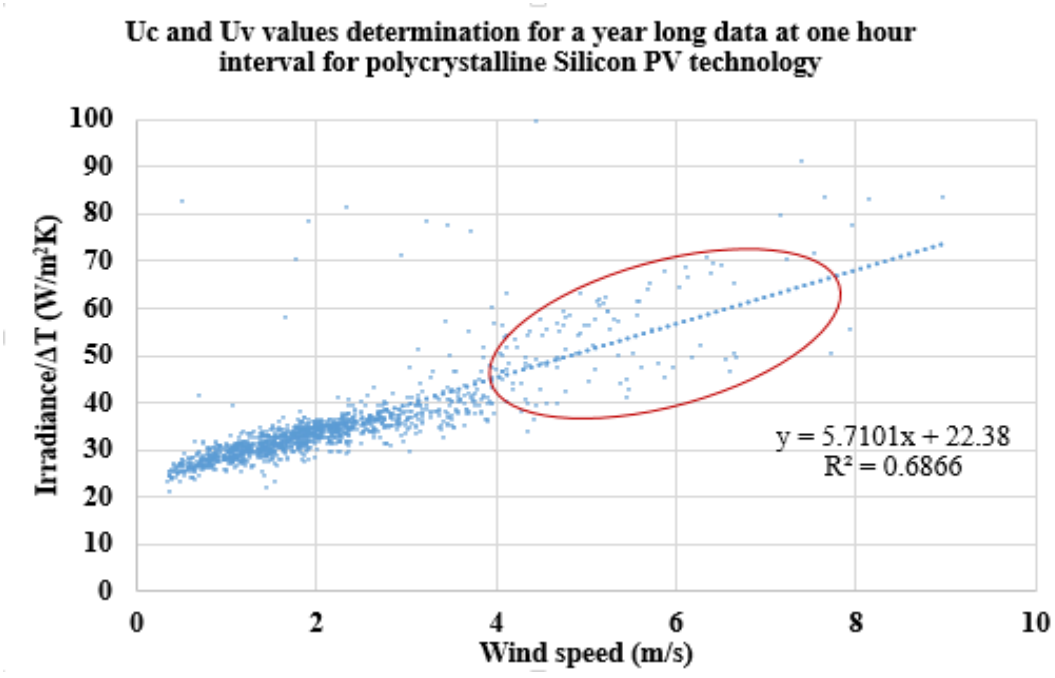

Figure 49: Determination of U_c and U_v Values for a Year-Long Data at One Hour Interval

A random pattern of data points was observed in Figure 49 for wind speed values of 4m/s and above. From feasibility point of view, wind speed values greater than 4m/s affects the energy yield of PV modules and might affect its performance. Therefore in this method, wind speed was limited to 4m/s. Figure 50 represents the U_c and U_v values for a yearlong data at one hour interval for polycrystalline Silicon PV technology after limiting the wind speed to 4m/s. The R-square value seems to be improved to 0.77.

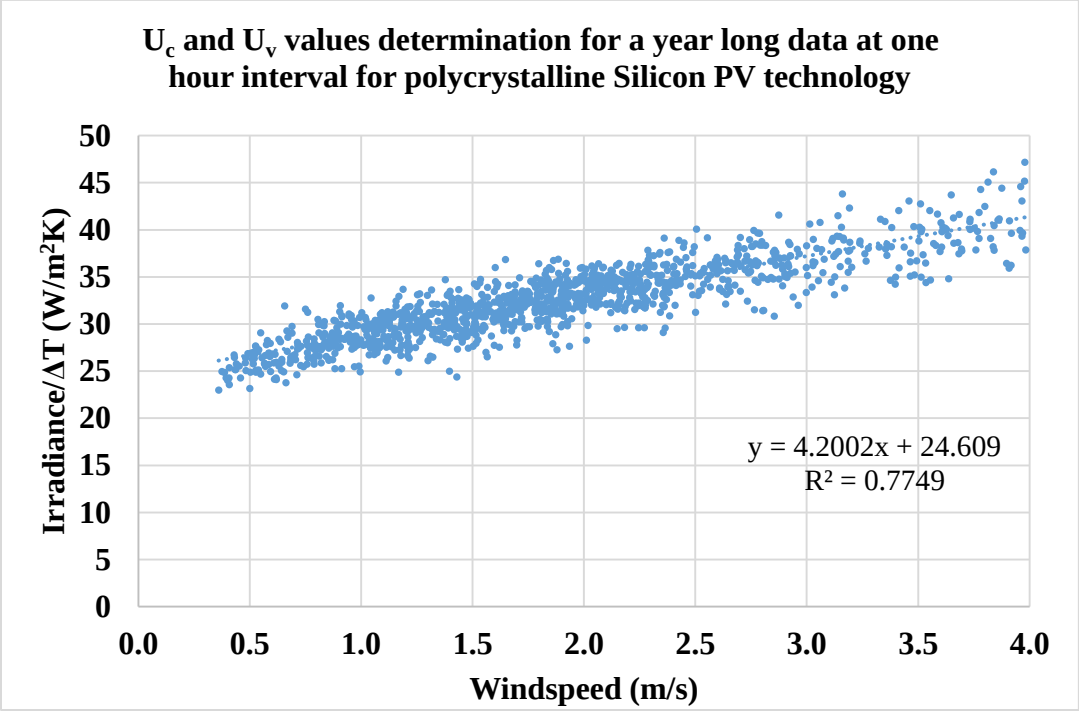

Figure 50: Determination of U_c and U_v Values for a Year-Long Data at One Hour Interval

These data points were further analyzed for model-adequacy checking. The unusual observations were removed and four-way analysis of residuals was performed. Figure 51 represents a sample model-adequacy check plots for PV technology module.

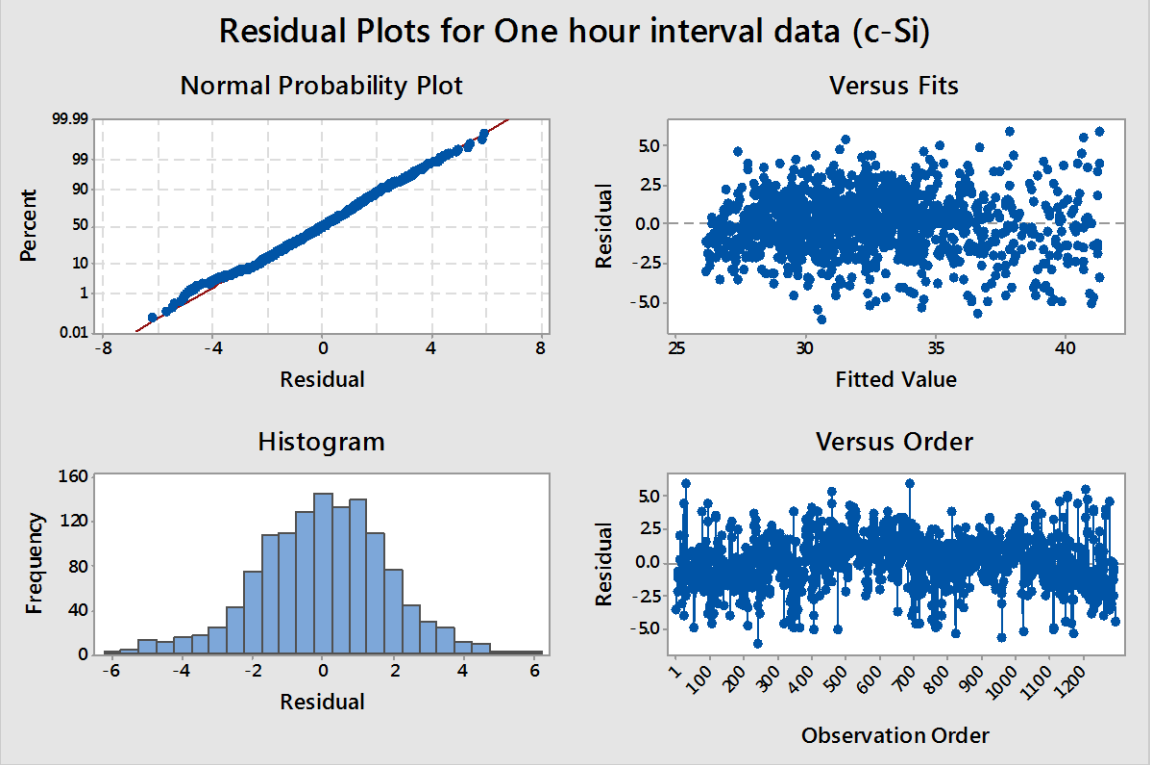

Figure 51: Residual Plots for a Year-Long Data (2001) at One Hour Interval for c-Si (polycrystalline Silicon) PV technology

It can be seen that the fitted values follow satisfactory pattern, the mean is normally distributed about zero and follows normal distribution. Therefore, the plots satisfy model adequacy check and the determination of U_c and U_v is statistically correlated. Moreover, the 95% confidence interval was obtained for each of the parameters.

Figure 52a and b represents the U_c and U_v values for all replicates of c-Si and thin film PV technology modules respectively.

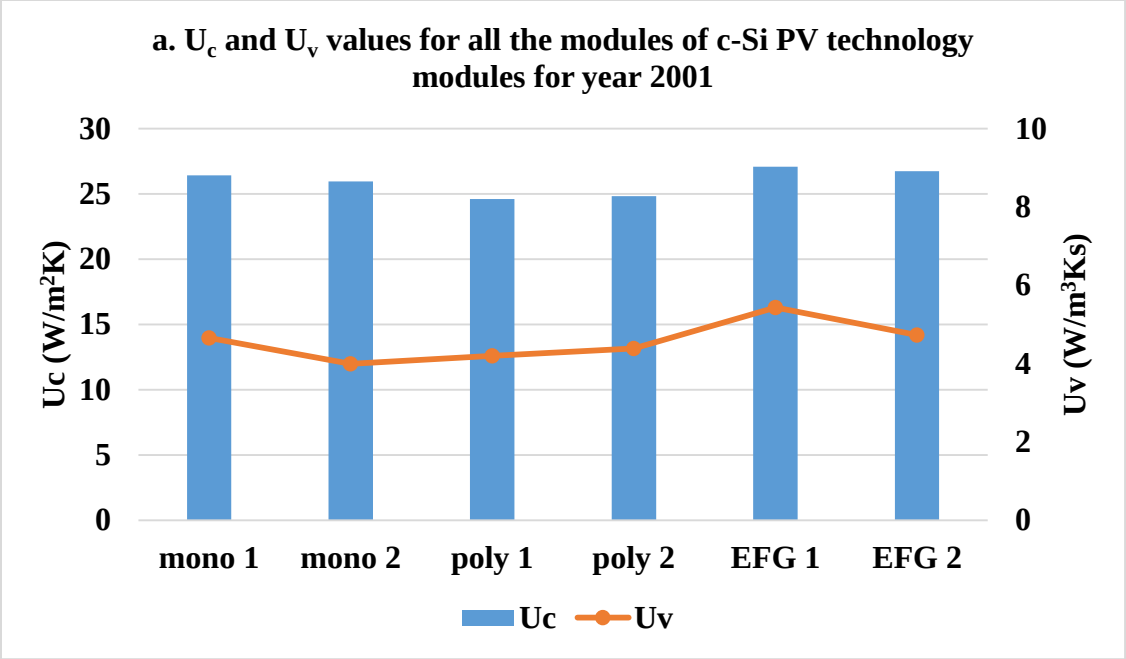

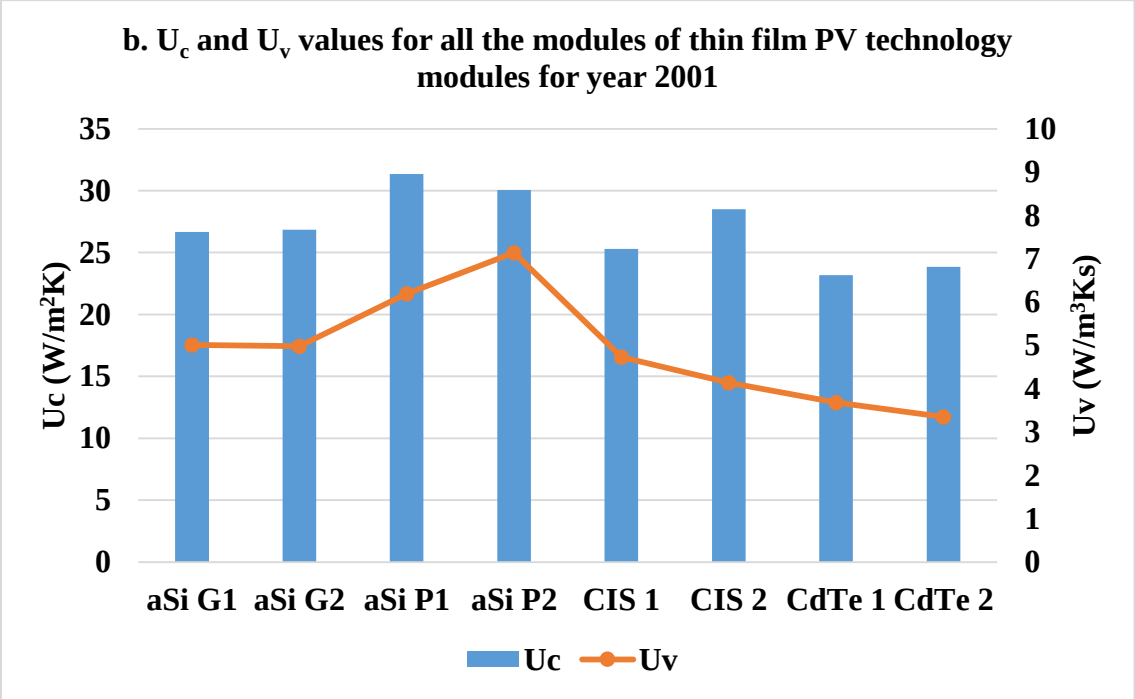

Figure 52: Uc and Uv Values for All the Modules of c-Si and Thin Film PV Technologies for year 2001

There is a stark difference in the values for the amorphous silicon technology with glass and Tefzel superstrate, because the modules with polymer superstrate operate at lower temperatures than those with glass superstrate. The following trend is observed in amorphous silicon PV modules:

U_c value for aSi with Tefzel superstrate > U_c value for aSi with Glass superstrate.

Two ANOVA designs were performed to determine significance of module replicates and PV technology on U_c and U_v values, if any. But the p-value for all the cases was obtained to be greater than 0.05 signifying no dominant effect as shown in Table 22 (a and b).

Table 22: ANOVA Design to determine Significance of Module Replicates (a. U_v Values)

Source	DF	Adj SS	Adj MS	F-Value	P-Value
Module	1	0.1015	0.1015	0.1	0.762
Error	12	12.7337	1.0611		
Total	13	12.8352			

Table 22: ANOVA Design to determine Significance of Module Replicates (b. U_c Values)

Source	DF	Adj SS	Adj MS	F-Value	P-Value
Module	1	0.3376	0.3376	0.06	0.809
Error	12	66.3226	5.5269		
Total	13	66.6602			

Figure 53 represents the U_c and U_v values for all PV technologies for a year-long data (2001) at one hour interval

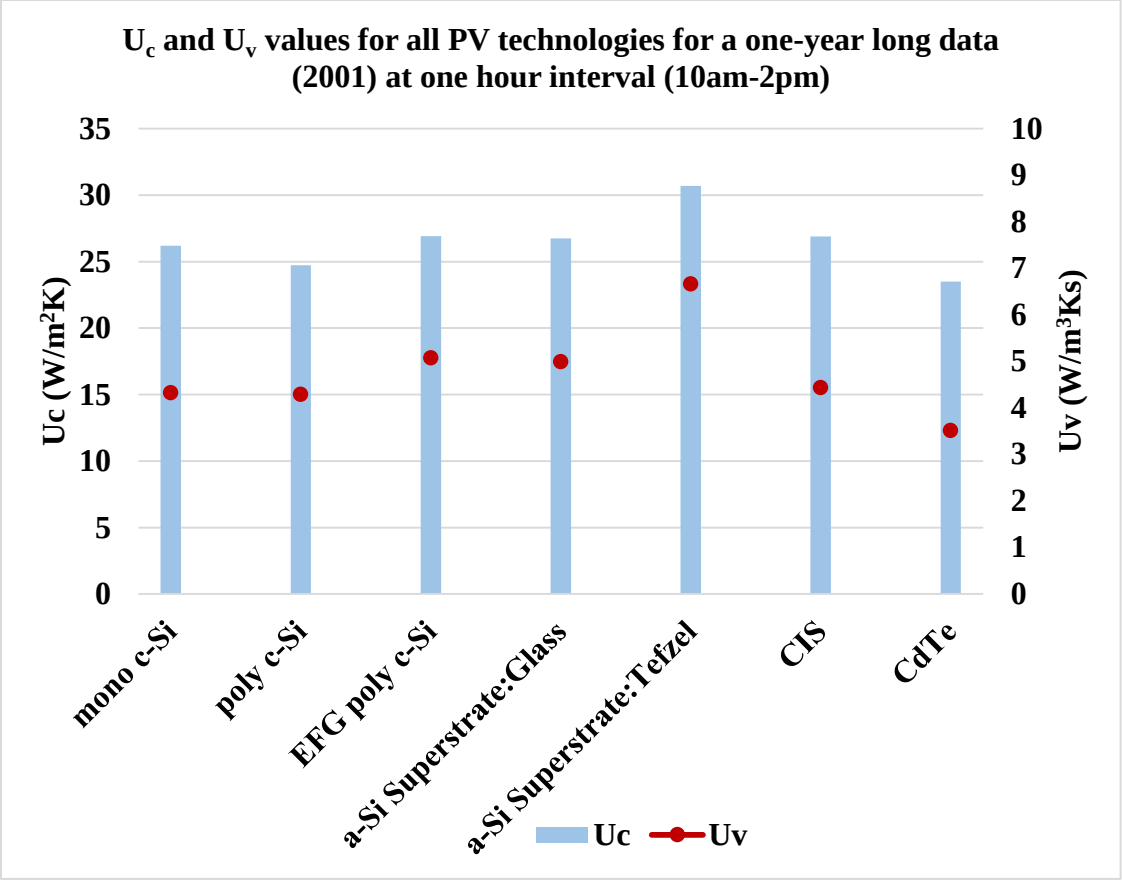

Figure 53: U_c and U_v Values for all PV Technologies for a One-Year Long Data (2001) at One Hour Interval (10am-2pm)

It can be observed from Figure 53 that the U_c and U_v value for CdTe technology is the lowest. This nature of CdTe modules operating at Pmax conditions is predicted to be because of G/G/FR construction type of the modules causing higher series resistance and I^2R heating loss. Therefore, considering all the PV technologies following trend is observed in the nature of U_c and U_v values.

Polymer-Polymer > Glass-Polymer > Glass-Glass PV technologies.

3.5 CONCLUSIONS

The year-long data (2001) at five minute interval was averaged into hourly data during the peak sun hours from 10am-2pm to determine the thermal model parameters Uc and U_v. The following conclusions can be interpreted.

- Limiting the wind speed to 4m/s gives statistically and practically correct Uc and U_v values. It eliminates the randomness in the data helping to statistically correlate the values and to improve the values for energy and performance models.
- The fitted values follow satisfactory pattern, the mean is normally distributed about zero and follows normal distribution and the Uc and U_v parameters have 95% confidence interval. Therefore it can be concluded that the plots satisfy model adequacy check and the determination of U_c and U_v is statistically correlated.
- ANOVA designs performed determine no significance of module replicates on Uc and U_v values.
- Considering all the PV technologies Uc and Uv value tend to follow the trend: Polymer-Polymer > Glass-Polymer > Glass-Glass PV technologies
- The U_c and U_v values of monocrystalline and polycrystalline PV technology modules were averaged to obtain one Uc and one Uv value for c-Si PV technology, which is used more than 80% in PV industry (wen average wind speed= 1.84 m/s): U_c = 25.46 W/m^{2}K and U_v = 4.31 W/m^{3}K.s

REFERENCES

[1] E. Skoplaki, J.A. Palyvos, "On the temperature dependence of photovoltaic module electrical performance: A review of efficiency/power correlations," *Solar Energy,* vol. 83, no. 5, pp. 614-624, 2009.

[2] Dyk, Edson L. Meyer and E. Ernest van, "Assessing the Reliability and Degradation of Photovoltaic Module Performance Parameters," in *IEEE transactions on Reliability*, 2004.

[3] "PV education," [Online]. Available: http://www.pveducation.org/pvcdrom/solar-cell-operation/effect-of-temperature.

[4] David King, Jay A. Kratochvil, and William E. Boyson, "Temperature coefficients for PV modules and arrays: Measurement methods, difficulties, and results," in *IEEE Photovoltaic Specialists Conference,* California, 1997.

[5] K. Emery, J. Burdick, Y. Caiyem, D. Dunlavy, H. Field, B. Kroposki, T. Moriarty, L. Ottoson, S. Rummel, T. Strand, and M.W. Wanlass, "Temperature dependence of photovoltaic cells, modules, and systems," in *IEEE Photovoltaics Specialists Conference*, Washington, 2002.

[6] C. Schwingshackl, M. Petittaa, J.E. Wagnera, G. Belluardo, D. Moser, M. Castellia, M. Zebischa and A. Tetzlaff, "Wind effect estimation on PV module temperature: Analysis of different techniques for an accurate estimation," *Energy Procedia,* pp. 77-86, 2013.

[7] Hans Goverde, Dirk Goossens, Jonathan Govaerts, Vikas Dubey, Francky Catthoor, Kris Baert, Jef Poortmans, Johan Driesen, "Spatial and temporal analysis of wind effects on PV module temperature and performance," *Suistainable Energy Technologies and Assessments,* vol. 11, pp. 36-41, 2015.

[8] Kurnik, J., Jankovec, M., Brecl, K., Topic, M.,, "Outdoor testing of PV module temperature and performance under different mounting and operational conditions," *Solar Energy Materials and Solar Cells,* vol. 95, no. 1, pp. 373-376, 2011.

[9] Umachandran, Neelesh, *Spatial Temperature Uniformity and Statistical Determination of Dominant Degradation Modes in PV Modules,* Master's Thesis, 2015.

[10] D.L.King, "Photovoltaic Module and Array Performance Characterization Methods for All System Operating Conditions," in *AIP Proceeding of NREL/SNL Photovoltaics Program Review Meeting*, New York, 1997.

[11] Faiman, David, "Assessing the Outdoor Operating Temperature of Photovoltaic Modules," *Photovoltaics Research and Applications*, pp. 307-315, 2008.

[12] D.L. King, W.E. Boyson, J.A. Kratochvill, "Sandia Report: Photovoltaic Array Performance Model," SANDIA, 2004.

[13] Li, Bo, *Outdoor photovoltaic module performance measurements- Implementation of Sandia National Laboratories method and improvement of thermal test bed,* Master's thesis:, 2006.

[14] Belmont, J., *26+ Year Old Photovoltaic Power Plant: Degradation and Reliability Evaluation of Crystalline Silicon Modules,",* 2013.

[15] Stein, Michaela G. Farr and Joshua S., "Spatial Variations in Temperature across a Photovoltaic Array," in *IEEE Photovoltaics Specialists Conference*, Colorado, 2014.

[16] C. M. Whitaker, et. al, "Effects of irradiance and Other Factors on PV Temperature Coefficients," in *IEEE Photovoltaic Specialists Conference*, 1991.

[17] Yedidi., Karan Rao, *Failure and Degradation Modes of PV modules in a Hot Dry Climate: Results after 16 years of field exposure,* Master's Thesis.

[18] Mallineni, Jaya Krishna, *Failure and Degradation Modes of PV modules in a Hot Dry Climate: Results after 4 and 12 years of field exposure,* Master's Thesis.

[19] William Hayes, Alex Panchula, and Lauren Nelson, "Thermal Modeling Accuracy of Hourly Averaged Data for Large Free Field Cadmium Telluride PV Arrays," in *IEEE Photovoltaic Specialists Conference*, Texas, 2012.

[20] M., Green, Solar Cells: Operating Principles, Technology and System Applications, Englewood Cliffs, N.J.: Prentice-Hall, Inc, 1982.

[21] Wohlgemuth J, Posbic J, Anderson J., "Energy ratings for PV modules," in *14th European Solar Energy Conference,*, Barcelona, Spain, 1997.

[22] Ty W. Neises, Sanford A. Klein and Douglas T. Reindl, "Development of a Thermal Model for Photovoltaics Modules and Analysis of NOCT Guidelines," *Solar Energy Engineering*, vol. 134, no. 1, 2011.

[23] Matthew Muller, Bill Marion, Jose Rodriguez, "Evaluating the IEC 61215 Ed.3 NMOT Procedure against the Existing NOCT Procedure with PV Modules in a Side-by-Side Configuration," in *IEEE Photovoltaic Specialists Conference*, Texas, 2012.

[24] "https://pvpmc.sandia.gov," [Online]. Available: https://pvpmc.sandia.gov/modeling-steps/2-dc-module-iv/cell-temperature/pvsyst-cell-temperature-model/.

[25] "PVSyst Help page," [Online]. Available: http://files.pvsyst.com/help/thermal_loss.htm.

[26] TamizhMani G, Ji L, Tang Y, Petacci L, Osterwald C., "Photovoltaic module thermal/wind performance: long-term monitoring and model development for energy rating," in *NCPV and Solar Program Review Meeting, Department of Energy*, Denver, CO, 2003.

APPENDIX A

TEMPERATURE COEFFICIENTS FOR VARIOUS MODULES AT FOUR DIFFERENT LOCATIONS

The tables and graphs for temperature coefficients for various modules at four different locations

1. CdTe PV technology

I-V Parameters	**Isc**	**Voc**	**Pm**
	(%/°C)	(%/°C)	(%/°C)
center	0.03%	-0.20%	-0.22%
corner	0.04%	-0.24%	-0.26%
long edge	0.04%	-0.22%	-0.24%
short edge	0.04%	-0.23%	-0.22%

2. a-Si PV technology

I-V Parameters	**Isc**	**Voc**	**Pm**
	(%/°C)	(%/°C)	(%/°C)
Centre	0.083	-0.42	-0.37
Corner	0.071	-0.36	-0.317
Long edge	0.071	-0.358	-0.316
Short Edge	0.071	-0.386	-0.34

3. c-Si PV technology with a black frame

I-V Parameters	**Isc**	**Voc**	**Pm**
	(%/°C)	(%/°C)	(%/°C)
Centre	0.041	-0.367	-0.54
Corner	0.037	-0.331	-0.49
Long edge	0.039	-0.351	-0.517
Short Edge	0.04	-0.355	-0.525

4. CIGS PV technology

I-V Parameters	**Isc**	**Voc**	**Pm**
	(%/°C)	(%/°C)	(%/°C)
Centre	0.023	-0.29	-0.38
Corner	0.023	-0.3114	-0.4
Long edge	0.019	-0.34	-0.43
Short Edge	0.028	-0.337	-0.43

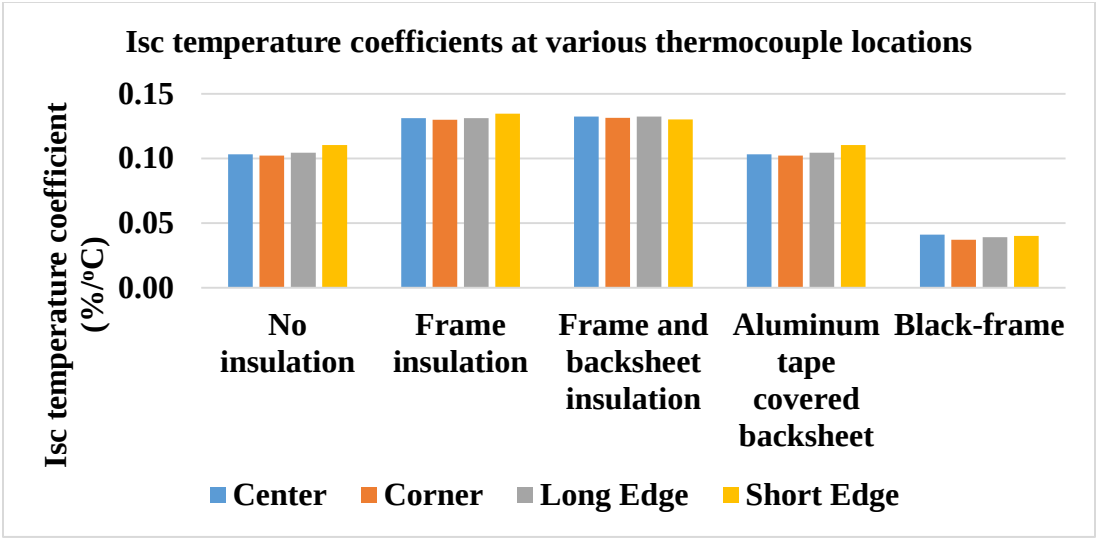
Isc temperature coefficients at various thermocouple locations
Isc temperature coefficient (%/°C)
0.15
0.10
0.05
0.00
No insulation
Frame insulation
Frame and backsheet insulation
Aluminum tape covered backsheet
Black-frame
Center
Corner
Long Edge
Short Edge

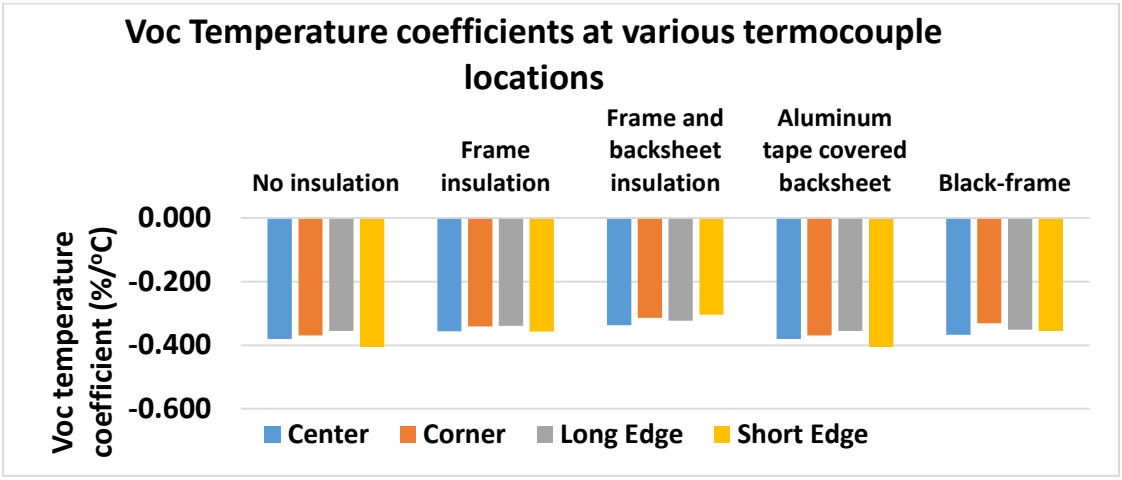
Voc Temperature coefficients at various termocouple locations
Voc temperature coefficient (%/°C)
0.000
-0.200
-0.400
-0.600
No insulation
Frame insulation
Frame and backsheet insulation
Aluminum tape covered backsheet
Black-frame
Center
Corner
Long Edge
Short Edge

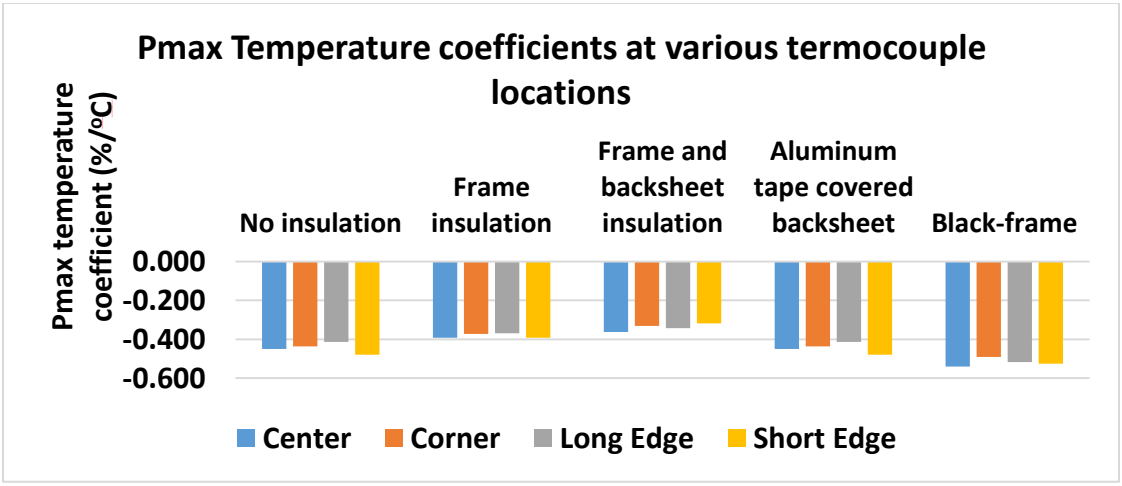
Pmax Temperature coefficients at various termocouple locations
Pmax temperature coefficient (%/°C)
0.000
-0.200
-0.400
-0.600
No insulation
Frame insulation
Frame and backsheet insulation
Aluminum tape covered backsheet
Black-frame
Center
Corner
Long Edge
Short Edge

APPENDIX B

PLANT LEVEL TEMPERATURE DISTRIBUTION FOR AZ3 AND AZ5 POWER PLANT

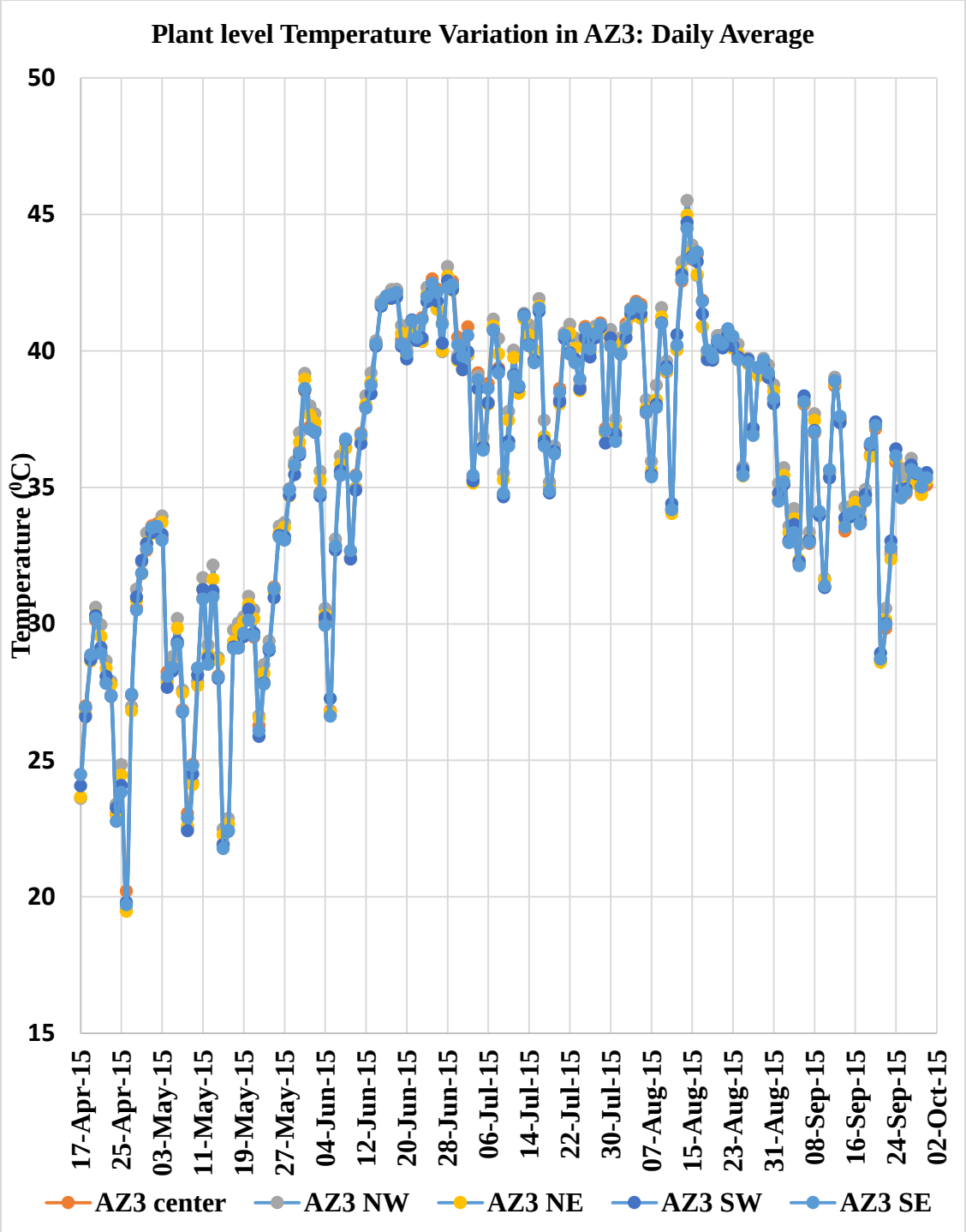
Plant level Temperature Variation in AZ3: Daily Average
Temperature (⁰C)
50
45
40
35
30
25
20
15
17-Apr-15
25-Apr-15
03-May-15
11-May-15
19-May-15
27-May-15
04-Jun-15
12-Jun-15
20-Jun-15
28-Jun-15
06-Jul-15
14-Jul-15
22-Jul-15
30-Jul-15
07-Aug-15
15-Aug-15
23-Aug-15
31-Aug-15
08-Sep-15
16-Sep-15
24-Sep-15
02-Oct-15
AZ3 center
AZ3 NW
AZ3 NE
AZ3 SW
AZ3 SE

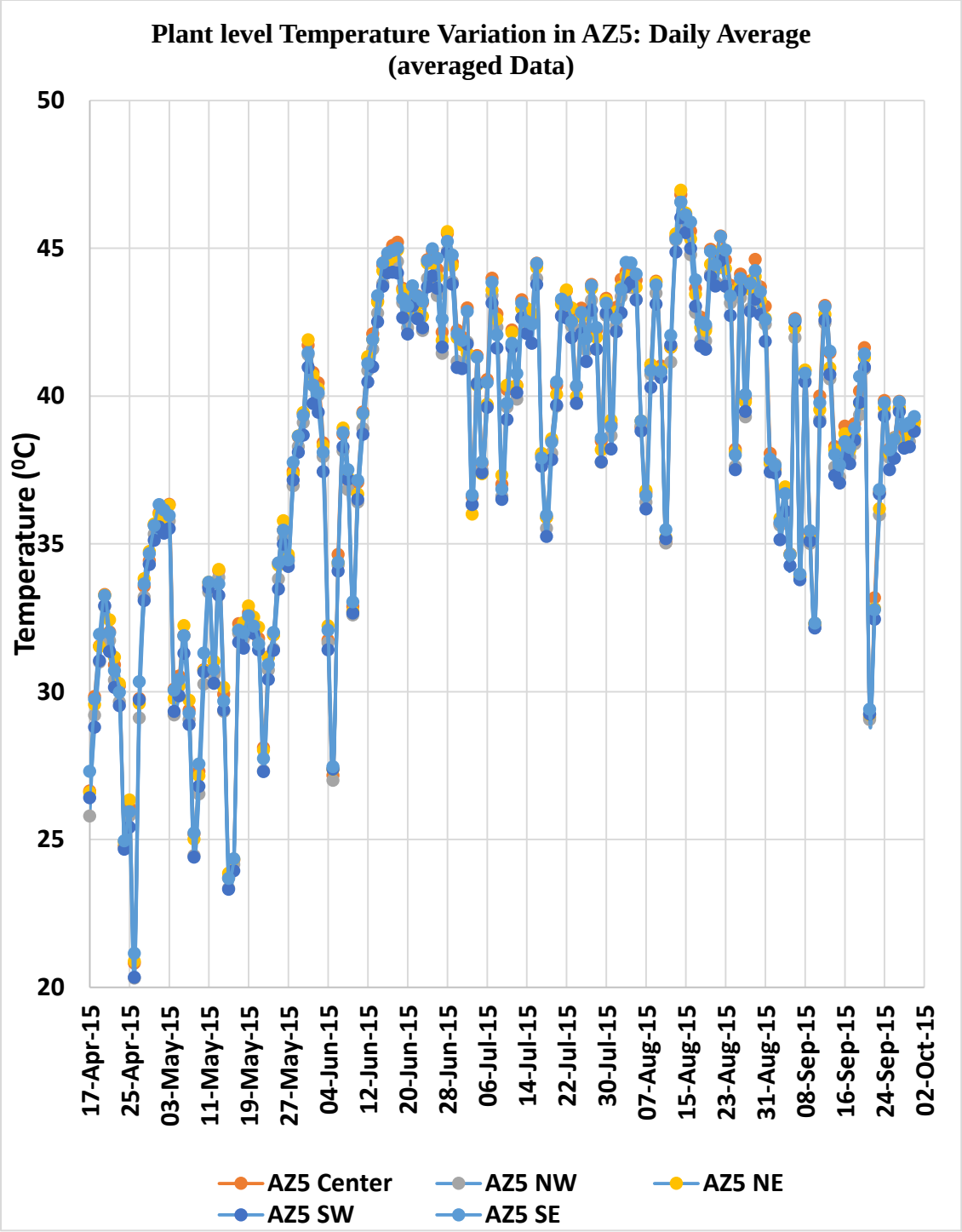
Plant level Temperature Variation in AZ5: Daily Average
(averaged Data)
Temperature (°C)
50
45
40
35
30
25
20
17-Apr-15
25-Apr-15
03-May-15
11-May-15
19-May-15
27-May-15
04-Jun-15
12-Jun-15
20-Jun-15
28-Jun-15
06-Jul-15
14-Jul-15
22-Jul-15
30-Jul-15
07-Aug-15
15-Aug-15
23-Aug-15
31-Aug-15
08-Sep-15
16-Sep-15
24-Sep-15
02-Oct-15
AZ5 Center
AZ5 NW
AZ5 NE
AZ5 SW
AZ5 SE

APPENDIX C

MODULE LEVEL TEMPERATURE VARIATION IN AZ3 AND AZ5

Module level temperature variation (Averaged data) in AZ3

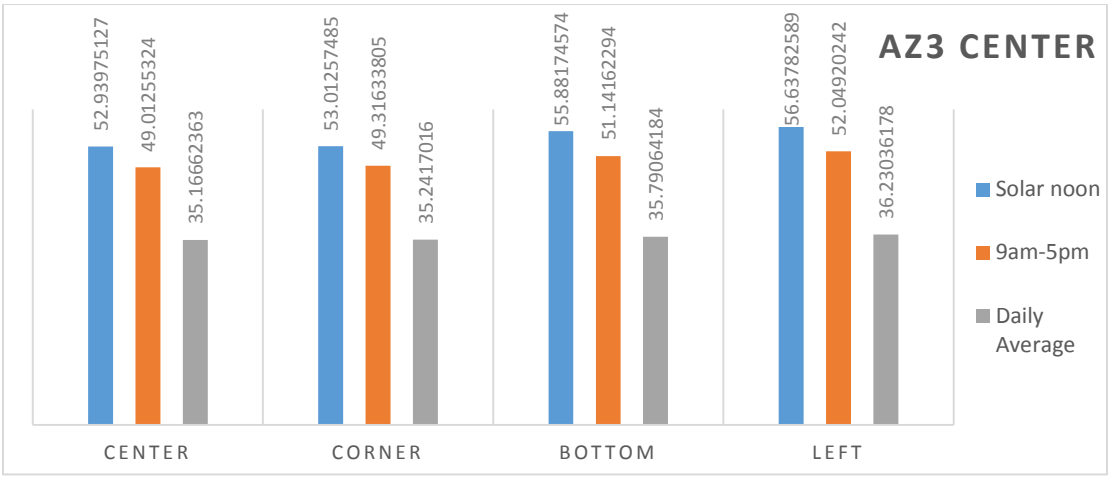

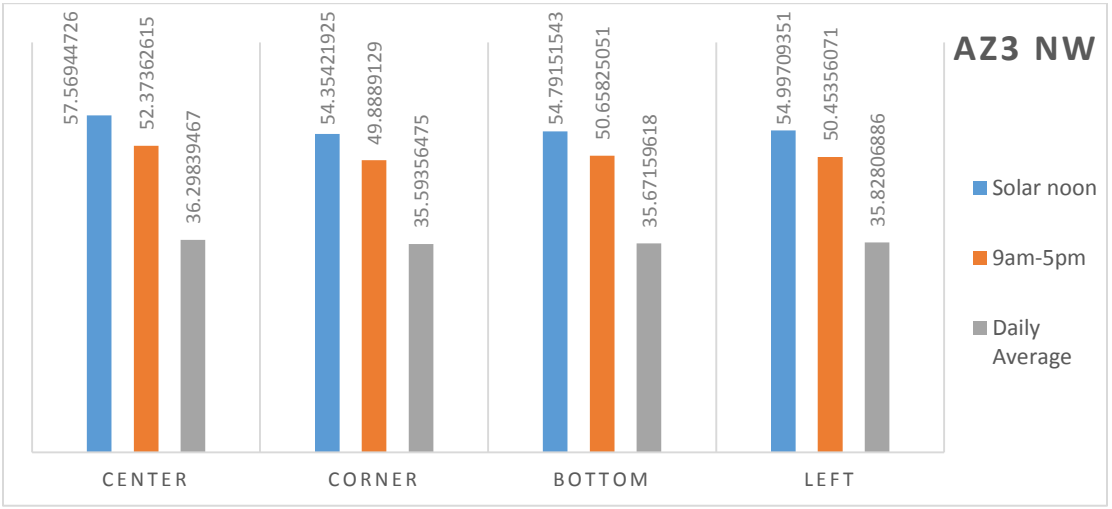

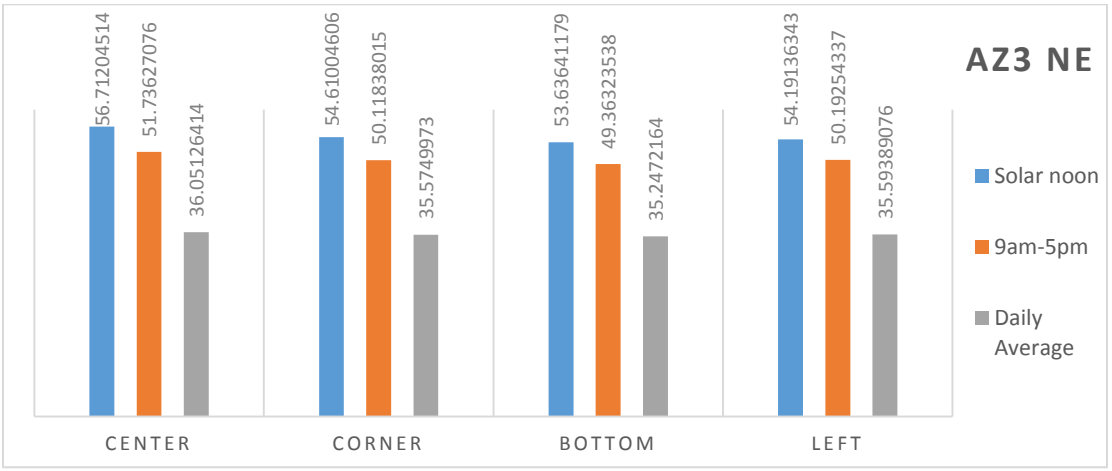

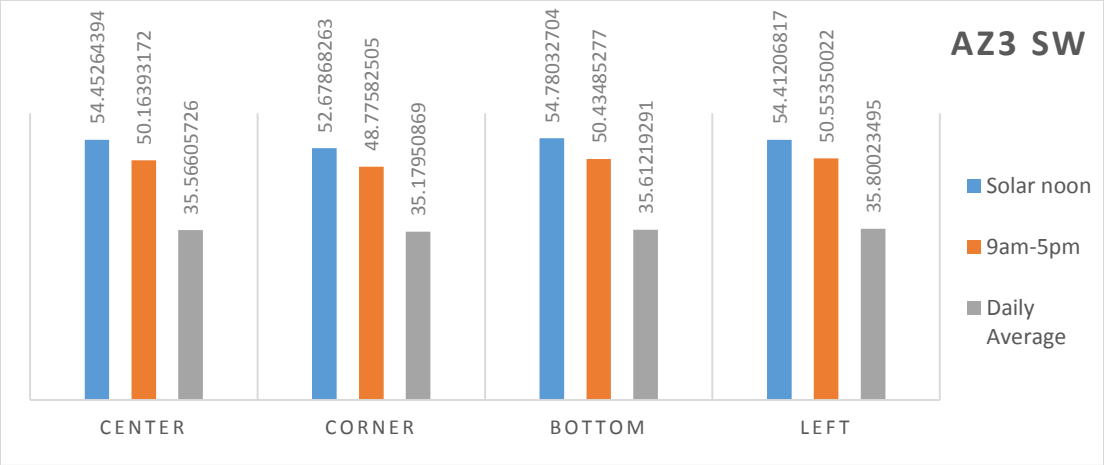
AZ3 SW
54.45264394
50.16393172
35.56605726
52.67868263
48.77582505
35.17950869
54.78032704
50.43485277
35.61219291
54.41206817
50.55350022
35.80023495
CENTER
CORNER
BOTTOM
LEFT
Solar noon
9am-5pm
Daily Average

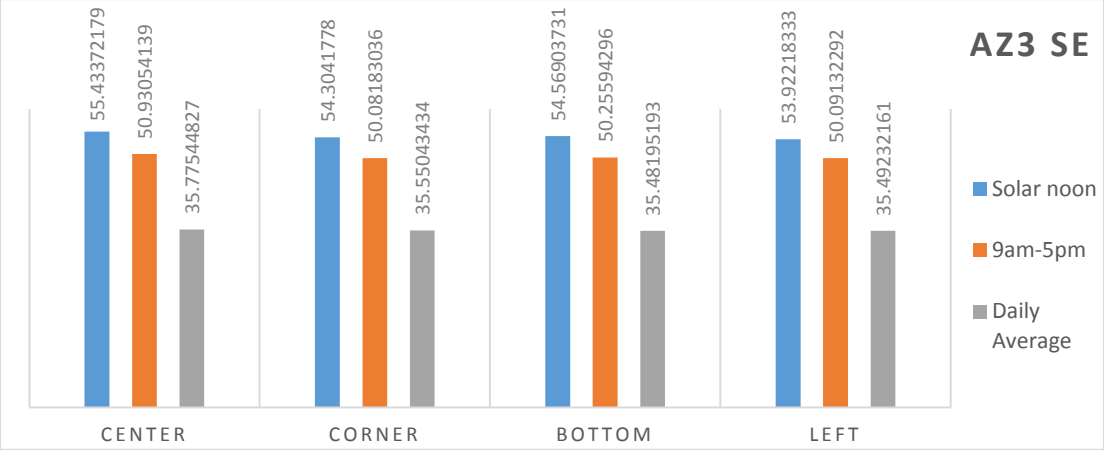
AZ3 SE
55.43372179
50.93054139
35.77544827
54.3041778
50.08183036
35.55043434
54.56903731
50.25594296
35.48195193
53.92218333
50.09132292
35.49232161
CENTER
CORNER
BOTTOM
LEFT
Solar noon
9am-5pm
Daily Average

Module level temperature variation (Averaged data) in AZ5

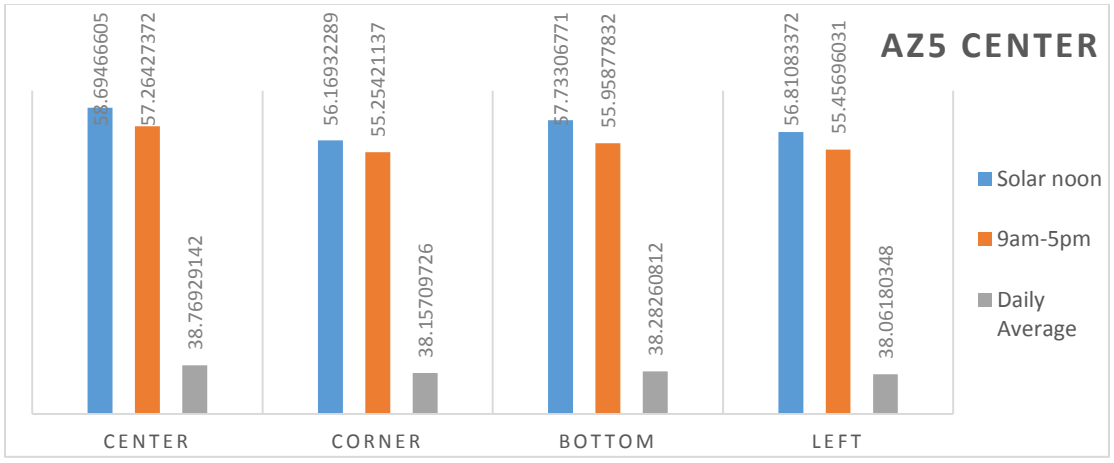

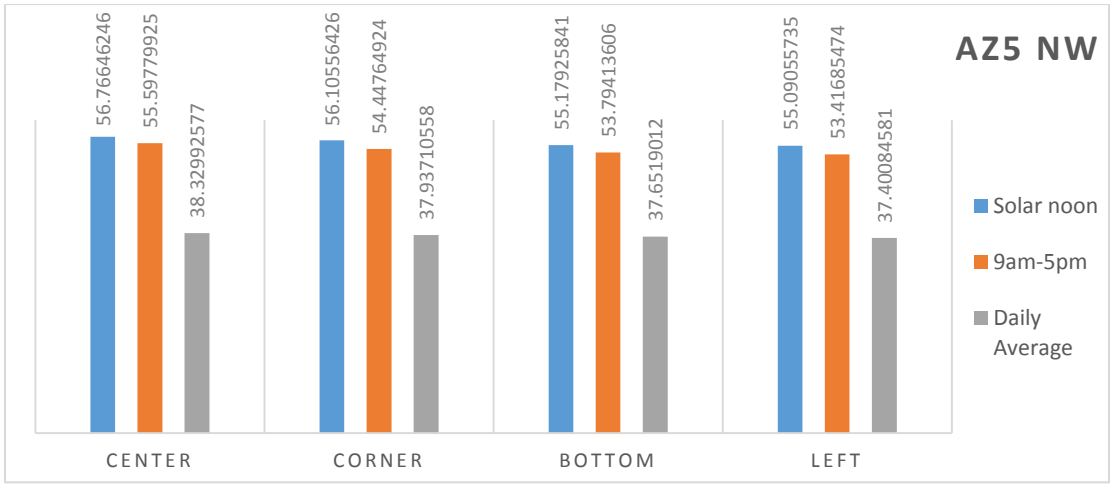

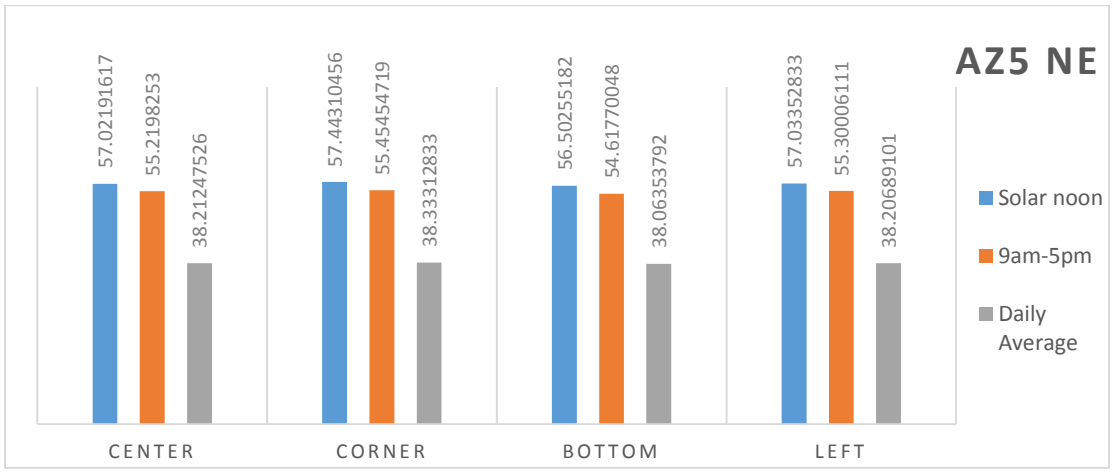

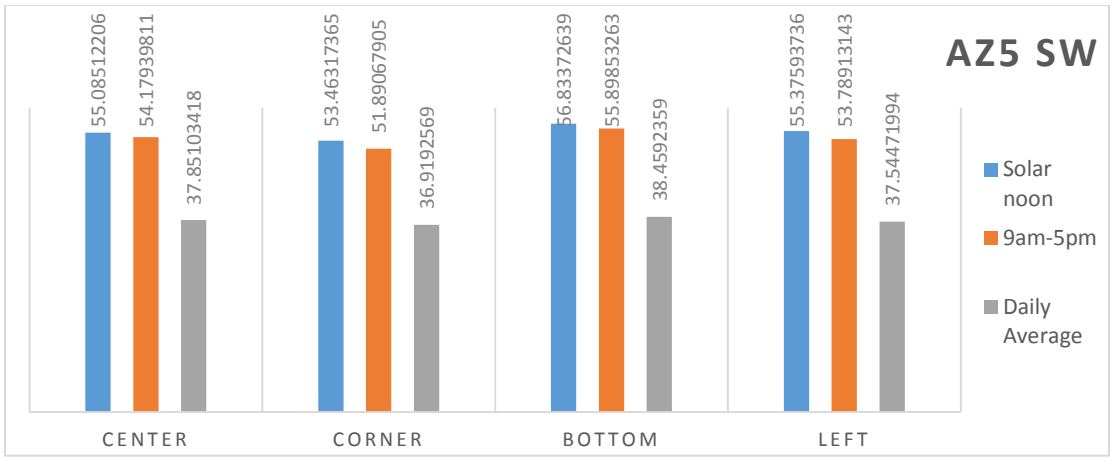
AZ5 SW
55.08512206
54.17939811
37.85103418
53.46317365
51.89067905
36.9192569
56.83372639
55.89853263
38.4592359
55.37593736
53.78913143
37.54471994
Solar noon
9am-5pm
Daily Average
CENTER
CORNER
BOTTOM
LEFT

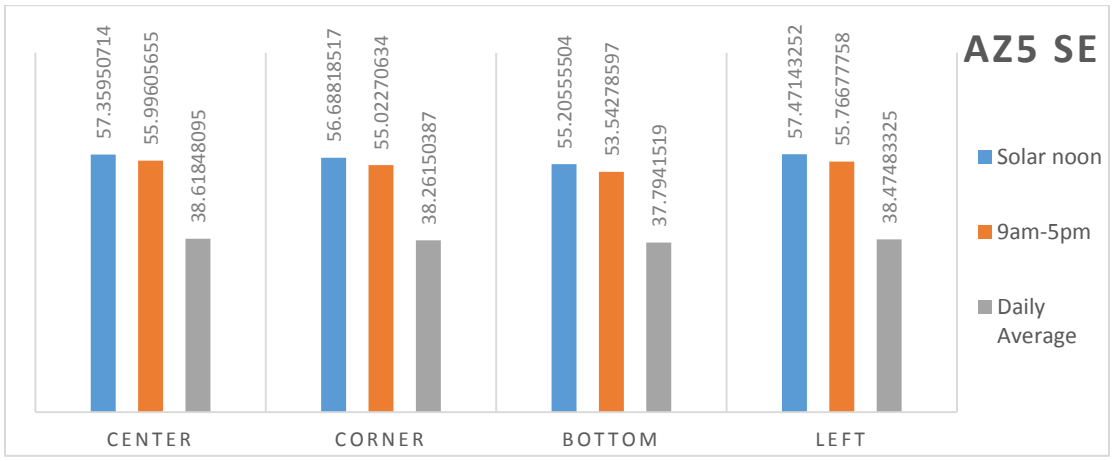
AZ5 SE
57.35950714
55.99605655
38.61848095
56.68818517
55.02270634
38.26150387
55.20555504
53.54278597
37.7941519
57.47143252
55.76677758
38.47483325
Solar noon
9am-5pm
Daily Average
CENTER
CORNER
BOTTOM
LEFT

APPENDIX D

U_C AND U_V VALUES FOR EACH MONTH OF A YEAR-LONG DATA (2001) AT FIVE-MINUTE INTERVAL FOR VARIOUS PV TECHNOLOGIES

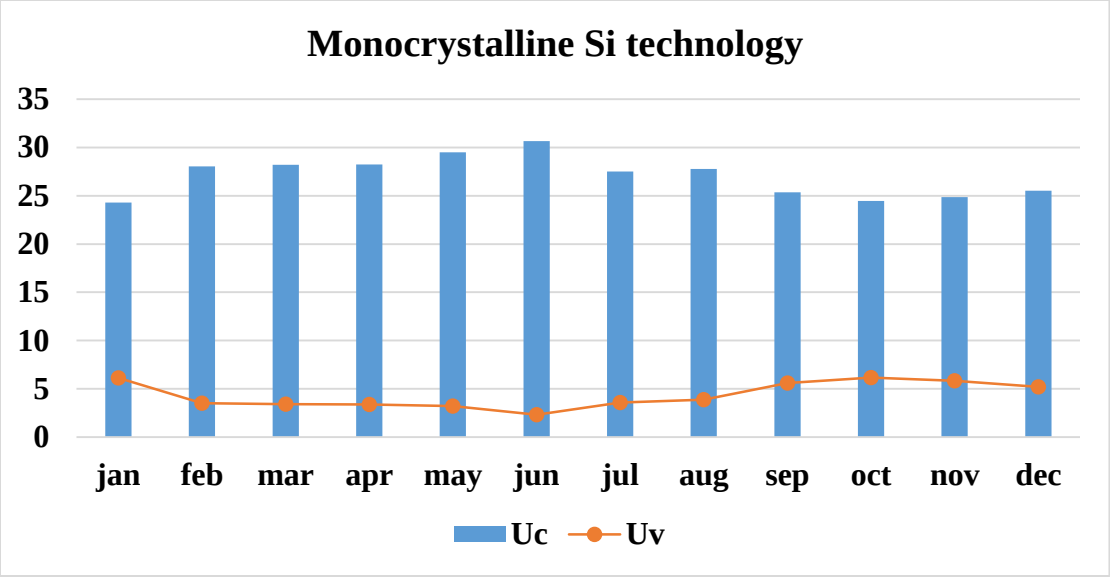
Monocrystalline Si technology
35
30
25
20
15
10
5
0
jan
feb
mar
apr
may
jun
jul
aug
sep
oct
nov
dec
Uc
Uv

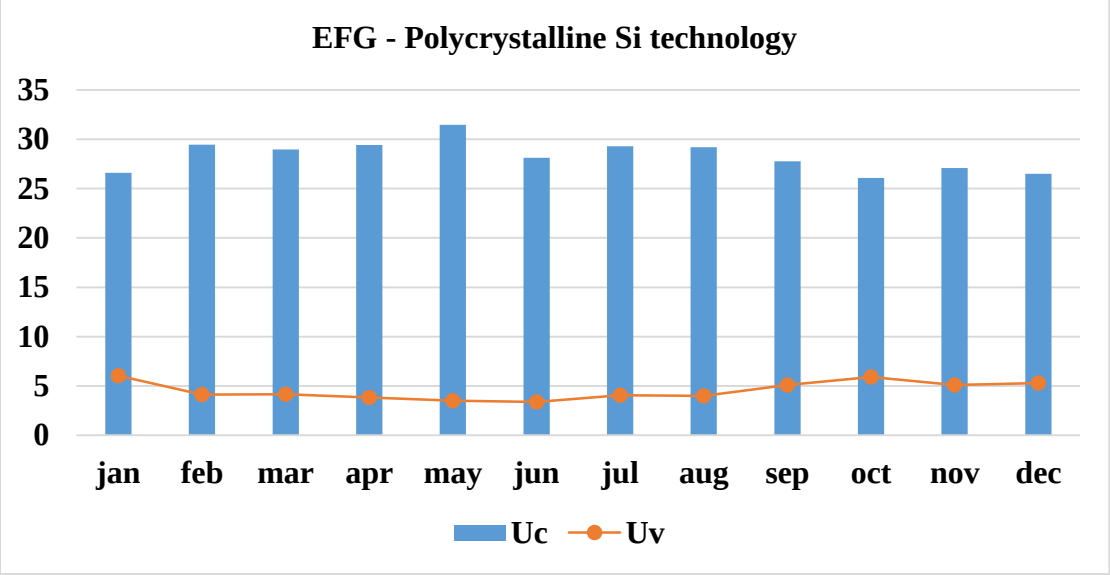
EFG - Polycrystalline Si technology
35
30
25
20
15
10
5
0
jan
feb
mar
apr
may
jun
jul
aug
sep
oct
nov
dec
Uc
Uv

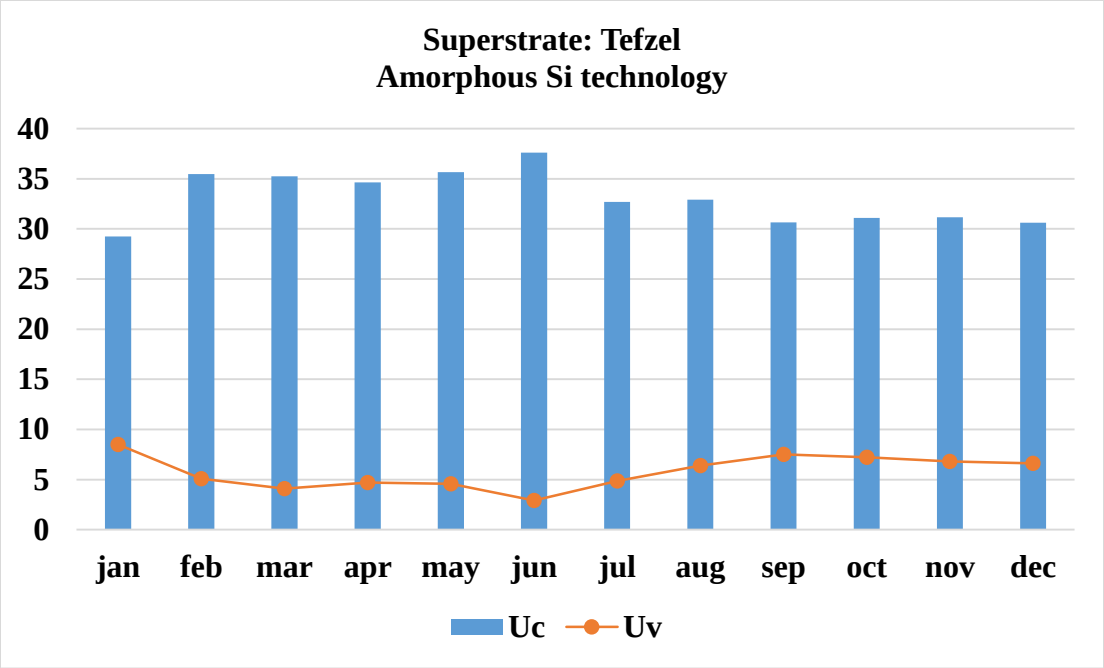
Superstrate: Tefzel
Amorphous Si technology
40
35
30
25
20
15
10
5
0
jan
feb
mar
apr
may
jun
jul
aug
sep
oct
nov
dec
Uc
Uv

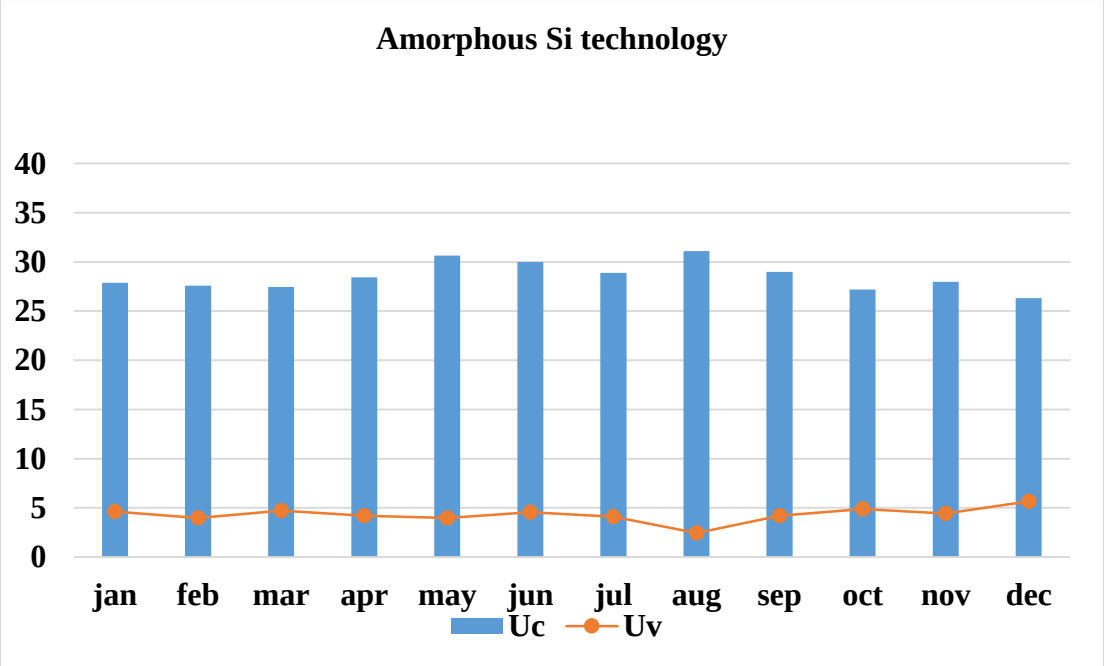
Amorphous Si technology
40
35
30
25
20
15
10
5
0
jan
feb
mar
apr
may
jun
jul
aug
sep
oct
nov
dec
Uc
Uv

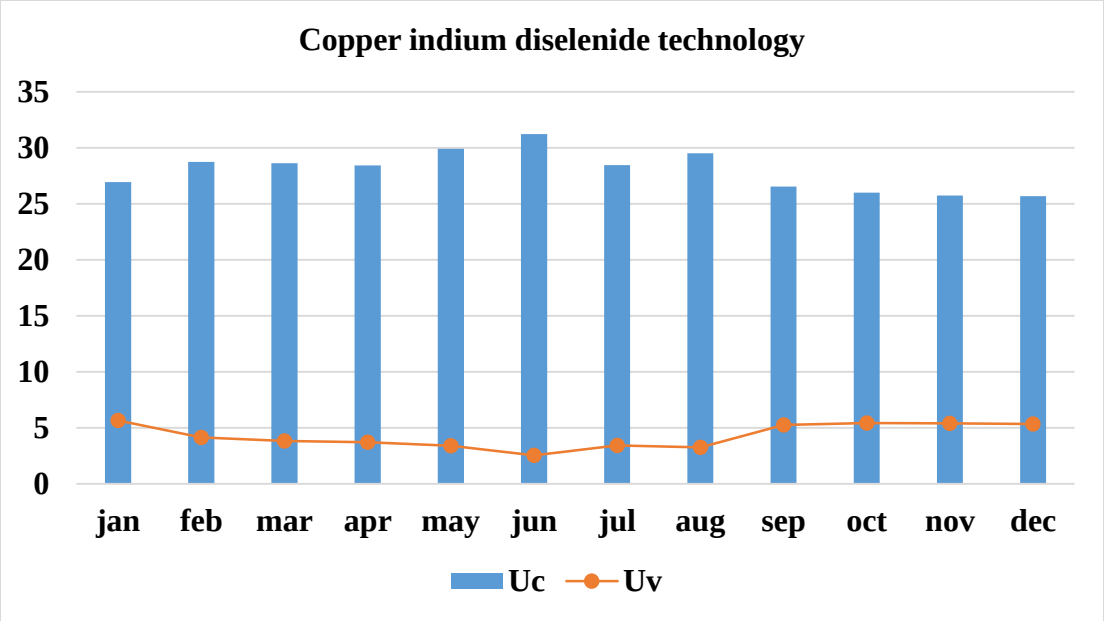
Copper indium diselenide technology
35
30
25
20
15
10
5
0
jan
feb
mar
apr
may
jun
jul
aug
sep
oct
nov
dec
Uc
Uv

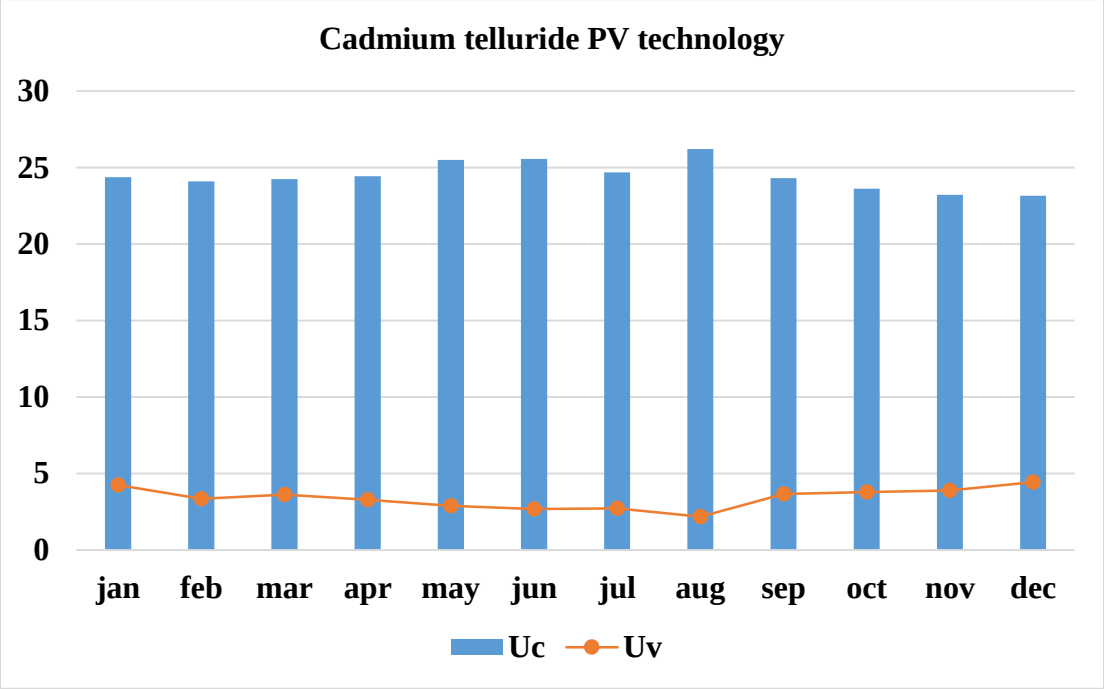
Cadmium telluride PV technology
30
25
20
15
10
5
0
jan
feb
mar
apr
may
jun
jul
aug
sep
oct
nov
dec
Uc
Uv